



HAL
open science

Intermittent transport processes on surfaces

Xuan Lan Phun

► **To cite this version:**

Xuan Lan Phun. Intermittent transport processes on surfaces. General Mathematics [math.GM].
Université d'Orléans, 2014. English. NNT : 2014ORLE2034 . tel-01128041

HAL Id: tel-01128041

<https://theses.hal.science/tel-01128041>

Submitted on 9 Mar 2015

HAL is a multi-disciplinary open access archive for the deposit and dissemination of scientific research documents, whether they are published or not. The documents may come from teaching and research institutions in France or abroad, or from public or private research centers.

L'archive ouverte pluridisciplinaire **HAL**, est destinée au dépôt et à la diffusion de documents scientifiques de niveau recherche, publiés ou non, émanant des établissements d'enseignement et de recherche français ou étrangers, des laboratoires publics ou privés.



UNIVERSITÉ D'ORLÉANS



***École doctorale Mathématiques, Informatiques, Physique
théorique et Ingénierie des systèmes***

Laboratoire : MAPMO

THÈSE présentée par :

Xuan Lan PHUN

soutenu le : **[25 Novembre 2014]**

pour obtenir le grade de : **Docteur de l'université d'Orléans**

Discipline/ Spécialité : **Mathématiques**

INTERMITTENT TRANSPORT PROCESSES ON SURFACES

THÈSE DIRIGÉE PAR :

Athanasios BATAKIS
Michel ZINSMEISTER

MCF, Université d'Orléans - Directeur de thèse
Professeur, Université d'Orléans - Co-directeur de
thèse

RAPPORTEURS :

Hermine BIERMÉ
Marcel FILOCHE

Professeur, Université de Poitiers
Directeur de recherches, École Polytechnique

JURY :

Stéphane SEURET

Président du jury, Professeur, Université Paris 12 Val
de Marne

Athanasios BATAKIS
Olivier BÉNICHOU
Hermine BIERMÉ
Marcel FILOCHE
Denis GREBENKOV
Luc HILLAIRET
Michel ZINSMEISTER

MCF, Université d'Orléans
Professeur, Université Pierre et Marie Curie
Professeur, Université de Poitiers
Directeur de recherches, École Polytechnique
Chargé de recherches, École Polytechnique
Professeur, Université d'Orléans
Professeur, Université d'Orléans

Remerciements

Ce manuscrit conclut trois ans de travail, et je tiens en ces quelques lignes à exprimer ma reconnaissance envers tous ceux qui de près ou de loin ont permis leur bon déroulement.

En premier lieu, je souhaiterais exprimer ma sincère gratitude à Athanasios Batakis et Michel Zinsmeister, mes directeur et co-directeur de thèse pour leur disponibilité, leur aide précieuse dans la réalisation de ma thèse en France. Leurs encouragements et leur soutien m'ont été d'un grand réconfort notamment lors de ma maladie. Je remercie tout particulièrement Michel pour sa générosité, ses conseils et sa patience. Les nombreuses discussions que nous avons eues ainsi que ses conseils sont pour beaucoup dans le résultat final de ce travail. Ses nombreuses relectures et corrections de cette thèse ont été très appréciables. Ses qualités humaines et sa gentillesse m'ont aussi beaucoup touchée.

J'adresse mes remerciements à Olivier Bénichou, Denis S. Grebenkov, Luc Hillairet et Raphaël Voituriez pour leur aide précieuse dans la rédaction d'articles que j'ai eu la chance de présenter en collaboration avec eux. J'exprime ma profonde gratitude à Monsieur Grebenkov avec qui j'ai eu l'opportunité de pouvoir travailler. Sa rigueur, sa capacité d'analyse des problèmes et ses très nombreuses connaissances m'ont permis de progresser.

Je remercie vivement les Professeurs Hermine Biermé et Marcel Filoche d'avoir accepté d'être rapporteurs de cette thèse. Leurs nombreuses remarques et suggestions ont beaucoup amélioré la qualité de ce mémoire. Je suis reconnaissante à Messieurs Olivier Bénichou, Denis S. Grebenkov, Luc Hillairet et Stéphane Seuret pour l'honneur qu'ils me font en acceptant d'être membres de mon jury.

Je souhaite aussi remercier les Professeurs qui ont participé au programme PUF. Ils nous ont donné l'occasion de travailler dans un bon environnement de recherche en France.

Inscrite en thèse de Mathématiques à l'Université d'Orléans, j'ai passé trois ans au sein du laboratoire MAPMO. Je sais gré à chaque membre du laboratoire et du département de son soutien et de ses témoignages d'amitié. Un merci tout particulier aux (ex-)thésards, à Marie-France Grespier, Anne Liger, Marie-Laurence Poncet, secrétaires du laboratoire du MAPMO pour leur convivialité et leurs encouragements.

Je tiens à remercier Pascal Omnes pour son amitié et ses encouragements. Mille mercis également à mes amis, Nga, Thuy, Kieu, Trang, Chuong, Bao, Hung, Hieu, Binh, Chi, Phuong, Tam, Nhat, Ky, Ly, Vladimir....avec qui j'ai partagé beaucoup de souvenirs pendant ces trois années loin de ma famille. Je souhaite remercier plus personnellement Nga et Bao pour m'avoir aidée à relire une partie de cette thèse et pour leurs précieux conseils. Leur profonde amitié m'a été d'un très grand soutien,

notamment dans les moments difficiles.

J'adresse un sincère remerciement à Jean-Yves, Nicole, Anaïs et Pierric Nourry ainsi que Victorialyne pour m'avoir accueillie au sein de leur famille.

J'ai une pensée particulière pour mes amis français, mes amis "internationaux" et mes autres amis vietnamiens que je ne peux pas citer ici.

Enfin, je tiens à exprimer la gratitude profonde de mon coeur à ma famille pour son amour et son soutien spirituel tout au long de ma vie.

Contents

1	INTRODUCTION	1
1.1	The model setting	1
1.2	Main results	3
2	MATHEMATICAL BACKGROUND	5
2.1	Separable Hilbert Space	5
2.1.1	Poisson summation formula	8
2.2	Operator theory	11
2.2.1	Compact operator	11
2.2.2	Self-adjoint operator	11
2.2.3	Spectral theorem	11
2.2.4	Sturm-Liouville theory	12
2.3	Discrete model for equations	13
2.3.1	Mean first-passage time for bulk diffusion	13
2.3.2	Mean first-passage time for surface diffusion	13
3	2D-CASE	17
3.1	Introduction	18
3.2	A self-adjoint operator formulation	19
3.2.1	Point-like target ($\epsilon = 0$)	23
3.2.2	Extended target ($\epsilon > 0$)	31
3.3	Numerical asymptotic behavior	36
4	3D-CASE	45
4.1	A self-adjoint operator formulation	46
4.1.1	Point-like target ($\epsilon = 0$ or $\alpha_\epsilon = 1$)	50
4.1.2	Extended target ($\epsilon > 0$ or $\alpha_\epsilon \in [-1, 1)$)	51
4.2	Numerical asymptotic behavior	54
5	TORUS CASE	63
5.1	A self-adjoint operator formulation	63
5.1.1	Point-like target ($\epsilon = 0$)	68
5.1.2	Extended target ($\epsilon > 0$)	72
5.2	Dependence on the value R	73

CONTENTS

5.3 Numerical asymptotic behavior	78
Appendix A Asymptotic behavior of the eigenvalues of the operator $V\tilde{T}V$	89
Appendix B Numerical computation of spectral characteristics	95
B.1 2-D case	95
B.2 3-D case	96
B.3 Rectangle case	98
Appendix C Proof of Theorem 5.1.1	101
Bibliographie	109

Chapter 1

INTRODUCTION

1.1 The model setting

What is the best strategy to find a missing object? It is clear that a systematic search may take a much longer time than a search involving some randomness. Let us look at a dog trying to find a ball in a garden. Typically, the dog will choose at random a direction, run for a (random) time in this direction and then search around the point it has reached for another random time. This means that not only the dog uses randomness, but also choose a two-phases strategy also called intermittent. The ballistic phases while the dog runs along straight lines alternate with some more systematic search following some kind of Brownian motion.

This intermittent dynamics can also be observed in many biological phenomena.

A typical example is water transport in confining media: the two phases are there diffusion in the bulk on one hand and surface exploration after adsorption (by hydrogen bond for instance). Other examples which are more linked to a strategy are facilitated search on DNA with phases of pure bulk diffusion and chain sliding, or vesicle transportation in living cells with phases of active transport by motor proteins or passive diffusion in the cytoplasm. This problem has been considered in [2, 4] and this Ph.D thesis is a continuation of this work.

The first model which was considered in the references [2, 4] (the model called 2-D) is that of a disk. A particle diffuses in it and seek to exit this disk through a "target", which is an interval on the boundary.

In order to reach this goal, the particle alternates diffusion steps in the disk with diffusion along the boundary circle after adsorption for instance by hydrogen bond or some similar physical phenomenon. This boundary phase consists in some Brownian motion within very small distance to the circle, small meaning of the order of the size of the atoms that are there. In particular we model the ending of this boundary phase by saying that the particle is located then at distance $a > 0$ (a is small that is of the order of the size of the atoms there) from the circle; it loses its attraction to the boundary and starts a new bulk diffusion from there. It is then reasonable

to say that boundary phases last for a random time following an exponential law. The parameters for this model are D_1 , D_2 , respectively the "speed" of diffusion on the boundary and the bulk phase, the small distance a , the parameter λ of the exponential law introduced before and ϵ which is half of the size of the target.

In [2], the authors show that for some values of D_1 , D_2 , a , ϵ there is indeed a choice of λ minimizing $\langle t_1 \rangle(\lambda)$, the expectation of the time necessary to reach the target. The problem can also be stated in 3-D, as it was already done in [2].

The purpose of this work is three-fold.

- (i) We begin by considering a model of surface-mediated diffusion with alternating phases of bulk and surface diffusion for a disk (2-D case). We provide rigorous mathematical formulation and resolution of the escape problem for surface-mediated diffusion. This formula involves the Sturm-Liouville theory applied to an appropriate self-adjoint operator. Considering an orthonormal basis of eigenvectors for this operator allows us to derive a new spectral representation of the mean exit time from the disk. In contrast to [1, 2, 17, 18] in which the mean exit time relied on matrix inversions, the new spectral representation is more explicit and particularly well-suited to investigate the asymptotic behavior of the mean exit time in the limit of large desorption rate λ . For a point-like target ($\epsilon = 0$), we obtain the asymptotic behavior: $\langle t_1 \rangle = A_1 \sqrt{\lambda} + A_2 + \frac{A_3}{\sqrt{\lambda}} + O\left(\frac{1}{\lambda}\right)$, with explicit formulas for coefficients A_i . For extended targets ($\epsilon > 0$), we establish the asymptotic approach to a finite limit \mathcal{T} . The main result of this work is a rigorous proof that $\langle t_1 \rangle$ is asymptotically increasing. In addition, we show numerical evidence that $\langle t_1 \rangle = \mathcal{T} - \frac{C_1}{\sqrt{\lambda}} + O\left(\frac{1}{\lambda}\right)$, with $C_1 > 0$. This statement implies a somewhat counter-intuitive conclusion that the pure bulk phase is never an optimal search strategy.
- (ii) From the model of the disk, we develop our problem to the models of the sphere (3-D case) and rectangle (Torus case). In these models, we investigate the similar problem as in the disk. In particular, by introducing self-adjoint operators, we use the orthonormal basis of eigenvectors of those operators to derive the spectral representation for $\langle t_1 \rangle$. Then we investigate the asymptotic behavior of $\langle t_1 \rangle$ at large λ for both cases $\epsilon = 0$ and $\epsilon > 0$. Especially, for 3-D case, mathematically, use the spectral representation shows that $\langle t_1 \rangle_{\epsilon=0}$ is always infinite (which is easily observed in physics). We also consider numerical asymptotic behavior of $\langle t_1 \rangle$ to show that $\langle t_1 \rangle_{\epsilon>0} = \mathcal{T} - \frac{C_1}{\sqrt{\lambda}} + O\left(\frac{1}{\lambda}\right)$ in these three models.
- (iii) We introduce a new model called rectangle or torus model. In this model the particle moves in the rectangle $[-\pi, \pi] \times [-R, R]$ whose sizes are pairwise identified (that is why we also call this model torus model) and we investigate how the shape elongation affects the mean exit time. Changing the rectangle aspect ratio, one can significantly reduce the mean exit time, enhancing the search efficiency $D_{2,crit}$ below which the surface diffusion is always optimal, and

prove that $D_{2,crit}$ monotonously grows with R . If D_2 is not too small, the "gain" of the intermittent search strategy over surface diffusion as a function of R is shown to have a maximum. In other words, for a given set of parameters (a, ϵ, D_1, D_2) the mean exit time can be optimized with respect to R , under the conditions that we identify.

1.2 Main results

In Ref.[2], the authors present a computation of the mean exit time $\langle t_1 \rangle$ to the target on the surface of a 2-D or 3-D spherical domain, which is based on an integral equation that can be solved analytically. Although an exact expression of $\langle t_1 \rangle$ can be given, it is not fully explicit, requiring the inversion of an infinite dimensional matrix. They then propose a method to approximate the mean exit time based on the fact that the matrix which they have to solve can be approximate by a diagonal matrix for small ϵ . They also show analytically that the mean exit time can be minimized as a function of the desorption rate from the surface.

Following their models, we introduce in chapter 3, 4 (2-D case and 3-D case) of this thesis another approach of the problem by using compact, self-adjoint operators. While not so different from [2], this approach is useful to control the resolvent of the main operator (or the infinite dimensional matrix in [2]) and allows us to use of the orthonormal basis of eigenvectors given by the spectral theorem for self-adjoint operators. This method lead us to obtain the spectral representation of the mean exit time, suitable in investigating the asymptotic behavior in the limit of large desorption rate λ .

With this approach, we prove that the mean exit time eventually increases at large λ . As a result, there exists a minimum at positive λ if the derivative $\frac{d\langle t_1 \rangle}{d\lambda}|_{\lambda=0} < 0$. This proof leads us to determine the critical ratio for D_2/D_1 , which called $(D_2/D_1)_{crit}$, so that $\langle t_1 \rangle$ has a minimum at some positive λ if $(D_2/D_1) > (D_2/D_1)_{crit}$. This critical ratio has already been established in [2], but our study is more rigorous.

In the general case of $\epsilon > 0$, we prove that $\langle t_1 \rangle$ converges to a finite limit as $\lambda \rightarrow \infty$.

Although the spectral representation of $\langle t_1 \rangle$ allows us to show that $\langle t_1 \rangle_{\epsilon>0}$ is eventually increasing to a finite limit, we cannot give an explicit asymptotic development for $\langle t_1 \rangle$. Therefore, in the rest of each chapter 3, 4, we use numerical computation to investigate the asymptotic behavior of the mean exit time. Even though our observations are conjectural, their validity is reinforced by the fact that they lead to the right asymptotics (Ref. [22, 20, 21]) in the limit $\epsilon \rightarrow 0$.

We also show the precise asymptotic development of the mean exit time for the case $\epsilon = 0$: in this case $\langle t_1 \rangle$ diverges as $\lambda \rightarrow \infty$ in 2-D case. The 3-D case is a different from the 2-D one in the sense that the exit time t_1 is infinite either from

the bulk or from the surface (while in 2-D, $t_1 < \infty$ a.s).

In Chapter 5, for the rectangle (Torus) case, we introduce a new geometry for the intermittent dynamics. The main interest in introducing this new model is that it introduces a new parameter, namely the modulus of the torus. Playing with this parameter allows us to address a question that was raised by Pierre Levitz: in most of the cases treated in [1] the value of the minimum $\langle t_1 \rangle_{\min}$ is not much smaller than $\langle t_1 \rangle(0)$ (the value of the mean exit time at $\lambda = 0$), at least not enough to be observed in an experiment, which would make it pointless to try to optimize $\langle t_1 \rangle$ in λ . However, in our setting, we find values of the modulus R for which $\langle t_1 \rangle_{\min} \leq 0.6 \langle t_1 \rangle(0)$, which is a ratio reachable by experiment.

Chapter 2

MATHEMATICAL BACKGROUND

In this chapter, we would like to present some mathematical facts that we use in this thesis.

2.1 Separable Hilbert Space

In this thesis, we approach the problem of searching time by introducing compact, self-adjoint operators, which have an orthonormal basis of eigenvectors that we put to use for our purposes. Therefore, in this section, we first would like to recall some properties of separable Hilbert space.

In this thesis we will consider several (real) Hilbert spaces, all of which being separable.

Every separable Hilbert space is unitarily equivalent to $\ell^2(\mathbb{N})$.

Therefore all separable Hilbert spaces have an orthonormal basis, i.e. an orthonormal family $(e_n)_{n \geq 0}$ such that $Vect(\{e_n\}_{n \geq 0})$ is dense in H .

In such a basis we have

$$f = \sum_{n=0}^{\infty} \langle f, e_n \rangle e_n, \quad (2.1.1)$$

this equality being seen as a limit in H of partial sums. Moreover, we have Parseval's formula

$$\|f\|^2 = \sum_{n=0}^{\infty} |\langle f, e_n \rangle|^2, \quad (2.1.2)$$

and $\langle f, g \rangle = \sum_{n=0}^{\infty} \langle f, e_n \rangle \langle g, e_n \rangle$. In the case when $H = L^2([-\pi, \pi])$ and $e_n := t \mapsto e^{int}$, Eq. (2.1.1) called the Fourier representation or Fourier series of f and $\langle f, e_n \rangle$ called Fourier coefficients of f .

Examples that we will use

Example 2.1.1 (Even Fourier series). In chapter 3 and chapter 5, at first our original system of equations is stated on $L^2([-\pi, \pi])$ space. However, by the symmetry of the problem, we consider the space of even functions in $L^2([-\pi, \pi])$ or equivalently the space $L^2([0, \pi])$, which is a separable Hilbert space.

In the language of Hilbert spaces, the set of functions $\{e_n, n \geq 0\}$, where $e_0 = \frac{1}{\sqrt{\pi}}$, $e_n = \sqrt{\frac{2}{\pi}} \cos n\theta, n \geq 1$, is an orthonormal basis for the space of $L^2([0, \pi])$ of square-integrable functions of $[-\pi, \pi]$. Indeed, this space is actually a separable Hilbert space with an inner product given for any two elements f and g by:

$$\langle f, g \rangle = \int_0^\pi f(x)g(x)dx.$$

For $m, n \geq 1$, we have that

$$\begin{aligned} \langle e_n, e_m \rangle &= \int_0^\pi \sqrt{\frac{2}{\pi}} \cos n\theta \sqrt{\frac{2}{\pi}} \cos m\theta d\theta \\ &= \begin{cases} \frac{2}{\pi} \int_0^\pi \frac{1}{2} [\cos(n+m)\theta + \cos(n-m)\theta] d\theta & \text{if } m \neq n \\ \frac{2}{\pi} \int_0^\pi (2 \cos 2n\theta + 1) d\theta & \text{if } m = n \end{cases} \\ &= \begin{cases} \frac{1}{\pi} \left[\frac{\sin(m+n)\theta}{m+n} + \frac{\sin(n-m)\theta}{n-m} \right] \Big|_0^\pi & \text{if } m \neq n \\ \frac{1}{\pi} \left(\frac{\sin 2n\theta}{2n} + \theta \right) \Big|_0^\pi & \text{if } m = n \end{cases} \\ &= \begin{cases} 0 & \text{if } m \neq n \\ 1 & \text{if } m = n \end{cases} \end{aligned}$$

If $n = 0$, then

$$\begin{aligned} \langle e_0, e_m \rangle &= \begin{cases} \int_0^\pi \frac{1}{\sqrt{\pi}} \sqrt{\frac{2}{\pi}} \cos m\theta d\theta & \text{if } m \neq 0 \\ \int_0^\pi \frac{1}{\sqrt{\pi}} \frac{1}{\sqrt{\pi}} d\theta & \text{if } m = 0 \end{cases} \\ &= \begin{cases} \frac{\sqrt{2}}{\pi} \frac{\sin m\theta}{m} \Big|_0^\pi & \text{if } m \neq 0 \\ \frac{1}{\pi} \theta \Big|_0^\pi & \text{if } m = 0 \end{cases} \\ &= \begin{cases} 0 & \text{if } m \neq 0 \\ 1 & \text{if } m = 0 \end{cases}. \end{aligned}$$

This proves that $(e_n)_{n \geq 0}$ is an orthonormal system. It remains that this system generates a dense subspace of $L^2([0, \pi])$. To prove that we consider a function f in $L^2([0, \pi])$ and extend to $[-\pi, \pi]$ as an even function \tilde{f} . We know that \tilde{f} is the limit in L^2 of its Fourier series, which is a cosine series.

A Fourier representation for a function f in this $L^2([0, \pi])$ is written as

$$f = \sum_{n=0}^{\infty} \langle f, e_n \rangle e_n = \sum_{n=0}^{\infty} a_n \cos nx.$$

where

$$a_0 = \frac{1}{\pi} \langle f, 1 \rangle = \frac{1}{\pi} \int_0^\pi f(x) dx,$$

$$a_n = \frac{2}{\pi} \langle f, \cos nx \rangle = \frac{2}{\pi} \int_0^\pi f(x) \cos nx dx.$$

Example 2.1.2 (Legendre polynomials). In chapter 4, we consider the following Laplace operators:

$$\left\{ \begin{array}{l} \Delta f(r, x) = \frac{1}{r^2} \frac{d}{dr} \left(r^2 \frac{df}{dr} \right) + \frac{1}{r^2} \Delta_\partial f(x), \end{array} \right. \quad (2.1.3)$$

$$\left\{ \begin{array}{l} \Delta_\partial f(x) = \frac{d}{dx} \left((1-x^2) \frac{df}{dx} \right), \end{array} \right. \quad (2.1.4)$$

with $r \in [0, 1]$, $x \in [-1, 1]$ (see Eqs. (4.1.5), (4.1.6)).

In order to solve these Laplacians, we have to look for homogeneous harmonic functions

$$f(r, \theta) = r^n g(\theta), \quad (2.1.5)$$

that is, solutions of Laplace equation $\Delta f = 0$.

We get

$$\Delta f = \frac{1}{r^2} \frac{d}{dr} \left(r^2 \frac{d(r^n g)}{dr} \right) + \frac{1}{r^2} (r^n g) \quad (2.1.6)$$

$$\begin{aligned} &= \frac{1}{r^2} \frac{d}{dr} (nr^{n+1} g) + r^{n-2} \Delta_\partial g \\ &= r^{n-2} (n(n+1)g + \Delta_\partial g). \end{aligned} \quad (2.1.7)$$

Consequently, $\Delta f = 0$ iff $\Delta_\partial g = -n(n+1)g$, that is g is an eigenfunction of Δ_∂ for the eigenvalue $-n(n+1)$.

The above equation $\Delta_\partial g = -n(n+1)g$ is defined on $L^2([-1, 1], dx)$, is equivalent to

$$(1-t^2)y'' - 2ty' + n(n+1)y = 0, \quad (2.1.8)$$

which called the general Legendre equation (Adrien-Marie Legendre, 1752-1833). The Legendre equation has regular singular points at -1 , 1 and ∞ . Since the Legendre equation is a second-order ordinary differential equation, it has two linearly independent solutions. A solution $P_n(t)$ which is regular at finite points called Legendre function of the first kind, while a solution $Q_n(t)$ which is singular at ± 1 is called a Legendre function of the second kind. If n is an integer, the function of the first kind reduces to a polynomial known as Legendre polynomial.

The Legendre polynomials can be defined in various way. One definition is in terms of Rodrigues' formula:

$$P_n(t) = \frac{1}{2^n n!} \frac{d^n}{dt^n} (t^2 - 1)^n. \quad (2.1.9)$$

In this version of Legendre polynomials they are normalized so that $P_n(1) = 1$. There is also the following recurrence relation:

$$\begin{aligned} P_0 &= 1 \\ P_1 &= t \\ (n+1)P_{n+1} &= (2n+1)tP_n - nP_{n-1}. \end{aligned}$$

In addition, the set of $\left\{ e_n \mid e_n(x) = \sqrt{\frac{2n+1}{2}} P_n(x), n \geq 0 \right\}$, where P_n are Legendre polynomials, is an orthonormal basis for the space $L^2([-1, 1], dx)$ of square-integrable functions on $[-1, 1]$. This space is a separable Hilbert space with an inner product given for two elements f, g by:

$$\langle f, g \rangle = \int_{-1}^1 f(x)g(x)dx.$$

A Fourier representation for a function f in this $L^2([-1, 1])$ is written as

$$f = \sum_{n=0}^{\infty} \langle f, e_n \rangle e_n = \sum_{n=0}^{\infty} a_n P_n(x),$$

where $a_n = \frac{2n+1}{2} \langle f, P_n(x) \rangle$.

2.1.1 Poisson summation formula

Proposition 2.1.1 (Poisson summation formula). *Let f be a continuous function in $L^1(\mathbb{R})$, and φ be defined by*

$$\varphi(t) = \frac{1}{2\pi} \int_{-\infty}^{+\infty} f(x)e^{-itx} dx, \quad (2.1.10)$$

If f satisfies these two conditions

- (i) $F(x) = \sum_{k=-\infty}^{+\infty} f(x + k2\pi\alpha)$ converges normally on $[-\pi, \pi]$.
- (ii) $\sum_{n=-\infty}^{+\infty} |\varphi(n/\alpha)| < \infty$,

then the function F is periodic with period $2\pi\alpha$, $\hat{F}(n) = \frac{1}{\alpha}\varphi(n/\alpha)$ and the Fourier series of F converges normally to F on $[-\pi\alpha, \pi\alpha]$. Hence, $F(x) = \sum_{n \in \mathbb{Z}} \frac{1}{\alpha}\varphi(n/\alpha)e^{inx/\alpha}$. In particular,

$$\sum_{k=-\infty}^{+\infty} f(k2\pi\alpha) = \sum_{n=-\infty}^{+\infty} \frac{1}{\alpha}\varphi(n/\alpha). \quad (2.1.11)$$

2.1. SEPARABLE HILBERT SPACE

Proof. We can easily observe that F is $2\pi\alpha$ -periodic. Considering the Fourier series representation of F , we get

$$F(x) = \sum_{n=-\infty}^{+\infty} \hat{F}(n) e^{\frac{inx}{\alpha}},$$

where

$$\hat{F}(n) = \frac{1}{2\pi\alpha} \int_{-\pi\alpha}^{\pi\alpha} F(x) e^{-inx/\alpha} dx \quad (2.1.12)$$

$$= \frac{1}{2\pi\alpha} \int_{-\pi\alpha}^{\pi\alpha} \sum_{k=-\infty}^{+\infty} f(x + k2\pi\alpha) e^{-inx/\alpha} dx. \quad (2.1.13)$$

Since $\sum_{k=-\infty}^{+\infty} f(x + 2k\pi\alpha)$ converges normally on $[-\pi\alpha, \pi\alpha]$, we can rearrange the sum and the integral of (2.1.12) and obtain

$$\begin{aligned} \hat{F}(n) &= \frac{1}{2\pi\alpha} \sum_{k=-\infty}^{+\infty} \int_{-\pi\alpha}^{\pi\alpha} f(x + 2k\pi\alpha) e^{-inx/\alpha} dx \\ &= \frac{1}{2\pi\alpha} \sum_{k=-\infty}^{+\infty} \int_{(2k-1)\pi\alpha}^{(2k+1)\pi\alpha} f(t) e^{-int/\alpha} dt \\ &= \frac{1}{2\pi\alpha} \int_{-\infty}^{+\infty} f(t) e^{-int/\alpha} dt \\ &= \frac{1}{\alpha} \varphi(n/\alpha). \end{aligned}$$

By the condition (ii) that $\sum_{n=-\infty}^{+\infty} |\varphi(n/\alpha)| < \infty$, we have $\sum_{n=-\infty}^{+\infty} \frac{1}{\alpha} \varphi(n/\alpha) e^{inx/\alpha}$ converges normally on \mathbb{R} towards a continuous function G and moreover $\hat{G}(n) = \frac{1}{\alpha} \varphi(n/\alpha) = \hat{F}(n)$, which implies that $G = F$. Therefore, by definition of the Fourier series of f , we have

$$F(x) = \sum_{n=-\infty}^{+\infty} \hat{F}(n) e^{\frac{inx}{\alpha}} = \sum_{n=-\infty}^{+\infty} \frac{1}{\alpha} \varphi(n/\alpha) e^{\frac{inx}{\alpha}}.$$

Choosing $x = 0$, we get

$$\sum_{k=-\infty}^{+\infty} f(2k\pi\alpha) = \sum_{n=-\infty}^{+\infty} \frac{1}{\alpha} \varphi\left(\frac{n}{\alpha}\right).$$

□

Take $f(x) = e^{-|x|}$, we will derive the identity

$$\frac{e^{2\pi\alpha} + 1}{e^{2\pi\alpha} - 1} = \frac{1}{\pi} \sum_{n=-\infty}^{\infty} \frac{\alpha}{n^2 + \alpha^2}. \quad (2.1.14)$$

2.1. SEPARABLE HILBERT SPACE

Indeed, we have that

$$\begin{aligned} \sup_{[-\pi\alpha, \pi\alpha]} |f(x + 2k\pi\alpha)| &= \sup_{[-\pi\alpha, \pi\alpha]} e^{-|x+2k\pi\alpha|} \\ &= \begin{cases} e^{-(2k-1)\pi\alpha}, & k \in \mathbb{Z}^+ \\ e^{(2k+1)\pi\alpha}, & k \in \mathbb{Z}^- \end{cases} \end{aligned}$$

We hence obtain that $\sum_{k \in \mathbb{Z}} \sup_{[-\pi\alpha, \pi\alpha]} |f(x + 2k\pi\alpha)| < \infty$ or $F(x) = \sum_{k \in \mathbb{Z}} |f(x + 2k\pi\alpha)|$ normally converges on $[-\pi, \pi]$.

We next consider

$$\begin{aligned} \varphi(t) &= \frac{1}{2\pi} \int_{-\infty}^{\infty} f(x) e^{-itx} dx \\ &= \frac{1}{2\pi} \int_{-\infty}^{\infty} e^{-|x|} e^{-itx} dx \\ &= \frac{1}{2\pi} \left(\int_{-\infty}^0 e^{x(1-it)} dx + \int_0^{\infty} e^{-x(1+it)} dx \right) \\ &= \frac{1}{2\pi} \left(\frac{1}{1-it} + \frac{1}{1+it} \right) \\ &= \frac{1}{\pi} \frac{1}{1+t^2}. \end{aligned}$$

We can observe that $\sum_{n=-\infty}^{\infty} |\varphi(n/\alpha)| < \infty$. Therefore, f satisfies two conditions of Proposition 2.1.1. By applying formula (2.1.11) for f , we get

$$\begin{aligned} \sum_{k=-\infty}^{+\infty} e^{-|2k\pi\alpha|} &= \sum_{n=-\infty}^{\infty} \frac{1}{\alpha} \frac{1}{\pi} \frac{1}{1 + \left(\frac{n}{\alpha}\right)^2} dx \\ &= \frac{1}{\pi} \sum_{n=-\infty}^{\infty} \frac{\alpha}{\alpha^2 + n^2} dx. \end{aligned} \tag{2.1.15}$$

Use the Taylor expansion $\frac{1}{1-x} = \sum_{n=0}^{\infty} x^n$, ($|x| < 1$), for the left-hand side of (2.1.15), we obtain

$$\begin{aligned} \sum_{k=-\infty}^{\infty} e^{-|2k\pi\alpha|} &= 2 \sum_{k=0}^{\infty} e^{-2k\pi\alpha} - 1 \\ &= \frac{2}{1 - e^{-2\pi\alpha}} - 1 \\ &= \frac{1 + e^{-2\pi\alpha}}{1 - e^{-2\pi\alpha}} \\ &= \frac{e^{2\pi\alpha} + 1}{e^{2\pi\alpha} - 1}. \end{aligned} \tag{2.1.16}$$

From Eqs. (2.1.15), (2.1.16), we obtain Eq. (2.1.14).

2.2 Operator theory

One of the main tools of this thesis is the use of spectral theorem for self-adjoint compact operators. We describe now this theory:

2.2.1 Compact operator

Definition 2.2.1 (Compact operator). Let E, F be two normed (real or complex) spaces; we say that a linear mapping u of E into F is compact iff for any bounded subset B of E , $u(B)$ is relatively compact in F . An equivalent condition is that for any bounded sequence (x_n) in E , there is a subsequence (x_{n_k}) such that the sequence $(u(x_{n_k}))$ converges in F .

Theorem 2.2.2. *The compact operator are a norm-closed, two-side, *-ideal in $\mathcal{L}(H)$. That is:*

1. *If $\{T_n\}$ is a sequence of compact operator and $T_n \rightarrow T$ in $\mathcal{L}(H)$, then T is compact.*
2. *If S is compact and T is bounded, then ST and TS are compact.*
3. *T is compact iff T^* is compact.*

2.2.2 Self-adjoint operator

Definition 2.2.3 (Adjoint operator). Let H be a Hilbert space and $u : E \rightarrow E$ a bounded operator, the adjoint u^* is defined by

$$\forall f, g \in H, \langle u(f), g \rangle = \langle f, u^*(g) \rangle$$

The adjoint u^* is unique and $(u^*)^* = u$.

If u is continuous, then u^* is continuous and $\|u^*\| = \|u\|$ in $\mathcal{L}(E)$.

Definition 2.2.4 (Self-adjoint operator). An operator u in a Hilbert space E is called self-adjoint (or hermitian) if $u^* = u$; the mapping $\langle x, y \rangle \rightarrow \langle u(x), y \rangle = \langle u(y), x \rangle$ is then a hermitian form on E . The self-adjoint operator u is called positive if the corresponding hermitian form is positive; one writes then $u \geq 0$.

2.2.3 Spectral theorem

Theorem 2.2.5 (Spectral theorem for compact self-adjoint operator). *Suppose T is a compact, self-adjoint operator on a Hilbert space E . There exists an orthonormal basis of E consisting of eigenvectors of T .*

The eigenvalues form a sequence converging to 0 and the eigenspaces associated to non-zero eigenvalues are finite dimensional.

2.2.4 Sturm-Liouville theory

We recall here the definitions of the Sobolev space H^1 and H_0^1 (Ref. [6])

Definition 2.2.6 (Sobolev space). Let $\Omega \subset \mathbb{R}^N$ be an open set and let $p \in \mathbb{R}$ with $1 \leq p \leq \infty$.

The Sobolev space $H^1(\Omega)$ defined by

$$H^1 = \{u \in L^2(\Omega) \mid \exists g_1, g_2, \dots, g_N \in L^2(\Omega) \text{ such that} \\ \int_{\Omega} u \frac{\partial \varphi}{\partial x_i} = - \int_{\Omega} g_i \varphi, \forall \varphi \in C_C^\infty(\Omega), i = \overline{1, N}\}$$

The space $H^1(\Omega)$ is a separable Hilbert space, equipped with the scalar product

$$\langle u, v \rangle_{H^1} = \langle u, v \rangle_{L^2} + \sum_{i=1}^N \left(\frac{\partial u}{\partial x_i}, \frac{\partial v}{\partial x_i} \right)_{L^2} = \int_{\Omega} uv + \sum_{i=1}^N \frac{\partial u}{\partial x_i} \frac{\partial v}{\partial x_i}.$$

The associated norm is

$$\|u\|_{H^1} = \left(\|u\|_2^2 + \sum_{i=1}^N \left\| \frac{\partial u}{\partial x_i} \right\|_2^2 \right)^{1/2}$$

$H_0^1(\Omega)$ denotes the closure of $C_C^1(\Omega)$ in $H^1(\Omega)$. The space H_0^1 , equipped with the H^1 scalar product, is a Hilbert space.

Theorem 2.2.7. *If $I = [a, b]$ is an interval on \mathbb{R} , $p \in C^1(I)$ is a function $\geq \alpha > 0$ on I , and $q \in C(I)$ is a real function. Then there exists a Hilbert basis (e_n) of $L^2(I)$ and a real sequence $\lambda_n \rightarrow +\infty$ such that $e_n \in C^2(I)$, $e_n(a) = e_n(b) = 0$ and*

$$-(pe_n')' + qe_n = \lambda_n e_n \tag{2.2.1}$$

on I .

Proposition 2.2.8. *For all $f \in L^2(I)$, there exists a unique function $u \in H^2(I) \cap H_0^1(I)$ such that*

$$-(pu')' + qu = f. \tag{2.2.2}$$

Let us define operator T on $L^2(I)$ such that $T(f) = u$.

Theorem 2.2.9. *The operator T is a compact, self-adjoint and positive.*

We have that $\ker T = 0$ and by the spectral theorem for the compact, self-adjoint operator, there exists a Hilbert basis of the eigenvectors of T and the associated eigenvalues form a real positive sequence $\mu_n = 1/\lambda_n$ which converge to 0.

2.3 Discrete model for equations

This section gives an explanation for the original equations (Eqs. (3.2.1), (3.2.2) in 2-D case or Eqs. (5.1.1), (5.1.2) in the rectangle case) that we use for our problems.

2.3.1 Mean first-passage time for bulk diffusion

Let us consider a symmetric domain D with the boundary ∂D . A particle starts at position z and moves inside the bulk (inside the domain) with a 2-D Brownian motion.

We aim to establish the equation of the time $t_2(z)$ for the particle starts at position $z = (x, y)$ inside the boundary to reach the target on the boundary. Let $\delta\theta$ be a step of motion and δt be the time increment between successive steps. The quantity $t_2(z)$ is the time for each path times the probability of the path, averaged over all particle trajectories:

$$\begin{aligned} t_2(z) &= \sum_k \mathcal{P}_k(z) (t_2)_k(z) \\ &= \sum_{i=1}^4 \frac{1}{4} (t_2(z_i) + \delta t) \\ &= \frac{1}{4} [t_2(x - \delta\theta, y) + t_2(x + \delta\theta, y) + t_2(x, y - \delta\theta) + t_2(x, y + \delta\theta)] + \delta t \end{aligned} \quad (2.3.1)$$

Eq. (2.3.1) implies

$$\frac{(\delta\theta)^2}{4\delta t} \Delta t_2 = -1, \quad (2.3.2)$$

where

$$\Delta t_2(x, y) = \frac{t_2(x - \delta\theta, y) + t_2(x + \delta\theta, y) + t_2(x, y - \delta\theta) + t_2(x, y + \delta\theta) - 4t_2(x, y)}{(\delta\theta)^2} \quad (2.3.3)$$

We assume that $\frac{(\delta\theta)^2}{4\delta t} = D_2$ for some positive constant D_2 (the diffusion coefficient of the Brownian motion in 2-D), then we get

$$D_2 \Delta t_2 = -1. \quad (2.3.4)$$

2.3.2 Mean first-passage time for surface diffusion

Here we consider a particle starts at position θ on the boundary ∂D of the symmetric domain D . In order to establish the equation for the diffusion on a 1-D

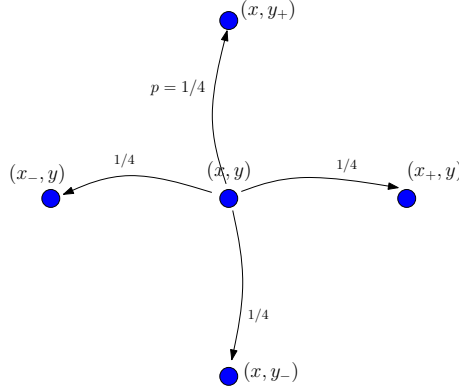


Figure 2.1: Discrete model of 2-D motion

symmetric boundary, we denote by $\delta\theta$ a step of motion and δt the time increment between successive steps. Let $t_1(\theta)$ be the mean time to reach the target when a particle starts at position θ on the boundary. We also let p be the probability for the Brownian motion to leave the boundary at position θ (on the boundary). In this model, we assume that $p = \lambda\delta t$, where λ is a positive constant.

The quantity t_1 is the time for each path times the transition probability of the path, average over all particle trajectories:

$$\begin{aligned} t_1(\theta) &= \frac{1-p}{2} [t_1(\theta - \delta\theta) + \delta t] + \frac{1-p}{2} [t_1(\theta + \delta\theta) + \delta t] + p [t_2(r_0, \theta)] \\ &= \frac{1-p}{2} t_1(\theta - \delta\theta) + \frac{1-p}{2} t_1(\theta + \delta\theta) + p t_2(r_0, \theta) + (1-p)\delta t, \end{aligned} \quad (2.3.5)$$

where (r_0, θ) the position inside the bulk.

From (2.3.5), one gets

$$\frac{(\delta\theta)^2}{2\delta t} \left[\frac{t_1(\theta + \delta\theta) + t_1(\theta - \delta\theta) - 2t_1(\theta)}{(\delta\theta)^2} \right] + \frac{1}{\delta t} \frac{p}{1-p} [t_2(r_0, \theta) - t_1(\theta)] = -1, \quad (2.3.6)$$

We assume that $\frac{(\delta\theta)^2}{2\delta t} = D_1$ for some positive constant D_1 (the diffusion coefficient of the Brownian motion).

Let $\delta t \rightarrow 0$, $\delta\theta \rightarrow 0$ and recall that $p = \lambda\delta t$, then we get the equation for the diffusion on the symmetric boundary:

$$D_1 t_1''(\theta) + \lambda [t_2(r_0, \theta) - t_1(\theta)] = -1. \quad (2.3.7)$$

Furthermore, we can show that the time that the particle remains on the boundary follows an exponential law with parameter λ .

Let us denote by X the index of the first step that the particle moves inside the bulk and Y the time that the particle remains on the boundary. Then we have

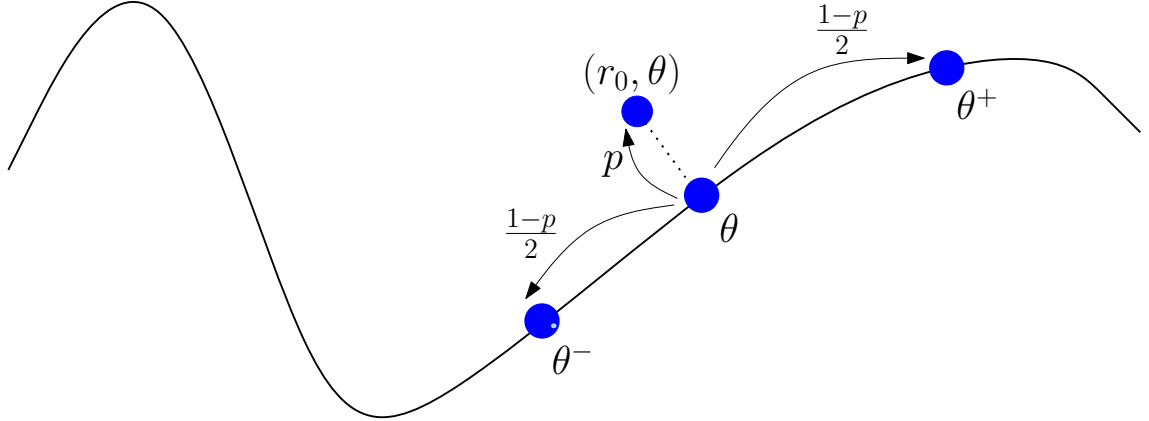


Figure 2.2: The movement of the particle on the boundary

$Y = (X - 1)\delta t$. We compute the probability of $\{X = n\}$, which means the event of the particle leave the boundary at n^{th} step

$$\mathbb{P}(X = n) = \mathbb{P}(X_1 = 1, \dots, X_{n-1} = 1, X_n = 0) = (1 - p)^{n-1}p, \quad (2.3.8)$$

where $\{X_i = 1\}$ (resp. $\{X_i = 0\}$) is the event that the particle stays on the boundary (resp. leaves the boundary) at step i .

Then we can compute the density function for Y

$$\begin{aligned} \mathbb{P}(Y = T) &= \mathbb{P}((X - 1)\delta t = T) = \mathbb{P}\left(X = \frac{T}{\delta t} + 1\right) \\ &= (1 - p)^{\frac{T}{\delta t}} p. \end{aligned} \quad (2.3.9)$$

We recall that $p = \lambda\delta t$, then

$$\mathbb{P}(Y = T) = (1 - \lambda\delta t)^{\frac{T}{\delta t}} \lambda\delta t \quad (2.3.10)$$

$$= e^{-\lambda T} \lambda\delta t, \quad (2.3.11)$$

since $\lim_{n \rightarrow \infty} \left(1 + \frac{\lambda}{n}\right)^n = e^\lambda$.

Hence, Y is a random variable has exponential distribution with rate parameter λ .

Chapter 3

2D-CASE

In this chapter, we solve the problem for the simplest model of the disk (Fig. 3.1). We start from the original system of equations for the exit time that has been introduced in Ref. [2] by using integral equations. However, our approach is different. We introduce two self-adjoint operators: a smoothing convolution operator V and a Sturm-Liouville operator \tilde{T} . Then we consider the self-adjoint operator $V\tilde{T}V$ for which we use an orthonormal basis of eigenvectors. This consideration allows us to obtain the spectral representation of $\langle t_1 \rangle$ and this is particularly appropriate to investigate the asymptotic behavior in the limit of large desorption rate λ .

We first consider $\langle t_1 \rangle$ for the case of point-like target (i.e. $\epsilon = 0$). In this case, we obtain a much more precise asymptotic development. We are able to derive an exact asymptotic of the behavior for $\langle t_1 \rangle_{\epsilon=0} = A_1\sqrt{\lambda} + A_2 + \frac{A_3}{\sqrt{\lambda}} + O\left(\frac{1}{\lambda}\right)$, where A_i are constants, by Theorem 3.2.1. Consequently, $\langle t_1 \rangle$ goes to infinity as $\lambda \rightarrow \infty$. In addition, we prove that $\frac{d\langle t_1 \rangle_{\epsilon=0}}{d\lambda} > 0$ at large λ . Therefore, there exists a minimum of $\langle t_1 \rangle_{\epsilon=0}$ at $\lambda > 0$ if $\left. \frac{d\langle t_1 \rangle_{\epsilon=0}}{d\lambda} \right|_{\lambda=0} < 0$. This property gives a method to determine the critical ratio for $\frac{D_2}{D_1}$ under which $\langle t_1 \rangle_{\epsilon=0}$ has a minimum at some positive λ . The critical ratio has already been studied in [2] but our conclusion is more rigorous.

In the next part, we study the case of extended target (i.e. $\epsilon > 0$). In previous research (Ref. [2]), the authors show the exact expression for the mean exit time and propose a method to approximate $\langle t_1 \rangle$, but they do not study its asymptotic behavior. In this work, although we cannot rigorously derive such a precise asymptotic development, we are able to prove that $\langle t_1 \rangle_{\epsilon>0}$ converges to a finite limit \mathcal{T} as $\lambda \rightarrow \infty$ (Theorem 3.2.3) and that $\langle t_1 \rangle_{\epsilon>0}$ increases at large λ (Theorem 3.2.4), thus providing a rigorous proof of the existence of the minimum of $\langle t_1 \rangle_{\epsilon>0}$ attained for some positive λ if $\left. \frac{d\langle t_1 \rangle_{\epsilon>0}}{d\lambda} \right|_{\lambda=0} < 0$. Therefore, the intermittent strategy is justified in this case. Moreover, this study shows that pure bulk dynamics is never optimal.

Although the consideration of the spectral representation of $\langle t_1 \rangle$ shows that

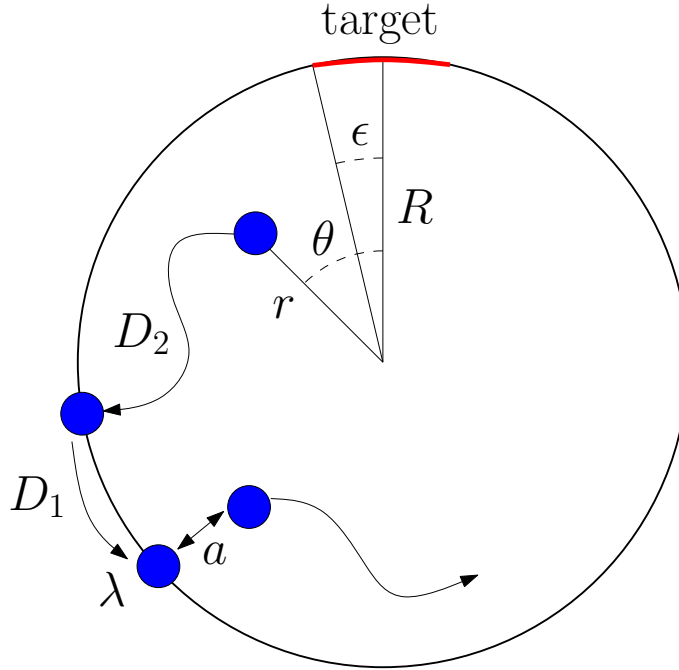


Figure 3.1: Surface-mediated diffusion in 2-D case

$\langle t_1 \rangle_{\epsilon > 0}$ is eventually increasing to a finite limit, we cannot rigorously derive a precise asymptotic development. We would obtain such a development if we knew the asymptotics for the eigenvalues λ_n and the spectral weight ψ_n . If we have proved rigorously that $\lambda_n \sim \frac{1}{n^2}$ (see Appendix A), the rest of the chapter consists in a numerical treatment giving evidence to the prediction $\psi_n \sim \frac{1}{n^3}$, and thus that $\langle t_1 \rangle_{\epsilon > 0} = \mathcal{T} - \frac{C_1}{\sqrt{\lambda}} + O\left(\frac{1}{\lambda}\right)$ with $C_1 > 0$. In addition, these considerations allow us to understand the transition between the $\epsilon > 0$ case and the pure point target one namely that $\langle t_1 \rangle \sim \ln \frac{1}{\epsilon}$ as $\epsilon \rightarrow 0$.

3.1 Introduction

Many transport and search processes exhibit intermittent character when different modes of motion are alternated. Typical examples are animals foraging (with phases of rapid relocation and slow exploration), facilitated search mechanism on DNA (with phases of pure bulk diffusion and chain sliding), vesicle transportation in living cells (with phases of active transport by motor proteins and passive diffusion in the cytoplasm), water transport in confining media (with phases of pure bulk diffusion and surface exploration) [4, 5]. The intermittence is often expected to facilitate transport and search processes, e.g., by reducing the mean search time necessary to reach a target (food, specific DNA sequence, nucleus, or reaction zone in the above examples). In particular, the mean exit time from a bounded domain

through an opening (a target) on the boundary has been actively studied during the last decade [11, 10]. For pure bulk diffusion, Singer *et al.* derived the asymptotic behavior of the mean exit time in the narrow escape limit (when the size of the target is small) [22, 20, 21, 19, 12]. Isaacson and Newby developed uniform in time asymptotic expansions in the target radius of the first passage time density for the diffusing molecule to find the target [9]. The escape problem for an intermittent process with phases of surface and pure bulk diffusion (the so-called surface-mediated diffusion) has been recently solved for rotation-invariant domains [1, 2]. The known eigenbasis for the Laplace operators governing pure bulk and surface diffusions allowed one to express the mean exit time in a closed matrix form. Under well-defined conditions, the mean exit time was shown to be minimized at an optimal desorption rate that characterizes switching from surface to pure bulk diffusion. These results have been extended in various directions [17, 18, 7, 8]. An alternative master equation approach for discrete (on-lattice) surface-mediated diffusion (also called the bulk-mediated surface diffusion) has been proposed [13, 16, 14, 15].

In the work, we propose a rigorous spectral analysis of the above escape problem. We focus on surface-mediated diffusion in the unit disk and derive a spectral representation of the mean exit time. This representation is well suited to investigate the asymptotic behavior of the mean exit time in the limit of large desorption rate λ . For a point-like target, we show that the mean exit time diverges as $\sqrt{\lambda}$. For extended targets, we establish the asymptotic approach to a finite limit. In both cases, the mean exit time is shown to asymptotically increase as λ tends to infinity. We also revise the optimality regime of surface-mediated diffusion. Although the presentation is limited to the unit disk, the spectral approach can be extended to other domains such as rectangles or spheres.

3.2 A self-adjoint operator formulation

We study the following model of surface-mediated diffusion in the unit disk $\mathbb{D} = \{z \in \mathbb{C} : |z| < 1\}$ whose boundary $\partial\mathbb{D}$ includes an exit (or a target) of angular size 2ϵ (i.e., an arc of the unit circle between $\pi - \epsilon$ and $\pi + \epsilon$), with $0 \leq \epsilon \leq \pi$. A starting point $e^{i\theta}$ is taken on the unit circle. If the starting point is located on the target then the process is immediately stopped. Otherwise, the particle moves along the circle according to a Brownian motion with the diffusion coefficient D_1 for a duration of $\min\{\tau_\lambda, \tau\}$, where τ_λ is a random variable with exponential law of parameter $\lambda \geq 0$, and τ is the first hitting time of the target. If $\tau \leq \tau_\lambda$ then the process stops. If $\tau > \tau_\lambda$ then the particle is relocated at time τ_λ along the normal inside the disk at a distance $0 < a \leq 1$ to start there a 2D Brownian motion with the diffusion coefficient D_2 . This motion is stopped after hitting back the unit circle, and the same procedure is restarted from this last hitting point. We define $t_1(\theta)$ as being the expected time to reach the target. Similarly, for $0 \leq r < 1$, we define $t_2(re^{i\theta})$ as being the expected time to reach the target starting from the point $re^{i\theta}$

inside the unit disk.

It has been shown in [2] that these two functions satisfy the following system of equations:

$$\begin{cases} D_1 \Delta_{S^1} t_1(\theta) + \lambda [t_2((1-a)e^{i\theta}) - t_1(\theta)] = -1 & (3.2.1) \\ D_2 \Delta t_2 = -1 & (3.2.2) \\ t_2(e^{i\theta}) = t_1(\theta) \quad (\theta \in [-\pi, \pi]) & (3.2.3) \\ t_1(\theta) = 0 \text{ if } \theta \in [-\pi, -\pi + \epsilon] \cup [\pi - \epsilon, \pi] & (3.2.4) \end{cases}$$

where

$$\Delta = \frac{\partial^2}{\partial r^2} + \frac{1}{r} \frac{\partial}{\partial r} + \frac{1}{r^2} \Delta_{S^1} \quad (3.2.5)$$

is Laplace operator in polar coordinates in \mathbb{R}^2 , and

$$\Delta_{S^1} = \frac{\partial^2}{\partial \theta^2} \quad (3.2.6)$$

is the Laplace operator on the boundary S^1 .

Let us notice that, by symmetry, $t_1(\theta)$ is an even function so it is sufficient to determine it on $L^2([0, \pi])$.

The solution to Eq. (3.2.2) is the sum of the particular solution $\frac{1-r^2}{4D_2}$ to the inhomogeneous (Poisson) equation $\Delta u = -\frac{1}{D_2}$, $u|_{\partial\mathbb{D}} = 0$, and the solution to the Dirichlet problem $\Delta v = 0$, $v|_{\partial\mathbb{D}} = t_1$.

Since t_1 is even it may be represented as a cosine series

$$t_1(\theta) = \sum_{n \geq 0} a_n \cos n\theta,$$

from which

$$t_2(re^{i\theta}) = \frac{1-r^2}{4D_2} + \sum_{n \geq 0} a_n r^n \cos n\theta.$$

Eq. (3.2.1) then becomes

$$t_1''(\theta) = -\frac{1}{D_1} \left(1 + \lambda \frac{1 - (1-a)^2}{4D_2} \right) + \frac{\lambda}{D_1} U(t_1)(\theta), \quad (3.2.7)$$

where U is the operator on $L^2([0, \pi])$ defined by

$$U \left(\sum_{n \geq 0} x_n \cos n\theta \right) = \sum_{n \geq 1} x_n (1 - (1-a)^n) \cos n\theta.$$

This operator can also be written as $U = V^2$, where

$$V \left(\sum_{n \geq 0} x_n \cos n\theta \right) = \sum_{n \geq 1} x_n \sqrt{1 - (1-a)^n} \cos n\theta. \quad (3.2.8)$$

3.2. A SELF-ADJOINT OPERATOR FORMULATION

Next we introduce the Sturm-Liouville operator T defined on $L^2([0, \pi - \epsilon])$ as $Tf = u$, where

$$\begin{cases} u'' = f \\ u'(0) = u(\pi - \epsilon) = 0. \end{cases} \quad (3.2.9)$$

The operator T is negative self-adjoint. Finally, we define $\tilde{T} = -\mathcal{E}T\mathcal{R}$ as an operator on $L^2([0, \pi])$, where $\mathcal{R} : L^2([0, \pi]) \rightarrow L^2([0, \pi - \epsilon])$ is the natural restriction, and $\mathcal{E} : L^2([0, \pi - \epsilon]) \rightarrow L^2([0, \pi])$ is the natural extension by 0. The operator \tilde{T} can be written explicitly as

$$\tilde{T}(f)(\theta) = \begin{cases} \int_{\theta}^{\pi - \epsilon} \left(\int_0^{\theta_1} f(\theta_2) d\theta_2 \right) d\theta_1, & 0 \leq \theta < \pi - \epsilon, \\ 0, & \pi - \epsilon \leq \theta \leq \pi. \end{cases} \quad (3.2.10)$$

One can easily check that the eigenbasis of this operator is

$$\nu_n = \frac{(1 - \epsilon/\pi)^2}{(n + 1/2)^2}, \quad u_n = \begin{cases} \sqrt{\frac{2}{\pi - \epsilon}} \cos\left(\frac{(n+1/2)\theta}{1 - \epsilon/\pi}\right), & 0 \leq \theta \leq \pi - \epsilon, \\ 0, & \pi - \epsilon \leq \theta \leq \pi. \end{cases} \quad (3.2.11)$$

These eigenvectors form an orthogonal basis of $L^2[0, \pi - \epsilon]$ by Sturm-Liouville theory.

Since T is negative, $-\mathcal{E}T\mathcal{R}$ is non-negative. Moreover, let us check that \tilde{T} is a self-adjoint operator on $L^2([0, \pi])$ since T is self-adjoint. Let f, g be in $L^2([0, \pi])$:

$$\begin{aligned} -\langle \tilde{T}f, \bar{g} \rangle &= \langle \mathcal{E}T\mathcal{R}f, \bar{g} \rangle = \int_0^{\pi - \epsilon} T(\mathcal{R}f) \bar{g} = \int_0^{\pi - \epsilon} T(\mathcal{R}f) \overline{\mathcal{R}g} \\ &= \int_0^{\pi - \epsilon} \mathcal{R}f \overline{T(\mathcal{R}g)} = \int_0^{\pi} f \overline{\mathcal{E}T\mathcal{R}(g)} = -\langle f, \overline{\tilde{T}g} \rangle, \end{aligned}$$

which proves the claim, since the operator $\mathcal{E}T\mathcal{R}$ is negative.

The operator \tilde{T} allows us to translate Eq. (3.2.7) into

$$t_1 = \frac{1}{D_1} \left(1 + \lambda \frac{1 - (1 - a)^2}{4D_2} \right) \tilde{T}(1) - \frac{\lambda}{D_1} \tilde{T}U(t_1). \quad (3.2.12)$$

From Eq. (3.2.12), which was actually stated in Ref. [2, 4], one can formally solve for t_1 in

$$t_1 = \frac{1}{D_1} \left(1 + \lambda \frac{1 - (1 - a)^2}{4D_2} \right) \left(I + \frac{\lambda}{D_1} \tilde{T}U \right)^{-1} (\tilde{T}(1)).$$

The problem is that $\tilde{T}U$ is not self-adjoint, as a consequence we would have a bad control of the resolvent $\left(I + \frac{\lambda}{D_1} \tilde{T}U \right)^{-1}$. The main idea to avoid this problem is to apply the operator V to both sides of Eq. (3.2.12) to get, writing $s_1 = V(t_1)$,

$$s_1 = \frac{1}{D_1} \left(1 + \lambda \frac{1 - (1 - a)^2}{4D_2} \right) V\tilde{T}(1) - \frac{\lambda}{D_1} V\tilde{T}V(s_1), \quad (3.2.13)$$

which can be solved in s_1 as

$$s_1 = \frac{1}{D_1} \left(1 + \lambda \frac{1 - (1-a)^2}{4D_2} \right) \left(I + \frac{\lambda}{D_1} V\tilde{T}V \right)^{-1} (\psi), \quad (3.2.14)$$

where $\psi = V\tilde{T}(1)$. This is an exact solution of the original problem for a fixed starting point. We emphasize that the operators V and \tilde{T} , as well as the function $\psi = V\tilde{T}(1)$, are given explicitly. At first thought, this representation looks similar to the mean exit time found in [2] (see also [17, 18]). Although both derivations are conceptually similar, the major advantage of the present approach is the use of the self-adjoint operator $V\tilde{T}V$. This feature allows one to invert the operator $(I + \frac{\lambda}{D_1} V\tilde{T}V)$ in Eq. (3.2.16) and to express the mean exit time in a spectral form (see below).

The case of a randomly distributed starting point on the circle with uniform law is of particular interest. This is equivalent to averaging the mean exit time over the starting points that we denote as

$$\langle t_1 \rangle = \frac{1}{\pi} \int_0^\pi d\theta t_1(\theta) = \frac{1}{\pi} \langle t_1, 1 \rangle.$$

Using Eqs. (3.2.12) and (3.2.14), we can write

$$\begin{aligned} \pi \langle t_1 \rangle &= \frac{1}{D_1} \left(1 + \lambda \frac{1 - (1-a)^2}{4D_2} \right) \langle \tilde{T}(1), 1 \rangle - \frac{\lambda}{D_1} \langle \tilde{T}V(s_1), 1 \rangle \\ &= \frac{1}{D_1} \left(1 + \lambda \frac{1 - (1-a)^2}{4D_2} \right) \langle \tilde{T}(1), 1 \rangle - \frac{\lambda}{D_1} \langle s_1, \psi \rangle, \end{aligned} \quad (3.2.15)$$

from which it follows that the knowledge of s_1 allows to compute $\langle t_1 \rangle$:

$$\langle t_1 \rangle = \frac{1}{\pi D_1} \left(1 + \lambda \frac{1 - (1-a)^2}{4D_2} \right) \left(\langle \tilde{T}(1), 1 \rangle - \frac{\lambda}{D_1} \left\langle \left(I + \frac{\lambda}{D_1} V\tilde{T}V \right)^{-1} \psi, \psi \right\rangle \right). \quad (3.2.16)$$

By spectral theorem there exists an orthonormal basis of $L^2([0, \pi])$ which diagonalizes the self-adjoint operator $V\tilde{T}V$. More precisely, $L^2([0, \pi])$ is the orthogonal direct sum of $\ker(V\tilde{T}V)$ and $\text{Im}(V\tilde{T}V)$ and we obtain this orthonormal basis by completing any orthonormal basis of $\ker(V\tilde{T}V)$ with the basis formed by the normalized eigenvectors associated with positive eigenvalues.

To identify these two spaces let us notice first that $\ker V$ is the one dimensional space of constant functions. Thus $\ker(V\tilde{T}V)$ is the space of functions $f \in L^2([0, \pi])$ such that $\tilde{T}(Vf)$ is constant. But since $\mathcal{R}Vf = (T(\mathcal{R}Vf))''$, $\mathcal{R}Vf \equiv 0$. Therefore we state that $f \in \ker(V\tilde{T}V) \Rightarrow \text{supp}(Vf) \subset [\pi - \epsilon, \pi]$, and this implication is easily seen to be an equivalence. With a slight abuse of language, we write $\ker(V\tilde{T}V) = V^{-1}(L^2(\pi - \epsilon, \pi))$. It follows that $\text{Im}(V\tilde{T}V) = V(L^2([0, \pi - \epsilon]))$.

We call $(e_n)_{n \geq 0}$ the orthonormal basis of $\text{Im}(V\tilde{T}V)$ such that $V\tilde{T}Ve_n = \lambda_n e_n$ and $\lambda_n \downarrow 0$ as $n \rightarrow \infty$.

When $\epsilon = 0$, the eigenbasis e_n is simply formed by cosine functions, and the analysis is straightforward (see below). When $\epsilon > 0$, we first observe that $\psi = V\tilde{T}(1) = V\tilde{T}(\varphi_0)$ (recall that ψ appears in Eq. (3.2.14)) where

$$\varphi_0 = \begin{cases} 1 & \text{on } [0, \pi - \epsilon), \\ -\frac{\pi - \epsilon}{\epsilon} & \text{on } [\pi - \epsilon, \pi]. \end{cases} \quad (3.2.17)$$

so that $\int_0^\pi \varphi_0 = 0$, and thus there exists $\psi_0 \in L^2([0, \pi])$ such that

$$\varphi_0 = V\psi_0. \quad (3.2.18)$$

It follows that $\psi \in \text{Im}(V\tilde{T}V)$ and we can write

$$\psi = \sum_{n \geq 1} \psi_n e_n, \quad (3.2.19)$$

with coefficients $(\psi_n)_n$ forming a sequence in $\ell^2(\mathbb{N})$, $\psi_n = \langle \psi, e_n \rangle$. Using this representation, Eq. (3.2.14) is formally solved as

$$s_1 = \frac{1}{D_1} \left(1 + \lambda \frac{1 - (1 - a)^2}{4D_2} \right) \sum_{n \geq 1} \frac{\psi_n}{1 + \frac{\lambda}{D_1} \lambda_n} e_n. \quad (3.2.20)$$

Plugging this expression into Eq. (3.2.16) we obtain

$$\langle t_1 \rangle = \frac{1}{\pi D_1} \left(1 + \lambda \frac{1 - (1 - a)^2}{4D_2} \right) \left[\langle \tilde{T}(1), 1 \rangle - \frac{\lambda}{D_1} \sum_{n \geq 0} \frac{\psi_n^2}{1 + \frac{\lambda}{D_1} \lambda_n} \right]. \quad (3.2.21)$$

This spectral representation is particularly well-suited for the asymptotic analysis of the mean exit time. We then consider the behavior of $\langle t_1 \rangle$ for distinguish cases of $\epsilon = 0$ and $\epsilon > 0$.

3.2.1 Point-like target ($\epsilon = 0$)

We first consider the case of $\epsilon = 0$. Although such a target is not accessible for 2D pure bulk diffusion, it can still be reached through 1D surface diffusion. In this case, one easily gets

$$\begin{cases} \tilde{T}(\cos n\theta) = -T(\cos n\theta) = \frac{\cos n\theta - (-1)^n}{n^2} & (n \geq 1), \\ \tilde{T}(1) = -T(1) = \frac{\pi^2 - \theta^2}{2}, \end{cases} \quad (3.2.22)$$

so that

$$\begin{cases} V\tilde{T}V(\cos n\theta) = \frac{1 - (1 - a)^n}{n^2} \cos n\theta & (n \geq 1), \\ V\tilde{T}V(1) = 0. \end{cases} \quad (3.2.23)$$

One concludes that

$$\lambda_n = \begin{cases} \frac{1-(1-a)^n}{n^2} & (n \geq 1), \\ 0 & (n = 0), \end{cases} \quad e_n = \begin{cases} \sqrt{2/\pi} \cos n\theta & (n \geq 1), \\ \sqrt{1/\pi} & (n = 0). \end{cases} \quad (3.2.24)$$

For $n \geq 1$, we have

$$\begin{aligned} \psi_n &= \langle \psi, e_n \rangle = \langle V\tilde{T}(1), e_n \rangle = \sqrt{2/\pi} \langle \tilde{T}(1), V(\cos n\theta) \rangle \\ &= \sqrt{2/\pi} \sqrt{1 - (1-a)^n} \left\langle \frac{\pi^2 - \theta^2}{2}, \cos n\theta \right\rangle = \sqrt{2\pi} \sqrt{1 - (1-a)^n} \frac{(-1)^{n+1}}{n^2}, \end{aligned} \quad (3.2.25)$$

while $\langle \psi, 1 \rangle = \langle V\tilde{T}(1), 1 \rangle = \langle \tilde{T}(1), V(1) \rangle = 0$. Substituting this expression into Eq. (3.2.21), we get

$$\begin{aligned} \langle t_1 \rangle_{\epsilon=0} &= \frac{1}{\pi D_1} \left(1 + \lambda \frac{1 - (1-a)^2}{4D_2} \right) \left(\langle \tilde{T}(1), 1 \rangle - \sum_{n \geq 1} \frac{2\pi \frac{\lambda}{D_1} (1 - (1-a)^n)}{n^2 \left(n^2 + \frac{\lambda}{D_1} (1 - (1-a)^n) \right)} \right) \\ &= \frac{1}{\pi D_1} \left(1 + \lambda \frac{1 - (1-a)^2}{4D_2} \right) \left(\langle \tilde{T}(1), 1 \rangle - 2\pi \sum_{n \geq 1} \frac{1}{n^2} \right. \\ &\quad \left. + 2\pi \sum_{n \geq 1} \frac{1}{n^2 + \frac{\lambda}{D_1} (1 - (1-a)^n)} \right). \end{aligned} \quad (3.2.26)$$

From Eq. (3.2.22), we get

$$\langle \tilde{T}(1), 1 \rangle_{\epsilon=0} = \int_0^\pi d\theta \frac{\pi^2 - \theta^2}{2} = \frac{1}{3}\pi^3. \quad (3.2.27)$$

We also know the value of the Riemann zeta function

$$\zeta(2) = \sum_{n \geq 1} \frac{1}{n^2} = \frac{\pi^2}{6}. \quad (3.2.28)$$

Plugging Eqs. (3.2.27) and (3.2.28) into Eq. (3.2.26) yields

$$\langle t_1 \rangle_{\epsilon=0} = \frac{2}{D_1} \left(1 + \lambda \frac{1 - (1-a)^2}{4D_2} \right) \sum_{n \geq 1} \frac{1}{n^2 + \frac{\lambda}{D_1} (1 - (1-a)^n)}. \quad (3.2.29)$$

We retrieved the exact representation of the mean exit time for point-like target that was first derived in [1]. Furthermore, as follows, we give an exact asymptotic behavior for this expression, show that $\langle t_1 \rangle_{\epsilon=0}$ is eventually increasing to infinity at large λ and determine the optimality condition for $\langle t_1 \rangle_{\epsilon=0}$ has a minimum.

Let us state the following theorem:

Theorem 3.2.1. *Let us define $I(\lambda) = \sum_{n \geq 1} \frac{1}{n^2 + \frac{\lambda}{D_1}(1 - \varepsilon_n)}$.*

If $\sum_{n \geq 1} n^4 \varepsilon_n < \infty$ then we have the asymptotic for $I(\lambda)$ such that

$$I(\lambda) = \frac{\pi\sqrt{D_1}}{2} \frac{1}{\sqrt{\lambda}} - \frac{D_1}{2\lambda} + \frac{D_1}{\lambda} \sum_{n \geq 1} \frac{\varepsilon_n}{1 - \varepsilon_n} + O\left(\frac{1}{\lambda^2}\right). \quad (3.2.30)$$

Proof. We can rewrite the sum $I(\lambda) = \sum_{n \geq 1} \frac{1}{n^2 + \frac{\lambda}{D_1}(1 - \varepsilon_n)}$ as

$$I(\lambda) = \sum_{n \geq 1} \frac{1}{n^2 + \frac{\lambda}{D_1}} + \frac{\lambda}{D_1} \sum_{n \geq 1} \frac{\varepsilon_n}{\left[n^2 + \frac{\lambda}{D_1}(1 - \varepsilon_n)\right] \left(n^2 + \frac{\lambda}{D_1}\right)} \quad (3.2.31)$$

Let us put

$$I_1(\lambda) = \sum_{n \geq 1} \frac{1}{n^2 + \frac{\lambda}{D_1}}, \quad (3.2.32)$$

and

$$I_2(\lambda) = \frac{\lambda}{D_1} \sum_{n \geq 1} \frac{\varepsilon_n}{\left[n^2 + \frac{\lambda}{D_1}(1 - \varepsilon_n)\right] \left(n^2 + \frac{\lambda}{D_1}\right)} \quad (3.2.33)$$

$$= \frac{D_1}{\lambda} \sum_{n \geq 1} \frac{\varepsilon_n}{\left(1 + \frac{n^2 D_1}{\lambda}\right) \left(1 - \varepsilon_n + \frac{n^2 D_1}{\lambda}\right)} \quad (3.2.34)$$

According to the Poisson summation formula (see the mathematical background 2.1.1), we get that

$$I_1(\lambda) = \sum_{n \geq 1} \frac{1}{n^2 + \frac{\lambda}{D_1}} = \frac{\pi\sqrt{D_1}}{2\sqrt{\lambda}} \frac{e^{2\pi\sqrt{\frac{\lambda}{D_1}}} + 1}{e^{2\pi\sqrt{\frac{\lambda}{D_1}}} - 1} - \frac{D_1}{2\lambda}, \quad (3.2.35)$$

$$\begin{aligned} &= \frac{\pi\sqrt{D_1}}{2\sqrt{\lambda}} + \frac{\pi\sqrt{D_1}}{2\sqrt{\lambda}} \frac{2}{e^{2\pi\sqrt{\frac{\lambda}{D_1}}} - 1} - \frac{D_1}{2\lambda}, \\ &= \frac{\pi\sqrt{D_1}}{2\sqrt{\lambda}} - \frac{D_1}{2\lambda} + O\left(e^{-2\pi\sqrt{\frac{\lambda}{D_1}}}\right), \end{aligned} \quad (3.2.36)$$

In order to estimate the second term $I_2(\lambda)$ we write

$$I_2(\lambda) = \frac{D_1}{\lambda} J_2(\lambda), \quad (3.2.37)$$

where

$$J_2(\lambda) = \sum_{n \geq 1} \frac{\varepsilon_n}{\left(1 + \frac{n^2 D_1}{\lambda}\right) \left(1 - \varepsilon_n + \frac{n^2 D_1}{\lambda}\right)}. \quad (3.2.38)$$

3.2. A SELF-ADJOINT OPERATOR FORMULATION

We have

$$\left| \frac{\varepsilon_n}{\left(1 + \frac{n^2 D_1}{\lambda}\right) \left(1 - \varepsilon_n + \frac{n^2 D_1}{\lambda}\right)} \right| \leq \left| \frac{\varepsilon_n}{1 - \varepsilon_n} \right|, \quad \forall n \geq 1. \quad (3.2.39)$$

Since $\sum_{n \geq 1} \varepsilon_n < \sum_{n \geq 1} n^4 \varepsilon_n < \infty$, there exists n_0 such that $\forall n \geq n_0$, $\varepsilon_n \leq 1/2$, which implies

$$\sum_{n \geq 1} \frac{\varepsilon_n}{1 - \varepsilon_n} \leq \sum_{n \geq 1} 2\varepsilon_n < \infty. \quad (3.2.40)$$

From (3.2.39), (3.2.40), by Lebesgue dominated convergence theorem, we obtain

$$J_2(\lambda) \rightarrow \sum_{n \geq 1} \frac{\varepsilon_n}{1 - \varepsilon_n} < \infty \text{ as } \lambda \rightarrow \infty. \quad (3.2.41)$$

We hence rewrite $J_2(\lambda)$ as

$$J_2(\lambda) = \sum_{n \geq 1} \frac{\varepsilon_n}{1 - \varepsilon_n} + \sum_{n \geq 1} K_n(\lambda), \quad (3.2.42)$$

where $K_n(\lambda) = \frac{\varepsilon_n}{\left(1 + \frac{n^2 D_1}{\lambda}\right) \left(1 - \varepsilon_n + \frac{n^2 D_1}{\lambda}\right)} - \frac{\varepsilon_n}{1 - \varepsilon_n}$.

We have

$$\begin{aligned} K_n(\lambda) &= -\frac{D_1}{\lambda} \frac{\varepsilon_n n^2}{1 - \varepsilon_n} \frac{2 - \varepsilon_n + \frac{n^2 D_1}{\lambda}}{\left(1 + \frac{n^2 D_1}{\lambda}\right) \left(1 - \varepsilon_n + \frac{n^2 D_1}{\lambda}\right)} \\ &= -\frac{D_1}{\lambda} \frac{\varepsilon_n (2 - \varepsilon_n) n^2}{(1 - \varepsilon_n)^2} \frac{1 + \frac{n^2}{D_1(2 - \varepsilon_n)}}{\left(1 + \frac{n^2 D_1}{\lambda}\right) \left(1 + \frac{n^2}{D_1(1 - \varepsilon_n)}\right)} \\ &= -\frac{D_1}{\lambda} \frac{\varepsilon_n (2 - \varepsilon_n) n^2}{(1 - \varepsilon_n)^2} - \frac{D_1}{\lambda} \frac{\varepsilon_n (2 - \varepsilon_n) n^2}{(1 - \varepsilon_n)^2} \left(\frac{1 + \frac{n^2}{D_1(2 - \varepsilon_n)}}{\left(1 + \frac{n^2 D_1}{\lambda}\right) \left(1 + \frac{n^2}{D_1(1 - \varepsilon_n)}\right)} - 1 \right) \\ &= -\frac{D_1}{\lambda} \frac{\varepsilon_n (2 - \varepsilon_n) n^2}{(1 - \varepsilon_n)^2} - \frac{D_1^2}{\lambda^2} \frac{\varepsilon_n (2 - \varepsilon_n) n^4}{(1 - \varepsilon_n)^2} \frac{\frac{1}{2 - \varepsilon_n} - \frac{1}{1 - \varepsilon_n} - 1 - \frac{n^2}{D_1(1 - \varepsilon_n)}}{\left(1 + \frac{n^2 D_1}{\lambda}\right) \left(1 + \frac{n^2}{D_1(1 - \varepsilon_n)}\right)} \\ &= -\frac{D_1}{\lambda} \varepsilon_n n^2 A_n(\lambda) - \frac{D_1^2}{\lambda^2} \varepsilon_n n^4 B_n(\lambda) \end{aligned} \quad (3.2.43)$$

where

$$A_n(\lambda) = \frac{(2 - \varepsilon_n)}{(1 - \varepsilon_n)^2}, \quad (3.2.44)$$

$$B_n(\lambda) = \frac{2 - \varepsilon_n}{(1 - \varepsilon_n)^2} \frac{\frac{1}{2 - \varepsilon_n} - \frac{1}{1 - \varepsilon_n} - 1 - \frac{n^2}{D_1(1 - \varepsilon_n)}}{\left(1 + \frac{n^2 D_1}{\lambda}\right) \left(1 + \frac{n^2}{D_1(1 - \varepsilon_n)}\right)} \quad (3.2.45)$$

3.2. A SELF-ADJOINT OPERATOR FORMULATION

The fact that $\sum_{n \geq 1} \varepsilon_n < \infty$ implies $|A_n(\lambda)| \leq 8$, and $|B_n(\lambda)| \leq \frac{1}{(1-\varepsilon_n)^2} \leq 4$, $\forall n \geq n_0$ which mean $A_n(\lambda)$ and $B_n(\lambda)$ are bounded.

Since $\sum_{n \geq 1} \varepsilon_n n^2 < \sum_{n \geq 1} \varepsilon_n n^4 < \infty$ and $A_n(\lambda), B_n(\lambda)$ bounded, we get $\sum_{n \geq 1} \varepsilon_n n^2 A_n(\lambda) < \infty$ and $\sum_{n \geq 1} \varepsilon_n n^4 B_n(\lambda) < \infty$.

Therefore,

$$\begin{aligned}
 I(\lambda) &= I_1(\lambda) + \frac{D_1}{\lambda} \sum_{n \geq 1} \frac{\varepsilon_n}{1 - \varepsilon_n} + \frac{D_1}{\lambda} \sum_{n \geq 1} \left(\frac{\varepsilon_n}{(1 + \frac{n^2 D_1}{\lambda})(1 - \varepsilon_n + \frac{n^2 D_1}{\lambda})} - \frac{\varepsilon_n}{1 - \varepsilon_n} \right) \\
 &= I_1(\lambda) + \frac{D_1}{\lambda} \sum_{n \geq 1} \frac{\varepsilon_n}{1 - \varepsilon_n} - \frac{D_1^2}{\lambda^2} \sum_{n \geq 1} \varepsilon_n n^2 A_n(\lambda) - \frac{D_1^3}{\lambda^3} \sum_{n \geq 1} \varepsilon_n n^4 B_n(\lambda) \\
 &= \frac{\pi \sqrt{D_1}}{2\sqrt{\lambda}} - \frac{D_1}{2\lambda} + \frac{D_1}{\lambda} \sum_{n \geq 1} \frac{\varepsilon_n}{1 - \varepsilon_n} + O\left(\frac{1}{\lambda^2}\right). \tag{3.2.46}
 \end{aligned}$$

□

We would like to show the asymptotic behavior of $\langle t_1 \rangle_{\varepsilon=0}$. For $0 < a < 1$, let us put $\varepsilon_n = (1-a)^n$ and note that $\sum_{n \geq 0} n^4 \varepsilon_n < \infty$. By applying Theorem 3.2.1 to Eq. (3.2.29), we can obtain the asymptotic for $\langle t_1 \rangle_{\varepsilon=0}$:

$$\begin{aligned}
 \langle t_1 \rangle_{\varepsilon=0} &= \frac{2}{D_1} \left(1 + \lambda \frac{1 - (1-a)^2}{4D_2} \right) \left(\frac{\pi \sqrt{D_1}}{2\sqrt{\lambda}} - \frac{D_1}{2\lambda} + \frac{D_1}{\lambda} \sum_{n \geq 1} \frac{\varepsilon_n}{1 - \varepsilon_n} + o\left(\frac{1}{\lambda}\right) \right) \\
 &= \frac{1 - (1-a)^2}{4D_2 \sqrt{D_1}} \pi \sqrt{\lambda} + \frac{1 - (1-a)^2}{4D_2} \left(2 \sum_{n \geq 1} \frac{\varepsilon_n}{1 - \varepsilon_n} - 1 \right) + \frac{\pi}{\sqrt{D_1}} \frac{1}{\sqrt{\lambda}} \\
 &\quad + \left(2 \sum_{n \geq 1} \frac{\varepsilon_n}{1 - \varepsilon_n} - 1 \right) \frac{1}{\lambda} + O\left(\frac{1}{\lambda^2}\right) \\
 &= A_1 \sqrt{\lambda} + A_2 + \frac{A_3}{\sqrt{\lambda}} + O\left(\frac{1}{\lambda}\right), \tag{3.2.47}
 \end{aligned}$$

where

$$A_1 = \frac{1 - (1-a)^2}{4D_2} \frac{\pi}{\sqrt{D_1}}, \tag{3.2.48}$$

$$A_2 = \frac{1 - (1-a)^2}{4D_2} \left(2 \sum_{n \geq 1} \frac{(1-a)^n}{1 - (1-a)^n} - 1 \right), \tag{3.2.49}$$

$$A_3 = \frac{\pi}{\sqrt{D_1}}. \tag{3.2.50}$$

Eq. (3.2.47) gives us the asymptotic behavior of $\langle t_1 \rangle_{\varepsilon=0}$. As a consequence, $\langle t_1 \rangle_{\varepsilon=0}$ tends to infinity as $\lambda \rightarrow \infty$.

3.2. A SELF-ADJOINT OPERATOR FORMULATION

We then show that $\langle t_1 \rangle_{\epsilon=0}$ is increasing at λ large enough ($\langle t_1 \rangle_{\epsilon=0}$ is eventually increasing). We compute $\frac{d\langle t_1 \rangle_{\epsilon=0}}{d\lambda}$ (from Eq. (3.2.29)) and show that $\frac{d\langle t_1 \rangle_{\epsilon=0}}{d\lambda} > 0$ for large λ :

$$\begin{aligned} \frac{d\langle t_1 \rangle_{\epsilon=0}}{d\lambda} &= \frac{2}{D_1} \left[\frac{1 - (1-a)^2}{4D_2} \sum_{n \geq 1} \frac{1}{n^2 + \frac{\lambda}{D_1}(1 - (1-a)^n)} \right. \\ &\quad \left. + \left(1 + \lambda \frac{1 - (1-a)^2}{4D_2} \right) \sum_{n \geq 1} \frac{\frac{1 - (1-a)^n}{D_1}}{\left(n^2 + \frac{\lambda}{D_1}(1 - (1-a)^n) \right)^2} \right] \end{aligned} \quad (3.2.51)$$

$$\begin{aligned} &= \frac{2D_1}{\lambda^2} \frac{1 - (1-a)^2}{4D_2} \left[\sum_{n \geq 1} \frac{n^2}{\left(1 - (1-a)^n + \frac{n^2 D_1}{\lambda} \right)^2} \right. \\ &\quad \left. - \frac{1}{D_1} \sum_{n \geq 1} \frac{1 - (1-a)^n}{\left(1 - (1-a)^n + \frac{n^2 D_1}{\lambda} \right)^2} \right]. \end{aligned} \quad (3.2.52)$$

Recall that $a \in (0, 1)$, there exists n_0 such that

$$n^2 - \frac{1 - (1-a)^n}{D_1} > 0, \quad \forall n \geq n_0. \quad (3.2.53)$$

We then rewrite Eq. (3.2.52) as

$$\frac{d\langle t_1 \rangle_{\epsilon=0}}{d\lambda} = \frac{2D_1}{\lambda^2} \frac{1 - (1-a)^2}{4D_2} \left[\sum_{n=1}^{n_0-1} \frac{n^2 - \frac{1 - (1-a)^n}{D_1}}{n^4 \left(\frac{1 - (1-a)^n}{n^2} + \frac{D_1}{\lambda} \right)^2} + \sum_{n=n_0}^{\infty} \frac{n^2 - \frac{1 - (1-a)^n}{D_1}}{n^4 \left(\frac{1 - (1-a)^n}{n^2} + \frac{D_1}{\lambda} \right)^2} \right]. \quad (3.2.54)$$

We have the first sum in Eq. (3.2.54) is finite which means there exists a positive M such that

$$\left| \sum_{n=1}^{n_0-1} \frac{n^2 - \frac{1 - (1-a)^n}{D_1}}{n^4 \left(\frac{1 - (1-a)^n}{n^2} + \frac{D_1}{\lambda} \right)^2} \right| \leq M, \quad \forall \lambda > 0. \quad (3.2.55)$$

Moreover, the numerator of the second sum is strictly positive (recall Eq. (3.2.53)), hence

$$\lim_{\lambda \rightarrow \infty} \sum_{n=n_0}^{\infty} \frac{n^2 - \frac{1 - (1-a)^n}{D_1}}{n^4 \left(\frac{1 - (1-a)^n}{n^2} + \frac{D_1}{\lambda} \right)^2} = \sum_{n=n_0}^{\infty} \frac{n^2 - \frac{1 - (1-a)^n}{D_1}}{(1 - (1-a)^n)^2} = +\infty. \quad (3.2.56)$$

By combining (3.2.55), (3.2.56) and using the fact that $D_1 > 0$, $D_2 > 0$, $0 < a < 1$, we obtain that $\frac{d\langle t_1 \rangle_{\epsilon=0}}{d\lambda} > 0$ when λ large enough which means $\langle t_1 \rangle_{\epsilon=0}$ is eventually

increasing, as illustrated on Fig. 3.2a.

Finally, we find the optimality condition for D_2 such that $\langle t_1 \rangle_{\epsilon=0}$ has a minimum at a positive λ . Since $\frac{d\langle t_1 \rangle_{\epsilon=0}}{d\lambda} > 0$ when λ large enough, a sufficient condition is that (use (3.2.51))

$$\left. \frac{d\langle t_1 \rangle_{\epsilon=0}}{d\lambda} \right|_{\lambda=0} = \frac{2}{D_1} \left(\frac{1 - (1-a)^2}{4D_2} \sum_{n \geq 1} \frac{1}{n^2} - \frac{1}{D_1} \sum_{n \geq 1} \frac{1 - (1-a)^n}{n^4} \right) < 0. \quad (3.2.57)$$

The Eq. (3.2.57) is equivalent to

$$\begin{aligned} \frac{1 - (1-a)^2}{4D_2} \frac{\pi^2}{6} &< \frac{1}{D_1} \sum_{n \geq 1} \frac{1 - (1-a)^n}{n^4} \\ \Leftrightarrow D_2 > D_{2,\text{crit}} &:= D_1 \frac{\pi^2(1 - (1-a)^2)}{24 \sum_{n \geq 1} \frac{1 - (1-a)^n}{n^4}}. \end{aligned} \quad (3.2.58)$$

We retrieved the optimality condition first reported in [1]. The relation (3.2.58) determines the critical value of the pure bulk diffusion coefficient $D_{2,\text{crit}}$, which for small a can be approximated as

$$\lim_{a \rightarrow 0} D_{2,\text{crit}} = D_1 \frac{\pi^2}{24} \frac{2a}{\sum_{n \geq 1} \frac{na}{n^4}} = D_1 \frac{\pi^2}{12\zeta(3)} \approx 0.68D_1. \quad (3.2.59)$$

If $\frac{D_2}{D_1} > \frac{D_{2,\text{crit}}}{D_1}$, then $\langle t_1 \rangle_{\epsilon=0}$ as a function of λ has a minimum at positive λ , and the intermittent search is optimal.

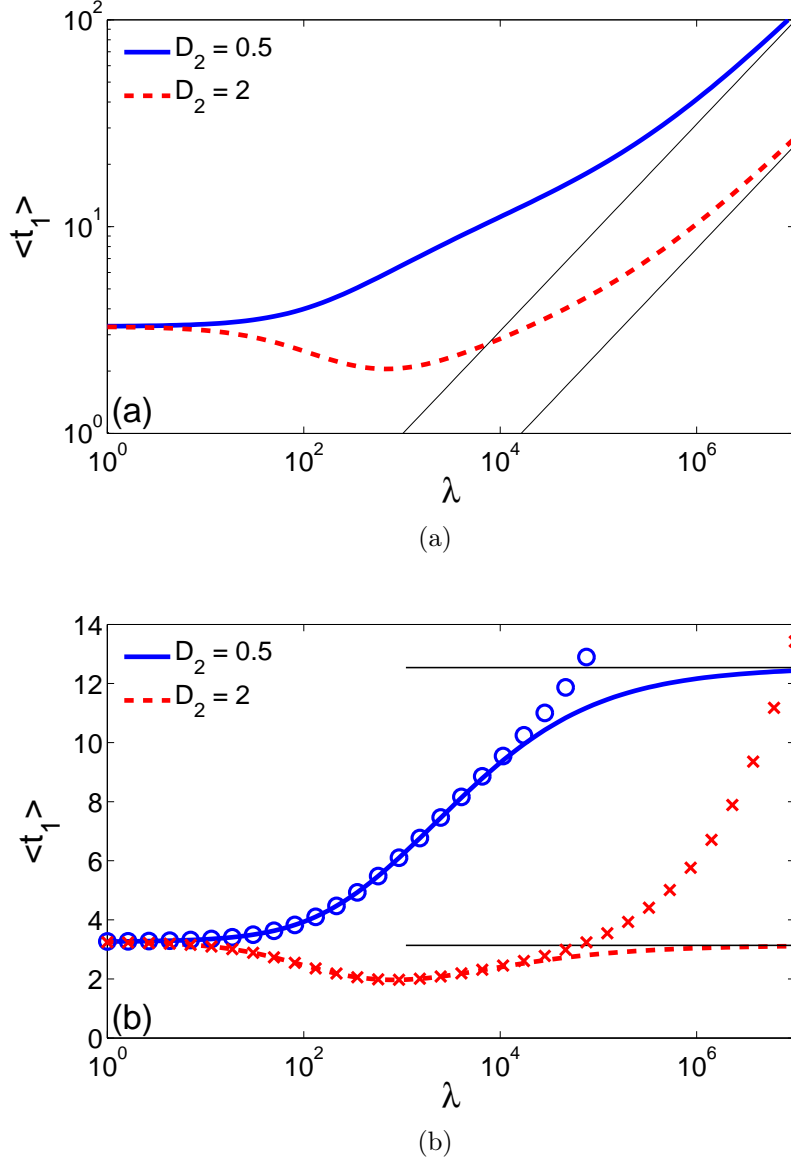


Figure 3.2: Mean exit time $\langle t_1 \rangle$ as a function of λ for $\epsilon = 0$ (a) and $\epsilon = 0.01$ (b), with $a = 0.01$ and $D_1 = 1$. When $D_2 = 0.5 < D_{2,\text{crit}}$ (blue solid line), $\langle t_1 \rangle$ monotonously increases with λ so that the smallest mean exit time corresponds to $\lambda = 0$ (surface diffusion without intermittence). When $D_2 = 2 > D_{2,\text{crit}}$ (red dashed line), $\langle t_1 \rangle$ starts first to decrease with λ , passes through a minimum and monotonously increases to infinity. For point-like target (a), thin solid lines indicate the leading term of the lower bound $\frac{1-(1-a)^2}{4D_2\sqrt{D_1}}\pi\sqrt{\lambda}$ from Eq. (3.2.47). Note that the upper bound, which is larger by $a^{-1/2}$, strongly overestimates the mean exit time. Finally, correction terms of the order $\lambda^{-1/2}$ are negligible for large λ . For extended target (b), horizontal lines indicate the limiting values of the mean exit time as $\lambda \rightarrow \infty$. Symbols present the diagonal approximation which is shown in [3].

3.2.2 Extended target ($\epsilon > 0$)

In contrast to a point-like target, the mean exit time $\langle t_1 \rangle$ to an extended target ($\epsilon > 0$) is expected to converge in a finite limit \mathcal{T} as $\lambda \rightarrow \infty$ because the mean exit time of reflecting Brownian motion (i.e., the limiting case $a = 0$) is finite (which is proved in [20]). In this section, we give a proof that $\langle t_1 \rangle$ converges to finite limit \mathcal{T} when $\lambda \rightarrow \infty$ for all a and then we analyze the asymptotic behavior of $\langle t_1 \rangle$.

We first prove the following theorem

Theorem 3.2.2. *For (λ_n) defined as the eigenvalues of the operator $V\tilde{T}V$ and (ψ_n) defined as the spectral weight of the function $V\tilde{T}(1)$ in the orthonormal basis (e_n) of the operator $V\tilde{T}V$, where V and \tilde{T} are defined in (3.2.8) and (3.2.10) we have*

- (i) $\sum_{n \geq 1} \frac{\psi_n^2}{\lambda_n} = \langle \tilde{T}(1), 1 \rangle$,
- (ii) $\sum_{n \geq 1} \frac{\psi_n^2}{\lambda_n^2} < +\infty$,
- (iii) $\sum_{n \geq 1} \frac{\psi_n^2}{\lambda_n^3} = +\infty$.

Proof. (i),(ii). First we define

$$\tilde{e}_n = \frac{1}{\lambda_n} \tilde{T}V e_n, \quad (3.2.60)$$

so that $V\tilde{e}_n = e_n$.

Recall $\psi = V\tilde{T}(1)$ (see Eq. (3.2.14)). Let $u \in L^2([0, \pi])$ such that $V(u) = 1$, hence $\psi = V\tilde{T}V(u)$. u must be of the form $\psi_0 + u^\perp$, where $u^\perp \in \ker(V\tilde{T}V)$ and ψ_0 defined in (3.2.18). Let

$$u_n = \langle u, e_n \rangle = \frac{1}{\lambda_n} \langle u, V\tilde{T}V e_n \rangle = \frac{1}{\lambda_n} \langle V\tilde{T}V u, e_n \rangle = \frac{\psi_n}{\lambda_n}. \quad (3.2.61)$$

This computation gives the proof of (ii) that $\sum_{n \geq 1} \frac{\psi_n^2}{\lambda_n^2} < \infty$.

Besides, since $V(u) = 1$, we have

$$\begin{aligned} \langle \tilde{T}(1), 1 \rangle &= \langle \tilde{T}V(u), V(u) \rangle \\ &= \langle V\tilde{T}V(u), u \rangle \\ &= \sum_{n \geq 1} \sum_{m \geq 1} u_n u_m \langle V\tilde{T}V(e_n), e_m \rangle \\ &= \sum_{n \geq 1} \frac{\psi_n^2}{\lambda_n}, \end{aligned} \quad (3.2.62)$$

which proves (i).

3.2. A SELF-ADJOINT OPERATOR FORMULATION

(iii). Equation (3.2.60) implies that, $-\lambda_n \tilde{e}_n'' = V e_n$ on $L^2([0, \pi - \epsilon])$. Let m, n be integers, and we establish:

$$\begin{aligned} \lambda_n \langle \tilde{e}_n', \tilde{e}_m' \rangle &= -\lambda_n \langle \tilde{e}_n'', \tilde{e}_m \rangle \\ &= \langle V e_n, \tilde{e}_m \rangle \\ &= \langle e_n, V \tilde{e}_m \rangle \\ &= \langle e_n, e_m \rangle = \delta_{m,n}. \end{aligned} \quad (3.2.63)$$

Setting $\epsilon_n = \sqrt{\lambda_n} \tilde{e}_n$, we get that (ϵ_n') is an orthonormal system of $L^2([0, \pi])$ due to (3.2.63).

Next assume that $\sum_{n \geq 1} \frac{\psi_n^2}{\lambda_n^3} < \infty$: then the above computation shows that $\sum_{n \geq 1} \frac{\psi_n}{\lambda_n} \tilde{e}_n$ is a function of the Sobolev space $H^1([0, \pi])$.

Before continuing, let us observe that the operator $I - V$ is regularizing which means for all $f \in L^2([0, \pi])$ we have $Vf = f + g$ where $g \in C^\infty([0, \pi])$.

This implies that

$$V \left(\sum_{n \geq 1} \frac{\psi_n}{\lambda_n} \tilde{e}_n \right) = \sum_{n \geq 1} \frac{\psi_n}{\lambda_n} \tilde{e}_n + g, \quad g \in C^\infty. \quad (3.2.64)$$

On the other hand

$$V \left(\sum_{n \geq 1} \frac{\psi_n}{\lambda_n} \tilde{e}_n \right) = \sum_{n \geq 1} \frac{\psi_n}{\lambda_n} e_n, \quad (3.2.65)$$

and thus $u_0 = \sum_{n \geq 1} \frac{\psi_n}{\lambda_n} e_n \in H^1$.

But u_0 minimizes $\|v\|_2^2$ on the set of v such that $\int_0^\pi (Vv - 1)^2 = 0$, $\int_{\pi-\epsilon}^\pi Vv = -(\pi - \epsilon)$. By the theory of constrained extrema, v must be of the form $\lambda V 1_{[\pi-\epsilon, \pi[} = \lambda 1_{[\pi-\epsilon, \pi[} + g$ with $g \in C^\infty$. But such a function cannot be in H^1 .

We have thus proven (iii). \square

Remark 3.2.1. Setting $\lambda = 0$ into Eq. (3.2.21), the expression (i) in Theorem 3.2.2 can be identified to the mean exit time for surface diffusion phase:

$$\langle t_1 \rangle_{\lambda=0} = \frac{1}{\pi D_1} \sum_{n \geq 1} \frac{\psi_n^2}{\lambda_n} = \frac{1}{\pi D_1} \langle \tilde{T}(1), 1 \rangle = \frac{(\pi - \epsilon)^3}{3\pi D_1}. \quad (3.2.66)$$

We may now state the main theorems of this work:

Theorem 3.2.3. The mean exit time $\langle t_1 \rangle$ defined in (3.2.21) converges to a finite limit as $\lambda \rightarrow \infty$.

Proof. We recall that

$$\langle t_1 \rangle = \frac{1}{\pi D_1} \left(1 + \lambda \frac{1 - (1 - a)^2}{4D_2} \right) \left[\langle \tilde{T}(1), 1 \rangle - \frac{\lambda}{D_1} \sum_{n \geq 0} \frac{\psi_n^2}{1 + \frac{\lambda}{D_1} \lambda_n} \right] \quad (3.2.21).$$

From theorem 3.2.2 we deduce

$$\lim_{\lambda \rightarrow \infty} \sum_{n \geq 1} \frac{\lambda \psi_n^2}{1 + \frac{\lambda}{D_1} \lambda_n} = D_1 \sum_{n \geq 1} \frac{\psi_n^2}{\lambda_n} = D_1 \langle \tilde{T}(1), 1 \rangle. \quad (3.2.67)$$

As a consequence, the quantity $\langle \tilde{T}(1), 1 \rangle - \frac{\lambda}{D_1} \sum_{n \geq 0} \frac{\psi_n^2}{1 + \frac{\lambda}{D_1} \lambda_n}$ converge to 0 as $\lambda \rightarrow \infty$.

Substituting $\langle \tilde{T}(1), 1 \rangle$ by $\sum_{n \geq 1} \frac{\psi_n^2}{\lambda_n}$ in Eq. (3.2.21) (use (i) in Theorem 3.2.2), we get

$$\begin{aligned} \langle t_1 \rangle &= \frac{1}{\pi D_1} \left(1 + \lambda \frac{1 - (1-a)^2}{4D_2} \right) \left[\sum_{n \geq 1} \frac{\psi_n^2}{\lambda_n} - \frac{\lambda}{D_1} \sum_{n \geq 1} \frac{\psi_n^2}{1 + \frac{\lambda}{D_1} \lambda_n} \right] \\ &= \frac{1}{\pi} \left(\frac{1}{\lambda} + \frac{1 - (1-a)^2}{4D_2} \right) \sum_{n \geq 1} \frac{\psi_n^2}{\lambda_n \left(\frac{D_1}{\lambda} + \lambda_n \right)}. \end{aligned} \quad (3.2.68)$$

This formula generalizes Eq. (3.2.29) to extended targets.

Theorem 3.2.2 also implies

$$\lim_{\lambda \rightarrow \infty} \sum_{n \geq 1} \frac{\psi_n^2}{\lambda_n \left(\frac{D_1}{\lambda} + \lambda_n \right)} = \sum_{n \geq 1} \frac{\psi_n^2}{\lambda_n^2} < \infty, \quad (3.2.69)$$

from which

$$\mathcal{T} := \lim_{\lambda \rightarrow \infty} \langle t_1 \rangle = \frac{1 - (1-a)^2}{4\pi D_2} \sum_{n \geq 1} \frac{\psi_n^2}{\lambda_n^2}, \quad (3.2.70)$$

i.e., we proved that the limit \mathcal{T} is finite and got its spectral representation. \square

Remark 3.2.2. Since $\langle t_1 \rangle \xrightarrow{\lambda \rightarrow \infty} \mathcal{T}$, we then rewrite $\langle t_1 \rangle$ as

$$\begin{aligned} \langle t_1 \rangle &= \frac{1}{\pi} \left(\frac{1}{\lambda} + \frac{1 - (1-a)^2}{4D_2} \right) \left[\sum_{n \geq 1} \frac{\psi_n^2}{\lambda_n^2} + \sum_{n \geq 1} \left(\frac{\psi_n^2}{\lambda_n \left(\frac{D_1}{\lambda} + \lambda_n \right)} - \frac{\psi_n^2}{\lambda_n^2} \right) \right] \\ &= \mathcal{T} + \frac{1}{\pi \lambda} \sum_{n \geq 1} \frac{\psi_n^2}{\lambda_n^2} - \frac{1}{\pi} \left(\frac{1}{\lambda} + \frac{1 - (1-a)^2}{4D_2} \right) \sum_{n \geq 1} \frac{\psi_n^2}{\lambda_n \left(\frac{D_1}{\lambda} + \lambda_n \right)} \end{aligned} \quad (3.2.71)$$

which leads us to

$$\mathcal{T} - \langle t_1 \rangle = -\frac{S}{\pi \lambda} + \frac{D_1}{\lambda} \frac{1 - (1-a)^2}{4\pi D_2} \sum_{n \geq 1} \frac{\psi_n^2}{\lambda_n^2 \left(\lambda_n + \frac{D_1}{\lambda} \right)} + \frac{D_1}{\pi \lambda^2} \sum_{n \geq 1} \frac{\psi_n^2}{\lambda_n^2 \left(\lambda_n + \frac{D_1}{\lambda} \right)}, \quad (3.2.72)$$

where $S = \sum_{n \geq 1} \frac{\psi_n^2}{\lambda_n^2}$.

Again, since $\lim_{\lambda \rightarrow \infty} \langle t_1 \rangle = \mathcal{T}$, the right-hand side of Eq. (3.2.72) must converges to

3.2. A SELF-ADJOINT OPERATOR FORMULATION

0 as $\lambda \rightarrow \infty$.

Besides, thank to Theorem 3.2.2 we have

$$\lim_{\lambda \rightarrow \infty} \sum_{n \geq 1} \frac{\psi_n^2}{\lambda_n^2 \left(\frac{D_1}{\lambda} + \lambda_n \right)} = \sum_{n \geq 1} \frac{\psi_n^2}{\lambda_n^3} = \infty. \quad (3.2.73)$$

Note that S is bounded (by (ii) in Theorem 3.2.2), from Eq. (3.2.73) we conclude that at large λ ,

$$\frac{D_1}{\lambda} \frac{1 - (1-a)^2}{4\pi D_2} \sum_{n \geq 1} \frac{\psi_n^2}{\lambda_n^2 \left(\lambda_n + \frac{D_1}{\lambda} \right)} \gg \frac{S}{\pi \lambda}, \quad (3.2.74)$$

and

$$\frac{D_1}{\lambda} \frac{1 - (1-a)^2}{4\pi D_2} \sum_{n \geq 1} \frac{\psi_n^2}{\lambda_n^2 \left(\lambda_n + \frac{D_1}{\lambda} \right)} \gg \frac{D_1}{\pi \lambda^2} \sum_{n \geq 1} \frac{\psi_n^2}{\lambda_n^2 \left(\lambda_n + \frac{D_1}{\lambda} \right)}. \quad (3.2.75)$$

Consequently, from (3.2.74), (3.2.75), we state that $\frac{D_1}{\lambda} \frac{1 - (1-a)^2}{4\pi D_2} \sum_{n \geq 1} \frac{\psi_n^2}{\lambda_n^2 \left(\lambda_n + \frac{D_1}{\lambda} \right)}$ is the leading term of the right-hand side of Eq. (3.2.72) and since $\mathcal{T} - \langle t_1 \rangle \xrightarrow{\lambda \rightarrow \infty} 0$, this leading term must tends to 0 as $\lambda \rightarrow \infty$. Hence, we can rewrite the third term $\frac{D_1}{\pi \lambda^2} \sum_{n \geq 1} \frac{\psi_n^2}{\lambda_n^2 \left(\lambda_n + \frac{D_1}{\lambda} \right)}$ in the right-hand side of Eq. (3.2.72) as $o\left(\frac{1}{\lambda}\right)$ and then we obtain the asymptotic behavior of $\langle t_1 \rangle$

$$\langle t_1 \rangle = \mathcal{T} - \frac{D_1}{\lambda} \frac{1 - (1-a)^2}{4\pi D_2} \sum_{n \geq 1} \frac{\psi_n^2}{\lambda_n^2 \left(\lambda_n + \frac{D_1}{\lambda} \right)} + \frac{S}{\pi \lambda} + o\left(\frac{1}{\lambda}\right). \quad (3.2.76)$$

Theorem 3.2.4. The function $\lambda \mapsto \langle t_1 \rangle$, where $\langle t_1 \rangle$ defined in (3.2.21), is eventually increasing as $\lambda \rightarrow +\infty$, or equivalently, $\frac{d\langle t_1 \rangle}{d\lambda} > 0$ at large λ . Moreover, if

$$\left. \frac{d\langle t_1 \rangle}{d\lambda} \right|_{\lambda=0} < 0,$$

then the function $\langle t_1 \rangle$ passes through a minimum.

Proof. Since (3.2.74) hold for large λ and S is bounded, the first correction term of Eq. (3.2.76) dominates over the second one, i.e.

$$\langle t_1 \rangle = \mathcal{T} - \frac{D_1}{\lambda} \frac{1 - (1-a)^2}{4\pi D_2} \sum_{n \geq 1} \frac{\psi_n^2}{\lambda_n^2 \left(\lambda_n + \frac{D_1}{\lambda} \right)} + O(\lambda^{-1}), \quad (3.2.77)$$

from which the principle part of $\langle t_1 \rangle$ is indeed non-decreasing as $\lambda \rightarrow \infty$.

To complete the proof, we differentiate Eq. (3.2.71) (the exchange of derivative and sum is easily established):

$$\pi \frac{d\langle t_1 \rangle}{d\lambda} = -\frac{S}{\lambda^2} + \frac{1}{\lambda^2} \frac{D_1 (1 - (1-a)^2)}{4D_2} \sum_{n \geq 1} \frac{\psi_n^2}{\lambda_n \left(\lambda_n + \frac{D_1}{\lambda} \right)^2} + \frac{D_1}{\lambda^3} \sum_{n \geq 0} \frac{\psi_n^2 (2\lambda_n + D_1/\lambda)}{\lambda_n^2 \left(\lambda_n + D_1/\lambda \right)^2}, \quad (3.2.78)$$

Since

$$\lim_{\lambda \rightarrow \infty} \sum_{n \geq 1} \frac{\psi_n^2}{\lambda_n \left(\lambda_n + \frac{D_1}{\lambda}\right)^2} = \sum_{n \geq 1} \frac{\psi_n^2}{\lambda_n^3} = +\infty \quad (3.2.79)$$

and

$$S = \sum_{n \geq 1} \frac{\psi_n^2}{\lambda_n^2} < \infty, \quad (3.2.80)$$

we imply for λ large enough,

$$\frac{1}{\lambda^2} \frac{D_1 (1 - (1 - a)^2)}{4D_2} \sum_{n \geq 1} \frac{\psi_n^2}{\lambda_n \left(\lambda_n + \frac{D_1}{\lambda}\right)^2} - \frac{S}{\lambda^2} > 0. \quad (3.2.81)$$

Besides, we also have $\frac{D_1}{\lambda^3} \sum_{n \geq 0} \frac{\psi_n^2 (2\lambda_n + D_1/\lambda)}{\lambda_n^2 (\lambda_n + D_1/\lambda)^2} \geq 0$. We hence imply that $\frac{d\langle t_1 \rangle}{d\lambda}$ is positive at large λ which means $\langle t_1 \rangle$ is asymptotically monotonously increasing. \square

Next, we find the optimality condition for D_2 such that $\langle t_1 \rangle_{\epsilon > 0}$ has a minimum at a positive λ . Returning to formula (3.2.21), we have

$$\begin{aligned} \pi \frac{d\langle t_1 \rangle}{d\lambda} &= \frac{1 - (1 - a)^2}{4D_1 D_2} \left[\langle \tilde{T}(1), 1 \rangle - \frac{\lambda}{D_1} \sum_{n \geq 1} \frac{\psi_n^2}{1 + \frac{\lambda \lambda_n}{D_1}} \right] \\ &+ \frac{1}{D_1} \left(1 + \frac{\lambda (1 - (1 - a)^2)}{4D_2} \right) \left[-\frac{1}{D_1} \sum_{n \geq 1} \frac{\psi_n^2}{1 + \frac{\lambda \lambda_n}{D_1}} + \frac{\lambda}{D_1} \sum_{n \geq 1} \frac{\psi_n^2 \frac{\lambda_n}{D_1}}{\left(1 + \frac{\lambda \lambda_n}{D_1}\right)^2} \right]. \end{aligned} \quad (3.2.82)$$

In particular, one gets

$$\pi \frac{d\langle t_1 \rangle}{d\lambda} \Big|_{\lambda=0} = \frac{1 - (1 - a)^2}{4D_1 D_2} \langle \tilde{T}(1), 1 \rangle + \frac{1}{D_1^2} \left[-\sum_{n \geq 1} \psi_n^2 \right]. \quad (3.2.83)$$

Since $\psi = V\tilde{T}(1) = \sum_{n \geq 1} \psi_n e_n$,

$$\pi \frac{d\langle t_1 \rangle}{d\lambda} \Big|_{\lambda=0} = \frac{1 - (1 - a)^2}{4D_1 D_2} \langle \tilde{T}(1), 1 \rangle - \frac{1}{D_1^2} \|V\tilde{T}(1)\|^2, \quad (3.2.84)$$

which becomes negative when

$$\|V\tilde{T}(1)\|^2 > \frac{D_1}{4D_2} (1 - (1 - a)^2) \langle \tilde{T}(1), 1 \rangle. \quad (3.2.85)$$

We recall that $\psi = V\tilde{T}(1) = V\tilde{T}(\varphi_0) = V\tilde{T}V(\psi_0)$ (as φ_0 defined in (3.2.17) and $\varphi_0 = V(\psi_0)$). Thus (3.2.85) is equivalent to

$$\|V\tilde{T}V(\psi_0)\|^2 > \frac{D_1}{4D_2} (1 - (1 - a)^2) \langle V\tilde{T}V(\psi_0), \psi_0 \rangle. \quad (3.2.86)$$

Remark 3.2.3. *The inequality (3.2.85) determines the critical value for the pure bulk diffusion coefficient $D_{2,\text{crit}}$ above which pure bulk excursions are beneficial. The existence of the optimal value λ (that minimizes the function $\langle t_1 \rangle$) depends on this ratio. If $D_2 > D_{2,\text{crit}}$, with*

$$D_{2,\text{crit}} = D_1 \frac{(1 - (1 - a)^2) \langle \tilde{T}(1), 1 \rangle}{4 \|V\tilde{T}(1)\|^2}, \quad (3.2.87)$$

then $\langle t_1 \rangle$ starts first to decrease with λ , passes through a minimum then monotonously increases. We retrieved the optimality condition first reported in [1]. Most importantly, we proved that this condition is necessary and sufficient for optimality of surface-mediated diffusion. In fact, the second optimality condition from [1], $\langle t_1 \rangle_{\lambda=0} < \langle t_1 \rangle_{\lambda=\infty}$, is not necessary because of the asymptotic growth of $\langle t_1 \rangle$ as $\lambda \rightarrow \infty$. In particular, the optimality diagrams from [1, 2] can be simplified by removing the region of pure bulk diffusion which is never an optimal search strategy.

Note that $\tilde{T}(1)(\theta) = \frac{(\pi - \epsilon)^2 - \theta^2}{2}$ for $\theta \in [0, \pi - \epsilon)$ (see (B.1.2)), we have

$$\begin{aligned} \psi(\theta) &= V\tilde{T}(1)(\theta) = V \left(\frac{(\pi - \epsilon)^2 - \theta^2}{2} \right) = V \left(\frac{2}{\pi} \sum_{n \geq 1}^{\infty} \cos n\theta \left\langle \frac{(\pi - \epsilon)^2 - \theta^2}{2}, \cos n\theta \right\rangle \right) \\ &= \frac{2}{\pi} \sum_{n \geq 1}^{\infty} \cos n\theta \sqrt{1 - (1 - a)^n} \left\langle \frac{(\pi - \epsilon)^2 - \theta^2}{2}, \cos n\theta \right\rangle \\ &= \frac{2}{\pi} \sum_{n \geq 1}^{\infty} \cos n\theta \sqrt{1 - (1 - a)^n} (-1)^{n-1} \frac{(\pi - \epsilon) \cos n\epsilon + \frac{\sin n\epsilon}{n}}{n^2}. \end{aligned} \quad (3.2.88)$$

Plugging (3.2.88) to (3.2.87), we obtain

$$D_{2,\text{crit}} = D_1 \frac{\pi(\pi - \epsilon)^3(1 - (1 - a)^2)}{24} \left(\sum_{n \geq 1} \frac{1 - (1 - a)^n}{n^4} \left[(\pi - \epsilon) \cos n\epsilon + \frac{\sin n\epsilon}{n} \right]^2 \right)^{-1}. \quad (3.2.89)$$

3.3 Numerical asymptotic behavior

In previous section, we showed the asymptotic behavior of $\langle t_1 \rangle_{\epsilon > 0}$ in Eq. (3.2.76). Nevertheless, it is not an explicit formula. We thus aim to precise the asymptotic behavior (3.2.76) of $\langle t_1 \rangle$ as $\lambda \rightarrow \infty$ by investigating on the eigenvalues λ_n and the spectral weights ψ_n . We first state the following theorem whose proof will be given in Appendix A:

Theorem 3.3.1. *Let $(\lambda_n)_{n \geq 1}$ be the decreasing sequence of eigenvalues of the operator $V\tilde{T}V$, where the operators \tilde{T} and V are defined in Eqs. (3.2.9) and (3.2.8). We have*

$$\lambda_n \sim A_\epsilon n^{-2}, \quad (3.3.1)$$

where A_ϵ depends only on ϵ .

3.3. NUMERICAL ASYMPTOTIC BEHAVIOR

Showing that $\lambda_n \sim n^{-2}$ has an significant role in presenting the asymptotic behavior of $\langle t_1 \rangle_{\epsilon > 0}$, but it is not sufficient. It is necessary to investigate the spectral weight ψ_n . We believe that the asymptotic behavior ψ_n^2 ,

$$\psi_n^2 \sim n^{-6}, \quad (3.3.2)$$

which is not proved rigorously. However, in this section, we focus on showing the numerical evidences for ψ_n^2 and also for λ_n . These results lead us to the behavior of $\langle t_1 \rangle$ in formula (3.3.13) and (3.3.14).

In addition, considering the numerical asymptotic behaviors of λ_n and ψ_n^2 also leads to the conclusion that $\mathcal{T} \sim \ln \frac{1}{\epsilon}$ in the case of $a \rightarrow 0$ as shown explicitly in Eq. (3.3.21).

For point-like target ($\epsilon = 0$), Eqs. (3.2.24) and (3.2.25) imply the existence of two distinct asymptotic behaviors for small a :

(i)

$$\lambda_n \simeq an^{-1}, \quad \psi_n^2 \simeq 2\pi an^{-3} \quad (na \ll 1), \quad (3.3.3)$$

i.e., there exists $c_1, c'_1, n_1, \epsilon_1$ such that for all $n \in [n_1, \frac{\epsilon_1}{a})$, we have

$$\frac{1}{c_1} < \left| \frac{\lambda_n}{an^{-1}} \right| < c_1, \quad \frac{1}{c'_1} < \left| \frac{\psi_n^2}{2\pi an^{-3}} \right| < c'_1.$$

(ii)

$$\lambda_n \simeq n^{-2}, \quad \psi_n^2 \simeq 2\pi n^{-4} \quad (na \gg 1) \quad (3.3.4)$$

i.e., there exists c_2, c'_2, n_2 such that for all n with $na \geq n_2$, we have

$$\frac{1}{c_2} < \left| \frac{\lambda_n}{n^{-2}} \right| < c_2, \quad \frac{1}{c'_2} < \left| \frac{\psi_n^2}{2\pi n^{-4}} \right| < c'_2.$$

For extended targets ($\epsilon > 0$), we do not have the explicit formulas for the eigenvalues λ_n and the spectral weights ψ_n^2 . Hence, this case is analyzed by numerical computations (see Appendix B.1 for computational details).

By observations, we distinguish two regimes for λ_n , as for the point-like target, for small and large n (see Figure 3.3):

(i)

$$\lambda_n \simeq \tilde{A}_{a,\epsilon} n^{-1} \quad (na \ll 1) \quad (3.3.5)$$

i.e., there exists c_1, n_1, ϵ_1 such that for all $n \geq n_1$ but $na < \epsilon_1$, we have

$$\frac{1}{c_1} < \left| \frac{\lambda_n}{\tilde{A}_{a,\epsilon} n^{-1}} \right| < c_1,$$

(ii)

$$\lambda_n \simeq A_\epsilon n^{-2} \quad (3.3.6)$$

i.e. there exists c_2, n_2 such that for all n with $na \geq n_2$ we have

$$\frac{1}{c_2} < \left| \frac{\lambda_n}{A_\epsilon n^{-2}} \right| < c_2,$$

where $\tilde{A}_{a,\epsilon}, A_\epsilon$ are two constants. The second (large n) asymptotic relation is proved with the constant A_ϵ does not depend on a by Theorem 3.3.1.

In turn, the transition between two asymptotic regimes is determined by $1/a$ (and is independent of ϵ). Note also that $A_\epsilon \rightarrow 1$ as $\epsilon \rightarrow 0$ according to Eq. (3.3.4). One can see that these asymptotic relations accurately approximate the eigenvalues λ_n . The behavior of A_ϵ is shown on Fig. 3.5a. As expected, it does not depend on a . These numerical results show the evidence for the expression:

$$A_\epsilon = (1 - \epsilon/\pi)^2, \quad (3.3.7)$$

which accurately reproduces A_ϵ on the whole range of ϵ from 0 to π .

According to (3.3.3), the coefficient $\tilde{A}_{a,\epsilon}$ is equal to a when $\epsilon = 0$. We plot therefore $\tilde{A}_{a,\epsilon}/a$ on Fig. 3.5b, where this ratio approaches 1 as $\epsilon \rightarrow 0$, and 0 as $\epsilon \rightarrow \pi$. Moreover, this ratio weakly depends on a (curves for $a = 0.001$ and $a = 0.1$ almost coincide).

Figure 3.4 shows that the asymptotic behavior of the spectral weights ψ_n^2 is more complicated. One can distinguish three asymptotic regimes:

(i)

$$\psi_n^2 \simeq \tilde{B}_{a,\epsilon} n^{-3} \quad (\max\{na, n\epsilon\} \ll 1), \quad (3.3.8)$$

i.e. there exists c_1, n_1, ϵ_1 such that for all $n \geq n_1$ but $\max\{na, n\epsilon\} < \epsilon_1$, we have

$$\frac{1}{c_1} < \left| \frac{\psi_n^2}{\tilde{B}_{a,\epsilon} n^{-3}} \right| < c_1,$$

(ii)

$$\psi_n^2 \simeq \tilde{B}'_{a,\epsilon} n^{-4} \quad (\min\{na, n\epsilon\} \ll 1 \ll \max\{na, n\epsilon\}), \quad (3.3.9)$$

i.e., there exists c_2, n_2, ϵ_2 such that for all n with $\max\{na, n\epsilon\} \geq n_2$ but $\min\{na, n\epsilon\} < \epsilon_2$, we have

$$\frac{1}{c_2} < \left| \frac{\psi_n^2}{\tilde{B}'_{a,\epsilon} n^{-4}} \right| < c_2,$$

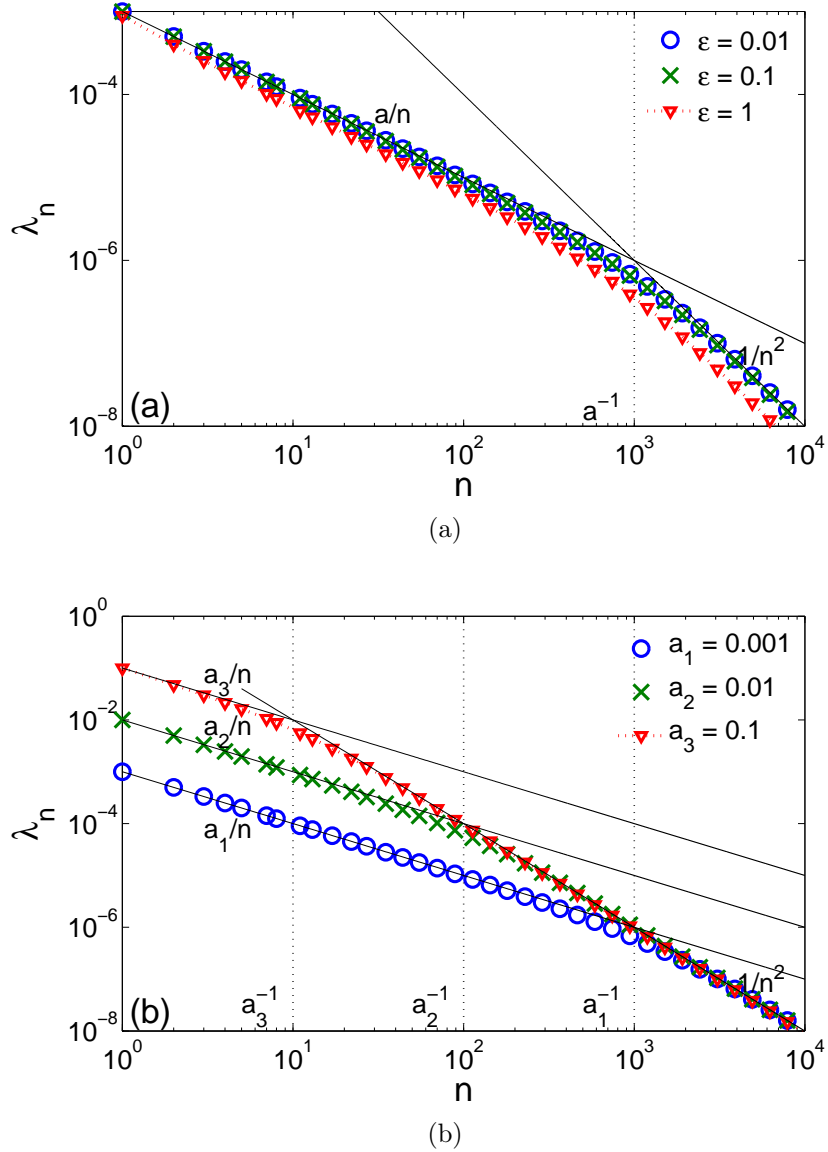


Figure 3.3: Eigenvalues λ_n of the operator $V\tilde{T}V$ for (a) $a = 0.001$ and three values ϵ : 0.01 (circles), 0.1 (crosses), and 1 (triangles); and (b) for $\epsilon = 0.01$ and three values of a : 0.001 (circles), 0.01 (crosses), and 0.1 (triangles). Solid lines show the asymptotic relations a/n and $1/n^2$, while vertical dotted lines indicate the separation $1/a$ between these asymptotic regimes. The coefficient A_ϵ in front of n^{-2} relation (see (3.3.6)) is close to 1 for all small targets, except for $\epsilon = 1$, see Eq. (3.3.7).

3.3. NUMERICAL ASYMPTOTIC BEHAVIOR

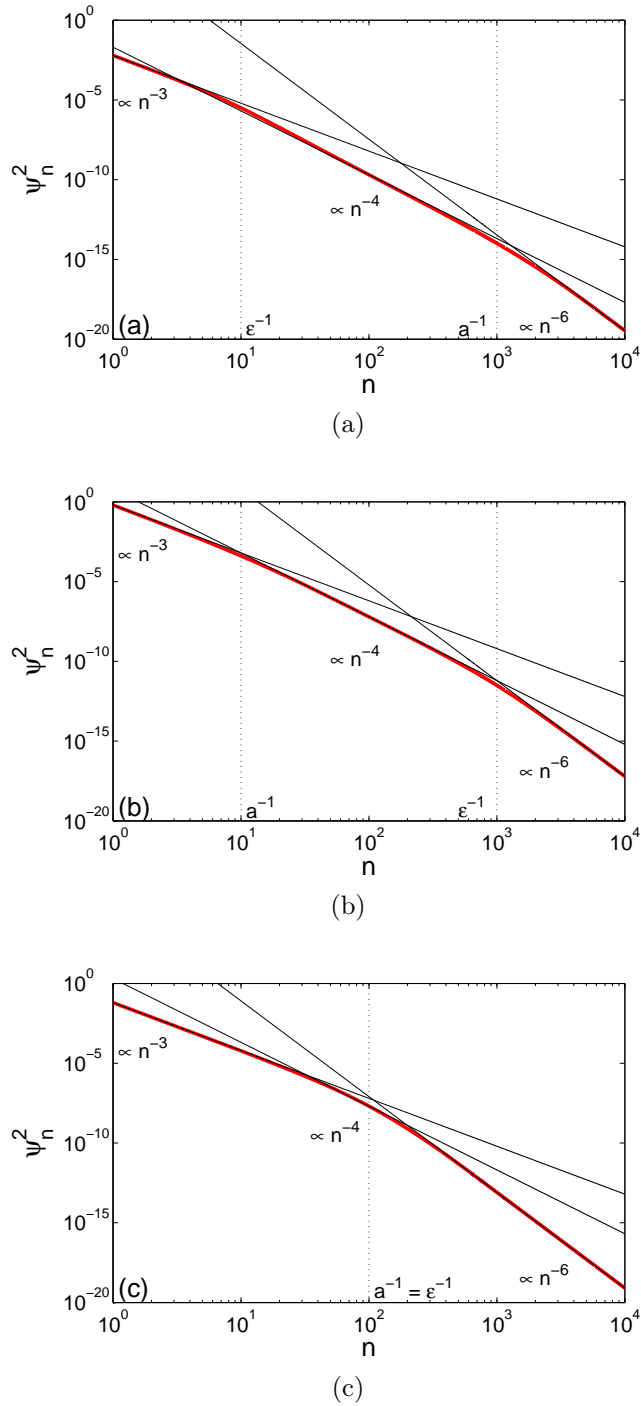


Figure 3.4: Spectral weights ψ_n^2 (shown by red solid line) for (a) $a = 0.001$ and $\epsilon = 0.1$; (b) $a = 0.1$ and $\epsilon = 0.001$; and (c) $a = \epsilon = 0.01$. In the first two plots, three asymptotic regimes can be distinguished according to Eqs. (3.3.8), (3.3.9), (3.3.10) while the intermediate regime disappears in the last plot.

(iii)

$$\psi_n^2 \simeq B_{a,\epsilon} n^{-6} \quad (\min\{na, n\epsilon\} \gg 1), \quad (3.3.10)$$

i.e., there exists c_3, n_3 such that for all n with $\min\{na, n\epsilon\} \geq n_3$, we have

$$\frac{1}{c_3} < \left| \frac{\psi_n^2}{B_{a,\epsilon} n^{-6}} \right| < c_3,$$

where $\tilde{B}_{a,\epsilon}, \tilde{B}'_{a,\epsilon}, B_{a,\epsilon}$ are constants.

In order to observe all three regimes, one needs $1 \ll \min\{1/a, 1/\epsilon\} \ll \max\{1/a, 1/\epsilon\}$, i.e., either $a \ll \epsilon \ll 1$, or $\epsilon \ll a \ll 1$. For instance, if a or ϵ is not small enough, the first regime with n^{-3} may not be well established (Fig. 3.4a, b). If $a \sim \epsilon$, the intermediate regime disappears, as illustrated on Fig. 3.4c. When $\epsilon \rightarrow 0$, $\max\{1/a, 1/\epsilon\} \rightarrow \infty$, the third regime disappears, and one retrieves two regimes for point-like targets.

The behavior of the coefficients $B_{a,\epsilon}$ and $\tilde{B}_{a,\epsilon}$ is shown on Fig. 3.5c,d. As expected from Eq. (3.3.3), $\tilde{B}_{a,\epsilon}/(2\pi a)$ approaches 1 as $\epsilon \rightarrow 0$ (point-like target). Moreover, such normalized coefficient weakly depends on a (at least for small a). The behavior of $B_{a,\epsilon}$ is more complicated. Given that \mathcal{T} should converge to the mean exit time for pure bulk diffusion, defined by $\langle t_1 \rangle_b$, as $a \rightarrow 0$ ($\langle t_1 \rangle_b = \lim_{a \rightarrow 0} \mathcal{T} = \lim_{a \rightarrow 0} \langle t_1 \rangle_{\lambda=\infty}$), from Eq. (3.2.70) one gets

$$\sum_{n \geq 1} \frac{\psi_n^2}{\lambda_n^2} \simeq \frac{2\pi D_2 \langle t_1 \rangle_b}{a}. \quad (3.3.11)$$

Since $\lambda_n \simeq A_\epsilon n^{-2}$ is independent of a , one concludes that $B_{a,\epsilon} \sim 1/a$ as $a \rightarrow 0$. For this reason, we plot $aB_{a,\epsilon}$ on Fig. 3.5c. For large ϵ , two curves for $a = 0.001$ and $a = 0.1$ do coincide, as expected. However, strong deviations emerge at small ϵ . In fact, one needs to consider much smaller a to get coinciding curves over the whole considered range of ϵ . We conclude that the reflection distance a plays an important role, especially for small targets.

Although the above asymptotic regimes for λ_n and ψ_n^2 remain conjectural, we will investigate their consequences for the asymptotic behavior of the mean exit time $\langle t_1 \rangle$. Using the asymptotic relations for large n , we get

$$\begin{aligned} \sum_{n \geq 1} \frac{\psi_n^2}{\lambda_n^2 (\lambda_n + \frac{D_1}{\lambda})} &\sim \int_1^\infty \frac{B_{a,\epsilon} x^{-6}}{A_\epsilon^2 x^{-4} (A_\epsilon x^{-2} + \frac{D_1}{\lambda})} dx \\ &= \frac{B_{a,\epsilon}}{A_\epsilon^3} \int_1^\infty \frac{dx}{1 + x^2 \frac{D_1}{\lambda A_\epsilon}} \sim \frac{B_{a,\epsilon}}{A_\epsilon^{5/2}} \frac{\pi}{2} \sqrt{\frac{\lambda}{D_1}}. \end{aligned} \quad (3.3.12)$$

Plugging (3.3.12) into (3.2.76), we get the asymptotic behavior of the mean exit time $\langle t_1 \rangle$

$$\langle t_1 \rangle = \mathcal{T} - \frac{C_1}{\sqrt{\lambda}} + O\left(\frac{1}{\lambda}\right), \quad (3.3.13)$$

3.3. NUMERICAL ASYMPTOTIC BEHAVIOR

where

$$C_1 = C_{a,\epsilon} \frac{\sqrt{D_1}}{D_2}, \quad C_{a,\epsilon} = (1 - (1 - a)^2) \frac{B_{a,\epsilon}}{8A_\epsilon^{5/2}}. \quad (3.3.14)$$

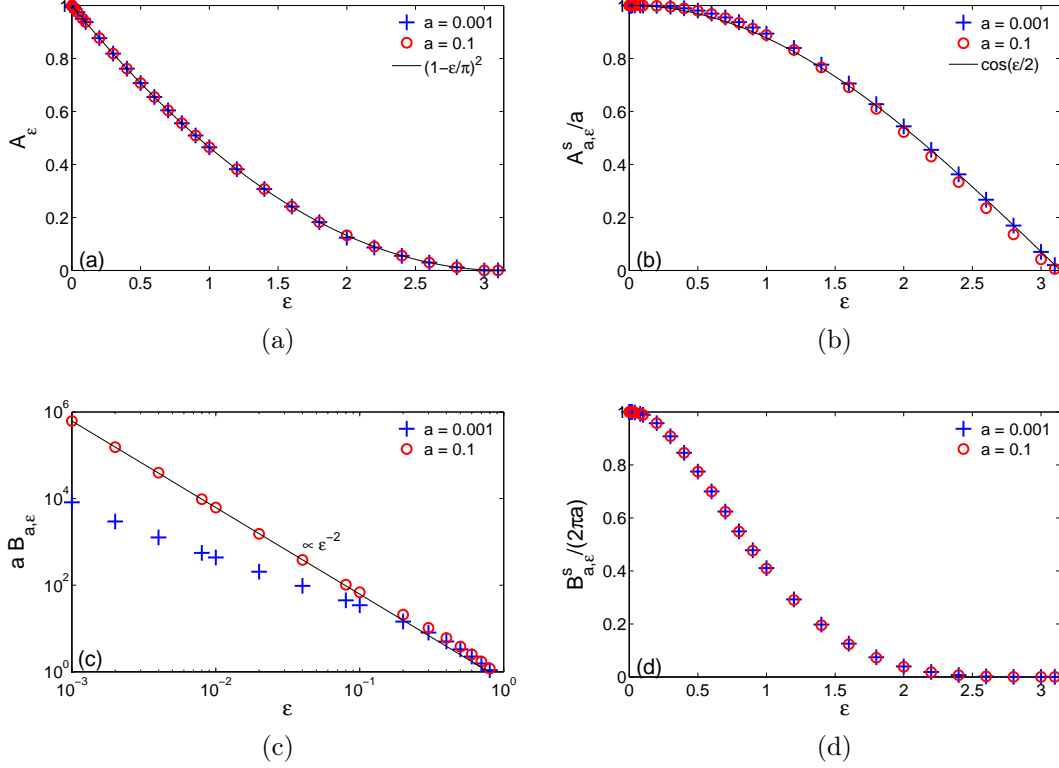


Figure 3.5: Coefficients A_ϵ , $\tilde{A}_{a,\epsilon}/a$, $aB_{a,\epsilon}$, and $\tilde{B}_{a,\epsilon}/a$ from Eqs. (3.3.5), (3.3.6) (3.3.8), (3.3.10) versus ϵ . Two curves for $a = 0.001$ and $a = 0.1$ coincide, that illustrates the independence of A_ϵ and \tilde{A}_ϵ/a of a .

For an accurate numerical computation of $\langle t_1 \rangle$, we consider the behavior of partial sums $f(N) = \sum_{n=1}^N \frac{\psi_n^2}{\lambda_n(\frac{D_1}{\lambda} + \lambda_n)}$ (note that $\langle t_1 \rangle$ is obtained in the limit $N \rightarrow \infty$ according to Eq. (3.2.68)). With the conjecture that $\psi_n^2 \sim n^{-6}$, we can check that for fixed λ ,

$$f(N) = f(\infty) - \frac{B_{a,\epsilon}}{A_\epsilon^2} \frac{1}{N} + \frac{B_{a,\epsilon}}{A_\epsilon^2} \left(\frac{D_1}{A_\epsilon \lambda} \right)^{3/2} \arctan \left(\sqrt{\frac{A_\epsilon \lambda}{D_1}} \frac{1}{N} \right) \quad (3.3.15)$$

$$= f(\infty) + \frac{c}{N} + o\left(\frac{1}{N}\right), \quad (3.3.16)$$

where $f(\infty) = \sum_{n=1}^{\infty} \frac{\psi_n^2}{\lambda_n(\frac{D_1}{\lambda} + \lambda_n)}$.

Indeed, we have that

$$f(\infty) = f(N) + \sum_{n=N}^{\infty} \frac{\psi_n^2}{\lambda_n \left(\frac{D_1}{\lambda} + \lambda_n \right)}. \quad (3.3.17)$$

Using again the asymptotic relations of λ_n and ψ_n^2 for large n , we obtain

$$\begin{aligned} \sum_{n=N}^{\infty} \frac{\psi_n^2}{\lambda_n \left(\frac{D_1}{\lambda} + \lambda_n \right)} &\sim \int_N^{\infty} \frac{B_{a,\epsilon} x^{-6}}{A_{\epsilon} x^{-2} \left(A_{\epsilon} x^{-2} + \frac{D_1}{\lambda} \right)} dx \\ &= \frac{B_{a,\epsilon}}{A_{\epsilon}^2} \int_N^{\infty} \frac{x^{-4} dx}{x^{-2} + \frac{D_1}{\lambda A_{\epsilon}}} \end{aligned} \quad (3.3.18)$$

By changing variable $t = x^{-1}$, we get

$$\begin{aligned} \sum_{n=N}^{\infty} \frac{\psi_n^2}{\lambda_n \left(\frac{D_1}{\lambda} + \lambda_n \right)} &\sim \frac{B_{a,\epsilon}}{A_{\epsilon}^2} \int_0^{1/N} \frac{t^2 dt}{t^2 + \frac{D_1}{\lambda A_{\epsilon}}} \\ &= \frac{B_{a,\epsilon}}{A_{\epsilon}^2} \left[\frac{1}{N} - \left(\frac{D_1}{\lambda A_{\epsilon}} \right)^{3/2} \arctan \left(\sqrt{\frac{A_{\epsilon} \lambda}{D_1}} \frac{1}{N} \right) \right], \end{aligned} \quad (3.3.19)$$

which implies Eq.(3.3.15).

In practice, we used the fourth order polynomial fit of $f(N)$ versus $1/N$ for N from 1000 to 20000 to extrapolate the value $f(\infty)$.

Figure 3.6 shows the mean exit time $\langle t_1 \rangle$ as a function of λ for a small target ($\epsilon = 0.01$) and two values of a : 0.01 and 0.001. In both cases, the mean exit time passes through a minimum at some intermediate desorption rate λ_c and then approaches the maximum as $\lambda \rightarrow \infty$. One can clearly see that the optimal value λ_c , as well as the height of the maximum at $\lambda \rightarrow \infty$, depend on a . Although both considered values $a = 0.001$ and $a = 0.01$ are small, the limiting mean exit time \mathcal{T} changes significantly. The asymptotic relation (3.3.13) (shown by thin solid lines) accurately captures the limiting behavior.

Furthermore, we consider the case of the double limit $\lambda \rightarrow \infty$ and $a \rightarrow 0$. When $\epsilon \rightarrow 0$, we use Eqs. (3.3.5) and (3.3.8) to get

$$\mathcal{T} = \frac{1 - (1 - a)^2}{4\pi D_2} \sum_{n \geq 1} \frac{\psi_n^2}{\lambda_n^2} \quad (3.3.20)$$

$$\begin{aligned} &= \frac{1 - (1 - a)^2}{4\pi D_2} \left(\sum_{n=1}^{1/\epsilon} \frac{\tilde{B}_{a,\epsilon} n^{-3}}{\tilde{A}_{a,\epsilon}^2 n^{-2}} + \sum_{n=1/\epsilon}^{\infty} \frac{\tilde{B}'_{a,\epsilon} n^{-4}}{\tilde{A}_{a,\epsilon}^2 n^{-2}} \right) \\ &= \frac{1 - (1 - a)^2}{4\pi D_2} \left(\frac{\tilde{B}_{a,\epsilon}}{\tilde{A}_{a,\epsilon}^2} \ln \frac{1}{\epsilon} + O(\epsilon) \right). \end{aligned} \quad (3.3.21)$$

3.3. NUMERICAL ASYMPTOTIC BEHAVIOR

This logarithmic divergence is similar to the result from Ref. [22, 20, 21] which describes the mean exit time for non-intermittent pure bulk diffusion (2D Brownian motion) in the narrow escape limit ($\epsilon \rightarrow 0$). Interestingly, the double limit can be taken separately: as $\lambda \rightarrow \infty$, the limiting value \mathcal{T} exists for any finite a .

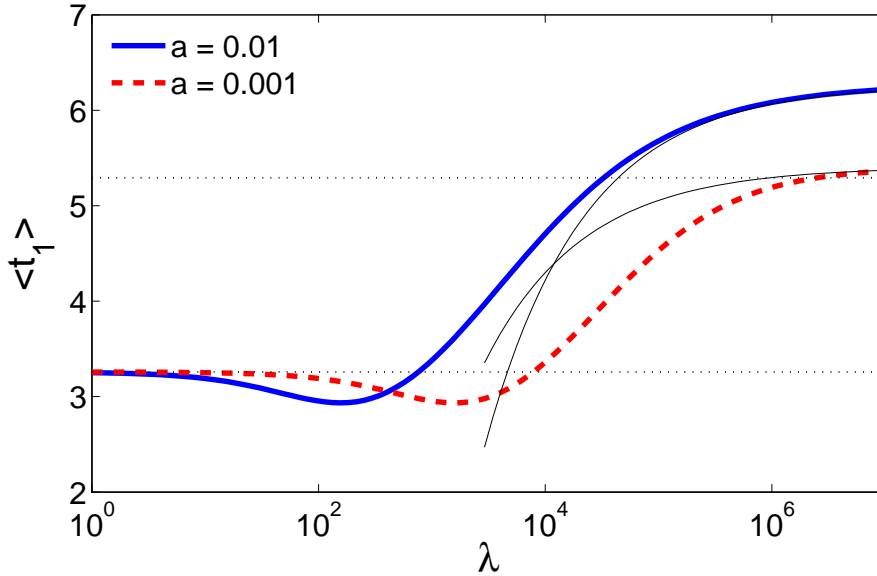


Figure 3.6: The mean exit time $\langle t_1 \rangle$ as a function of λ for $\epsilon = 0.01$, $D_1 = D_2 = 1$, and two values of a : 0.01 (solid line) and 0.001 (dashed line). Two horizontal lines indicate the mean exit times for surface diffusion $\langle t_1 \rangle_{\lambda=0} \approx 3.2586$ from Eq.(3.2.66) and for pure bulk diffusion $\langle t_1 \rangle_b = \lim_{a \rightarrow 0} \langle t_1 \rangle_{\lambda=\infty} \approx 5.2929$ from which showed in [3]. Thin lines show the asymptotic behavior (3.3.13) where \mathcal{T} and C_1 are computed from Eqs. (3.2.70), (3.3.14).

Chapter 4

3D-CASE

Chapter 4 is the analogue of chapter 3 for the sphere (Fig. 4.1). We investigate here the analogous problem, that is we consider the given system of equations of the exit time on the sphere (which has been shown in [2]) and by using self-adjoint operators, we find the spectral representation for $\langle t_1 \rangle$. As in the case of the disk, we can prove that $\langle t_1 \rangle_{\epsilon > 0}$ is eventually increasing to a finite limit \mathcal{T} at $\lambda \rightarrow \infty$.

Since we improve the model from 2-D into 3-D, in this chapter, we also study the numerical asymptotic behavior of $\langle t_1 \rangle_{\epsilon > 0}$ and obtain $\langle t_1 \rangle_{\epsilon > 0} = \mathcal{T} - \frac{C_1}{\sqrt{\lambda}} + O\left(\frac{1}{\lambda}\right)$.

The main differences between the 3-D case and the 2-D one are that:

- In a sphere, a point-like target ($\epsilon = 0$) is not reachable neither from the bulk nor from the surface.

In 2-D case, a random variable $X(\theta, \omega)$, which is the time for a particle starts at position θ from the 1-D surface to reach a point-like target, is finite almost surely and $t_1(\theta) = \int X(\theta, \omega) dP(\omega) = E[X(\theta, \omega)]$ is also finite but $\langle t_1 \rangle \rightarrow +\infty$ as $\lambda \rightarrow +\infty$.

In 3-D case, it is intuitively clear that the time to reach the point-like target either from the surface or from the bulk is infinite almost surely because the Brownian motion does not hit a point neither in 2-D nor in 3-D. This implies that $t_1 = E[X(\theta, \omega)] = \infty$ and $\langle t_1 \rangle = +\infty$, where $X(\theta, \omega)$ is the time for a particle to reach the point-like target from the 2-D surface. We can retrieve that $t_1 = +\infty$ by computation using the spectral representation for t_1 (see section 4.1.1).

- The role played by $(\cos n\theta)$ in 2-D is now replaced by the Legendre polynomials $(P_n(x))$.

In 2-D, we use the $\{\cos n\theta\}$ as an orthogonal basis in $L^2([0, \pi])$. It has an important role in solving Laplace equation on \mathbb{R}^2 , since $\{\cos n\theta\}$ are the eigenfunctions of the Laplacian Δ_{S^1} on the sphere \mathbb{S}^1 (defined in (3.2.6)).

In 3-D, we have to solve the Laplacian in \mathbb{R}^3 . By cylindrical symmetry, our problem becomes solving the Laplacian Δ^1 on $L^2([0, 1] \times [0, \pi])$ (defined in (2.1.3)) which depends only on two variables: the radius distance r and the polar angle θ (see Example 2.1.2 in the Mathematical Backgrounds). It would

be useful if we use the eigenfunctions of the Laplacian $\Delta_{S^2}^1$ on the sphere S^2 (defined in (2.1.6)), which are the Legendre polynomials $\{P_n(\cos \theta)\}$ as an orthogonal basis to solve the problem. By changing the variable $x = \cos \theta$, the space $L^2([0, \pi], \sin \theta d\theta)$ changes into $L^2([-1, 1], dx)$ and the Legendre polynomials we considered are now $\{P_n(x)\}$ (see Example 2.1.2 in the Mathematical Backgrounds).

The self-adjoint operators T that we introduce in each chapter is a particular case for the inverse of the Laplacians Δ_{S^1} on the boundary S^1 (2-D), or $\Delta_{S^2}^1$ on the boundary S^2 (3-D). Therefore, investigating each problem in the basis set by the eigenvectors of the Laplacian $\Delta_{S^1}^{-1}$ (in 2-D) and $\Delta_{S^2}^{-1}$ (in 3-D) plays an important role.

However, finding the eigenvalues and eigenvectors of operator T in this chapter is not obvious. We have a much more limited knowledge of the quantities involved in 3-D than in 2-D. For instance, in 2-D, we know the exact value of $\lambda_n(\tilde{T}) = \frac{(1-\epsilon/\pi)^2}{n(n+1)} \sim A_\epsilon n^{-2}$ and we are able to show that the coefficient $A_\epsilon = \left(1 - \frac{\epsilon}{\pi}\right)^2$, converges to 1 as $\epsilon \rightarrow 0$, while in 3-D we cannot. Besides, the numerical computation becomes more complicated with the Legendre polynomials $P_n(x)$ than with $\cos n\theta$. This leads us to limit the numerical computation to $\epsilon < 0.7$.

- Considering the numerical asymptotic behavior of the eigenvalues λ_n and the spectral weights ψ_n leads us to draw out the asymptotic behavior of \mathcal{T} as $\epsilon \rightarrow 0$. In 2-D, we showed that $\mathcal{T} \sim \ln \frac{1}{\epsilon}$ when $a \rightarrow 0$. In 3-D, we will show that when $a \rightarrow 0$ for small ϵ , $\mathcal{T} \sim \frac{1}{\epsilon}$ (Eq. (4.2.11)).

As we shall see the rest is similar.

4.1 A self-adjoint operator formulation

Similar to 2D case, we introduce the model for the intermittent dynamics for 3D case as follows:

The particle moves in a sphere of radius 1. Let ϵ, a be small positive numbers. The target is a small region of the sphere such that the elevation angle (in standard spherical coordinates) is between 0 and ϵ .

The starting point (θ, ϕ) is chosen on the surface of the unit sphere. If it is inside the target, the process is immediately stopped. If not then the particle moves on the surface of the sphere according to a 2-D Brownian motion with speed D_1 for a duration of $\min(T, \tau)$ where T is a random variable with exponential law of parameter $\lambda > 0$ and τ is the hitting time of the target. If $\tau \leq T$ then the process stops. If $\tau > T$ then we move the particle at time T along the normal inside the sphere at a distance a and start there a 3-D Brownian motion with speed D_2 stopped when we hit back the boundary, from there we start the same procedure. Due to the cylindrical symmetry, our problem is independent of the azimuthal angle ϕ . We define $t_1(\theta)$ as being the expected time to reach the target. Similarly we define, for

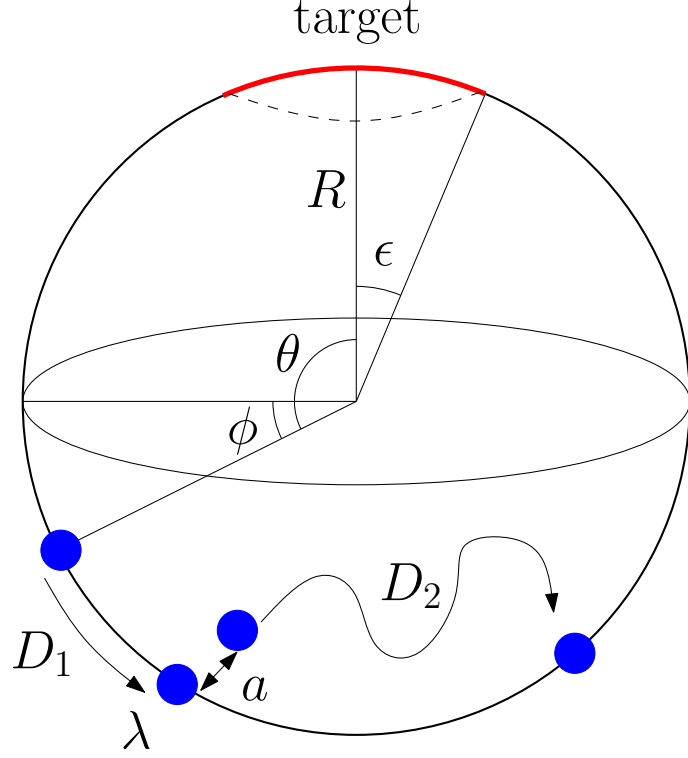


Figure 4.1: Surface-mediated diffusion in 3-D case

$0 \leq r < 1$ and $\theta \in \mathbb{R}$, $t_2(r, \theta)$ as the expected time necessary to reach the target starting at the point $z = (r, \theta)$.

Two functions $t_1(\theta)$ and $t_2(r, \theta)$ satisfy the following system of equations (see Ref. [2]):

$$\left\{ \begin{array}{l} D_1 \left(\frac{\partial^2 t_1}{\partial \theta^2} + \frac{1}{\tan \theta} \frac{\partial t_1}{\partial \theta} \right) + \lambda [t_2(1 - a, \theta) - t_1(\theta)] = -1 \text{ for } \theta \in [\epsilon, \pi] \end{array} \right. \quad (4.1.1)$$

$$\left\{ \begin{array}{l} D_2 \left(\frac{\partial^2}{\partial r^2} + \frac{2}{r} \frac{\partial}{\partial r} + \frac{1}{r^2} \frac{\partial^2}{\partial \theta^2} + \frac{1}{r^2} \frac{1}{\tan \theta} \frac{\partial}{\partial \theta} \right) t_2(r, \theta) = -1 \end{array} \right. \quad (4.1.2)$$

$$\left\{ \begin{array}{l} t_2(1, \theta) = t_1(\theta) \text{ } (\theta \in [0, \pi]) \end{array} \right. \quad (4.1.3)$$

$$\left\{ \begin{array}{l} t_1(\theta) = 0 \text{ if } \theta \in [0, \epsilon] \end{array} \right. \quad (4.1.4)$$

Let us put $x = \cos \theta$ then the space $L^2([0, \pi], -\sin \theta d\theta)$ transforms to $L^2([-1, 1], dx)$.

The original equations thus become

$$\begin{cases} D_1 \frac{d}{dx} \left((1-x^2) \frac{dt_1}{dx} \right) + \lambda [t_2(1-a, x) - t_1(x)] = -1 \text{ for } x \in [-1, \alpha_\epsilon], & (4.1.5) \\ D_2 \left(\frac{d^2 t_2(r, x)}{dr^2} + \frac{2}{r} \frac{dt_2(r, x)}{dr} + \frac{1}{r^2} \frac{d}{dx} \left((1-x^2) \frac{dt_2(r, x)}{dx} \right) \right) = -1, & (4.1.6) \\ t_2(1, x) = t_1(x), & (4.1.7) \\ t_1(x) = 0 \text{ for } x \in [\alpha_\epsilon, 1], & (4.1.8) \end{cases}$$

where

$$\alpha_\epsilon = \cos \epsilon. \quad (4.1.9)$$

In order to solve Eq. (4.1.6), we write $t_2(r, x)$ as $u(r) + v(r, x)$ where $u(r) = \frac{1-r^2}{6D_2}$ is the particular solution to the inhomogeneous (Poisson) equation $\Delta u = -\frac{1}{D_2}$, $u|_{\partial S} = 0$, and $v(r, x)$ is the solution to the Dirichlet problem $\Delta v = 0$, $v|_{\partial S} = t_1$.

Using the Legendre polynomial for the expansion of t_1 we get

$$t_1(x) = \sum_{n \geq 0} a_n P_n(x), \quad (4.1.10)$$

where P_n stands for the Legendre polynomial of order n . Then, we can rewrite t_2 in the following form

$$t_2(r, x) = \frac{1-r^2}{6D_2} + \sum_{n \geq 0} r^n a_n P_n(x). \quad (4.1.11)$$

We again define operators U, V on $L^2([-1, 1])$ which satisfy that $U = V^2$

$$U \left(\sum_{n \geq 0} a_n P_n(x) \right) = \sum_{n \geq 1} a_n (1 - (1-a)^n) P_n(x), \quad (4.1.12)$$

$$V \left(\sum_{n \geq 0} a_n P_n(x) \right) = \sum_{n \geq 1} a_n \sqrt{1 - (1-a)^n} P_n(x). \quad (4.1.13)$$

By using these operators, Eq. (4.1.5) thus is rewritten as

$$D_1 \frac{d}{dx} \left((1-x^2) \frac{dt_1}{dx} \right) = -1 - \lambda \frac{1 - (1-a)^2}{6D_2} + \lambda U(t_1), \quad (4.1.14)$$

We hence get the solution t_1

$$t_1 = \frac{1}{D_1} \left(1 + \lambda \frac{1 - (1-a)^2}{6D_2} \right) \tilde{T}(1) - \frac{\lambda}{D_1} \tilde{T}U(t_1). \quad (4.1.15)$$

where \tilde{T} is defined by

$$\tilde{T} = -\mathcal{E}T\mathcal{R}, \quad (4.1.16)$$

with T is an operator defined on $L^2([-1, \alpha_\epsilon])$, $Tf = y$ means

$$\begin{cases} \frac{d}{dx} \left((1-x^2) \frac{dy}{dx} \right) = f(x); x \in [-1, \alpha_\epsilon] \\ y(\alpha_\epsilon) = 0 \text{ and } y \text{ does not blow up at } x = -1, \end{cases} \quad (4.1.17)$$

$$(4.1.18)$$

the operator $\mathcal{R} : L^2([-1, 1]) \rightarrow L^2([-1, \alpha_\epsilon])$ is the natural restriction, and $\mathcal{E} : L^2([-1, \alpha_\epsilon]) \rightarrow L^2([-1, 1])$ is the natural extension by 0.

We note that T is a compact, self-adjoint and non-positive operator, by the same method as in 2-D, we get that \tilde{T} is an self-adjoint, non-negative operator on $L^2([-1, 1])$. We next apply the operator V to both sides of Eq. (4.1.15) to get, writing $s_1 = V(t_1)$,

$$s_1 = \frac{1}{D_1} \left(1 + \lambda \frac{1 - (1-a)^2}{6D_2} \right) V\tilde{T}(1) - \frac{\lambda}{D_1} V\tilde{T}V(s_1), \quad (4.1.19)$$

which can be solved in s_1 as

$$s_1 = \frac{1}{D_1} \left(1 + \lambda \frac{1 - (1-a)^2}{6D_2} \right) \left(I + \frac{\lambda}{D_1} V\tilde{T}V \right)^{-1} (\psi), \quad (4.1.20)$$

where $\psi = V\tilde{T}(1)$.

The property self-adjoint of the operator $V\tilde{T}V$ allows us to invert the operator $(I + \frac{\lambda}{D_1} V\tilde{T}V)$ in Eq. (4.1.20) and to express the mean exit time in a spectral form. We are interested in the case of a randomly distributed starting point on the sphere with uniform law which equivalentents to averaging the mean exit time over the starting points as

$$\langle t_1 \rangle = \frac{1}{2} \int_{-1}^1 t_1(x) dx = \frac{1}{2} \langle t_1, 1 \rangle. \quad (4.1.21)$$

Using Eqs. (4.1.15) and (4.1.20), we can write

$$\begin{aligned} 2\langle t_1 \rangle &= \frac{1}{D_1} \left(1 + \lambda \frac{1 - (1-a)^2}{6D_2} \right) \langle \tilde{T}(1), 1 \rangle - \frac{\lambda}{D_1} \langle \tilde{T}V(s_1), 1 \rangle \\ &= \frac{1}{D_1} \left(1 + \lambda \frac{1 - (1-a)^2}{6D_2} \right) \langle \tilde{T}(1), 1 \rangle - \frac{\lambda}{D_1} \langle s_1, \psi \rangle, \end{aligned} \quad (4.1.22)$$

from which it follows that the knowledge of s_1 allows to compute $\langle t_1 \rangle$:

$$\langle t_1 \rangle = \frac{1}{2D_1} \left(1 + \lambda \frac{1 - (1-a)^2}{6D_2} \right) \left(\langle \tilde{T}(1), 1 \rangle - \frac{\lambda}{D_1} \left\langle \left(I + \frac{\lambda}{D_1} V\tilde{T}V \right)^{-1} \psi, \psi \right\rangle \right). \quad (4.1.23)$$

As the same reason as in $2D$ case, there is an orthonormal basis $(e_n)_{n \geq 0}$ on $L^2([-1, 1])$ of $\text{Im}(V\tilde{T}V)$ such that $V\tilde{T}Ve_n = \lambda_n e_n$ and $\lambda_n \downarrow 0$ as $n \rightarrow \infty$.

When $\epsilon = 0$ i.e. $\alpha_\epsilon = 1$, the eigenbasis (e_n) is Legendre polynomials of order n , $e_n = P_n(x)$. When $\epsilon > 0$ i.e. $\alpha_\epsilon < 1$, for $\psi = V\tilde{T}(1)$ defined in (4.1.20), one can prove that $\psi \in \text{Im}(V\tilde{T}V)$ as in 2-D and write

$$\psi = \sum_{n \geq 1} \psi_n e_n, \quad (4.1.24)$$

with coefficients $\psi_n = \langle \psi, e_n \rangle$ is a sequence in $\ell^2(\mathbb{N})$. Using this representation, we solve Eq. (4.1.20):

$$s_1 = \frac{1}{D_1} \left(1 + \lambda \frac{1 - (1-a)^2}{6D_2} \right) \sum_{n \geq 1} \frac{\psi_n}{1 + \frac{\lambda}{D_1} \lambda_n} e_n. \quad (4.1.25)$$

Plugging this expression into Eq. (4.1.23) we obtain

$$\langle t_1 \rangle = \frac{1}{2D_1} \left(1 + \lambda \frac{1 - (1-a)^2}{6D_2} \right) \left[\langle \tilde{T}(1), 1 \rangle - \frac{\lambda}{D_1} \sum_{n \geq 1} \frac{\psi_n^2}{1 + \frac{\lambda}{D_1} \lambda_n} \right]. \quad (4.1.26)$$

In the following subsections, we investigate the asymptotic behavior of the mean exit time for the cases of $\epsilon = 0$ and $\epsilon > 0$ by using this spectral representation.

4.1.1 Point-like target ($\epsilon = 0$ or $\alpha_\epsilon = 1$)

In this situation, a target is unreachable either from the bulk or from the surface. A mathematical explanation can be seen as follows.

We note that the operator \tilde{T} can be written explicitly as

$$\tilde{T}(f)(\theta) = \begin{cases} \int_x^{\alpha_\epsilon} \frac{1}{1-x_1^2} \left(\int_{-1}^{x_1} f(x_2) dx_2 \right) dx_1, & -1 \leq x < \alpha_\epsilon, \\ 0, & \alpha_\epsilon \leq x \leq 1. \end{cases} \quad (4.1.27)$$

From which, refer to [2], we can get for $n \geq 1$

$$\tilde{T}(P_n)(x) = \begin{cases} -T(P_n)(x) = \int_x^{\alpha_\epsilon} \frac{1}{1-x_1^2} \left(\int_{-1}^{x_1} P_n(x_2) dx_2 \right) dx_1 = \frac{P_n(x) - P_n(\alpha_\epsilon)}{n(n+1)}, & -1 \leq x < \alpha_\epsilon, \\ 0, & \alpha_\epsilon \leq \theta \leq 1, \end{cases} \quad (4.1.28)$$

and for $n = 0$

$$\tilde{T}(P_0)(x) = \tilde{T}(1)(x) = \begin{cases} -T(1)(x) = \int_x^{\alpha_\epsilon} \frac{1}{1-x_1^2} \left(\int_{-1}^{x_1} dx_2 \right) dx_1 = \ln \frac{1-x}{1-\alpha_\epsilon}, & -1 \leq x < \alpha_\epsilon, \\ 0, & \alpha_\epsilon \leq x \leq 1. \end{cases} \quad (4.1.29)$$

In the case of $\epsilon = 0$, one easily gets

$$\begin{cases} \tilde{T}(P_n)(x) = -T(P_n)(x) = \frac{1}{n(n+1)} [P_n(x) - 1] & (n \geq 1), \\ \tilde{T}(1)(x) = -T(1)(x) = +\infty & (n = 0). \end{cases} \quad (4.1.30)$$

Assume that operator $\left(I + \frac{\lambda}{D_1} \tilde{T}U\right)^{-1}$ exists then (4.1.15) can be rewritten as

$$t_1 = \frac{1}{D_1} \left(1 + \lambda \frac{1 - (1-a)^2}{6D_2}\right) \left(I + \frac{\lambda}{D_1} \tilde{T}U\right)^{-1} \tilde{T}(1) \quad (4.1.31)$$

The right-hand side of (4.1.31) equals to infinity because of (4.1.30). It implies that $t_1(x)$ must be infinity when $\alpha_\epsilon = 1$ and certainly, $\langle t_1 \rangle_{\epsilon=0} = \langle t_1 \rangle_{\alpha_\epsilon=1} = +\infty$.

4.1.2 Extended target ($\epsilon > 0$ or $\alpha_\epsilon \in [-1, 1)$)

When $\epsilon > 0$, as for the disk, it can be shown that the mean exit time $\langle t_1 \rangle$ is eventually increasing to a finite limit \mathcal{T} as $\lambda \rightarrow \infty$.

Although in 3-D case, there are differences in definition of the operators V and \tilde{T} from 2-D case, we still can state the same theorem as Theorem 3.2.2 whose proof is completely the same in $L^2[-1, 1]$ space.

Theorem 4.1.1. *For (λ_n) defined as the eigenvalues of the operator $V\tilde{T}V$ and (ψ_n) defined as the spectral weight of the function $V\tilde{T}(1)$ in the orthonormal basis (e_n) of the operator $V\tilde{T}V$, where V and \tilde{T} are defined in (3.2.8) and (4.1.17) we have*

- (i) $\sum_{n \geq 1} \frac{\psi_n^2}{\lambda_n} = \langle \tilde{T}(1), 1 \rangle$,
- (ii) $\sum_{n \geq 1} \frac{\psi_n^2}{\lambda_n^2} < +\infty$,
- (iii) $\sum_{n \geq 1} \frac{\psi_n^2}{\lambda_n^3} = +\infty$.

We note that from (4.1.29) we have

$$\langle \tilde{T}(1), 1 \rangle = \int_{-1}^{\alpha_\epsilon} \tilde{T}(1) dx = \int_{-1}^{\alpha_\epsilon} \ln \frac{1-x}{1-\alpha_\epsilon} dx = 2 \left(\ln \frac{2}{1-\alpha_\epsilon} - \frac{1+\alpha_\epsilon}{2} \right). \quad (4.1.32)$$

We hence get the following remark from Eq. (4.1.26):

Remark 4.1.1. *The mean exit time for surface diffusion phase is:*

$$\langle t_1 \rangle_{\lambda=0} = \frac{1}{2D_1} \langle \tilde{T}(1), 1 \rangle = \frac{1}{D_1} \left(\ln \frac{2}{1-\alpha_\epsilon} - \frac{1+\alpha_\epsilon}{2} \right). \quad (4.1.33)$$

Due to theorem 4.1.1, we obtain the following Theorems 4.1.2 and 4.1.3 which can be proved in a similar way with Theorems 3.2.3 and 3.2.4.

Theorem 4.1.2. *The mean exit time $\langle t_1 \rangle$ defined by (4.1.26) converges to a finite limit \mathcal{T} as $\lambda \rightarrow \infty$, where*

$$\mathcal{T} := \lim_{\lambda \rightarrow \infty} \langle t_1 \rangle = \frac{1 - (1 - a)^2}{12D_2} \sum_{n \geq 1} \frac{\psi_n^2}{\lambda_n^2}. \quad (4.1.34)$$

Remark 4.1.2. *From Theorem 4.1.2 and Theorem 4.1.1, we obtain the asymptotic behavior for $\langle t_1 \rangle$:*

$$\langle t_1 \rangle = \mathcal{T} - \frac{D_1}{\lambda} \frac{1 - (1 - a)^2}{12D_2} \sum_{n \geq 1} \frac{\psi_n^2}{\lambda_n^2 (\lambda_n + \frac{D_1}{\lambda})} + \frac{S}{2\lambda} + o\left(\frac{1}{\lambda}\right), \quad (4.1.35)$$

where $S = \sum_{n \geq 1} \frac{\psi_n^2}{\lambda_n^2}$.

From Remark 4.1.2 and Theorems 4.1.1, 4.1.2 we obtain

Theorem 4.1.3. *The function $\lambda \mapsto \langle t_1 \rangle$, where $\langle t_1 \rangle$ defined in Eq. (4.1.26), is eventually increasing as $\lambda \rightarrow +\infty$. Moreover, if*

$$\left. \frac{d\langle t_1 \rangle}{d\lambda} \right|_{\lambda=0} < 0, \quad (4.1.36)$$

then the function $\langle t_1 \rangle$ passes through a minimum.

Figure 4.2 shows that there is a critical value of D_2 , $D_{2,crit}$, such that if $D_2 > D_{2,crit}$, the mean exit time $\langle t_1 \rangle$ first decreases with λ , passes through a minimum at $\lambda > 0$ and then increases to a finite limit. Vice versa, if $D_2 < D_{2,crit}$, the mean exit time monotonously increases with λ to a finite limit.

Thank to Theorem 4.1.3, we get the following remark:

Remark 4.1.3. *Theorem (4.1.3) allows us to determine the critical value for the bulk diffusion coefficient, $D_{2,crit}$, which bulk excursions are beneficial. The existence of the optimal value λ (that minimizes the function $\langle t_1 \rangle$) depends on this value. If $D_2 > D_{2,crit}$, with*

$$D_{2,crit} = D_1 \frac{(1 - (1 - a)^2) \langle \tilde{T}(1), 1 \rangle}{6 \|V\tilde{T}(1)\|^2} \quad (4.1.37)$$

Refer to Eq. (B.1.8), we have

$$\begin{aligned} \|V\tilde{T}(1)\|^2 &= \sum_{n=1}^{\infty} \psi_n^2 \\ &= \sum_{n \geq 1} \frac{(1 - (1 - a)^n) (2n + 1)}{4n^2(n + 1)^4} [(n + 1 + n\alpha_\epsilon)P_n(\alpha_\epsilon) + P_{n-1}(\alpha_\epsilon)]^2 \end{aligned} \quad (4.1.38)$$

Plugging (4.1.32) and (4.1.38) into (4.1.37), we obtain

$$D_{2,\text{crit}} = D_1 \frac{2(1 - (1 - a)^2)}{6} \left(\ln \frac{2}{1 - \alpha_\epsilon} - \frac{\alpha_\epsilon + 1}{2} \right) \left(\sum_{n \geq 1} \frac{(1 - (1 - a)^n)(2n + 1)}{4n^2(n + 1)^4} [(n + 1 + n\alpha_\epsilon)P_n(\alpha_\epsilon) + P_{n-1}(\alpha_\epsilon)]^2 \right)^{-1}, \quad (4.1.39)$$

then $\langle t_1 \rangle$ starts first to decrease with λ , passes through a minimum at $\lambda > 0$ then monotonously increases. We again retrieved the optimality condition for 3-D case reported in [1].

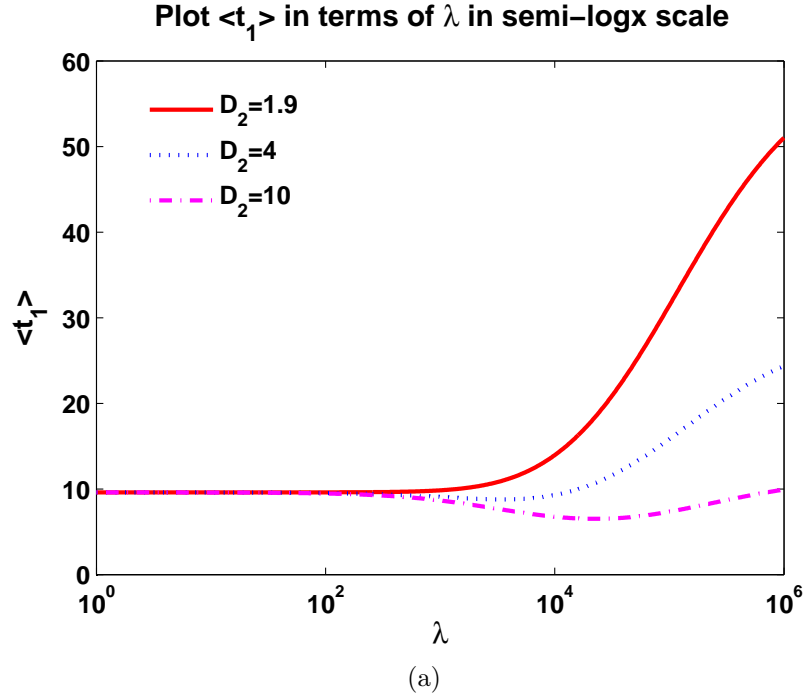


Figure 4.2: Mean exit time $\langle t_1 \rangle$ as a function of λ for $\epsilon = 0.01$ with $a = 0.001$ and $D_1 = 1$. When $D_2 = 1.9 < D_{2,\text{crit}} \approx 1.9997$ (blue solid line), $\langle t_1 \rangle$ monotonously increases with λ so that the smallest mean exit time corresponds to $\lambda = 0$ (surface diffusion without intermittence). When $D_2 = 4$ (or $D_2 = 10$) $> D_{2,\text{crit}}$ (red dashed line), $\langle t_1 \rangle$ starts first to decrease with λ , passes through a minimum and monotonously increases to infinity.

4.2 Numerical asymptotic behavior

This section aims to show the numerical asymptotic behavior of $\langle t_1 \rangle$ ($\epsilon > 0$) by investigating the asymptotic relations of λ_n and ψ_n (as in 2-D case). There are some restrictions in this 3-D case:

- Since the numerical computation becomes more complicated with the Legendre polynomials $P_n(x)$ (n big) in this 3-D case than with $\cos n\theta$ in 2-D case (see Section B.2) when ϵ is big ($\epsilon \geq 0.7$), we limit ourselves in the cases of $\epsilon \leq 0.7$.
- In 3-D case, we cannot give a rigorous proof for the asymptotic behavior of λ_n as $n \rightarrow \infty$ since we do not know the eigenvalues of the operator \tilde{T} , $\lambda_n(\tilde{T})$. However, we believe that $\psi_n^2 \sim \frac{1}{n^6}$ as $n \rightarrow \infty$ which as a result leads us to the asymptotic behavior $\mathcal{T} - \langle t_1 \rangle_{\epsilon > 0} \sim \frac{1}{\sqrt{\lambda}}$ (see (4.2.9) and (4.2.10)).

The difference compares to 2-D case is the behavior of the mean exit time for non-intermittent pure bulk diffusion $\mathcal{T} \sim 1/\epsilon$ (see Eq. (4.2.11)) while in 2-D case, we have $\mathcal{T} \sim \ln(1/\epsilon)$.

We can see Appendix B.2 for computational details of the eigenvalues λ_n and the spectral weight ψ_n^2 .

We first plot λ_n versus n (in the log-log scale) (Fig. 4.3) and observe that there are two distinguish regimes for the eigenvalues λ_n , for small and large n :

(i)

$$\lambda_n \simeq \tilde{A}_{a,\epsilon} n^{-1} \quad (na \ll 1), \quad (4.2.1)$$

i.e. there exists c_1, n_1, ϵ_1 such that for all $n \geq n_1$ but $na < \epsilon_1$, we have

$$\frac{1}{c_1} < \left| \frac{\lambda_n}{\tilde{A}_{a,\epsilon}} \right| < c_1,$$

(ii)

$$\lambda_n \simeq A_\epsilon n^{-2} \quad (na \gg 1), \quad (4.2.2)$$

i.e., there exists c_2, n_2, ϵ_2 such that for all n with $na \geq n_2$, we have

$$\frac{1}{c_2} < \left| \frac{\lambda_n}{A_\epsilon} \right| < c_2,$$

where $\tilde{A}_{a,\epsilon}$ and A_ϵ are two constants.

From Fig. 4.3, we can see that A_ϵ does not depend on a and it is close to 1 when ϵ is close to 0. We also can state a conjecture that the transition between two asymptotic regimes is determined by $1/a$ (and is independent of ϵ).

In the case of the sphere, we do not have the explicit computation of $\lambda_n(\tilde{T})$. Therefore, we cannot find the exact formula of A_ϵ . Nevertheless, since the operator \tilde{T} does

4.2. NUMERICAL ASYMPTOTIC BEHAVIOR

not depend on a A_ϵ does not depend on a , moreover, the numerical results suggest that $A_\epsilon \rightarrow 1$ as $\epsilon \rightarrow 0$ (see Fig. 4.5a).

We then plot ψ_n^2 versus n (in the log-log scale) (Fig.4.4). In 3-D case, the asymptotic behavior of ψ_n^2 is more complicated than in 2-D case. We can distinguish three asymptotic regimes:

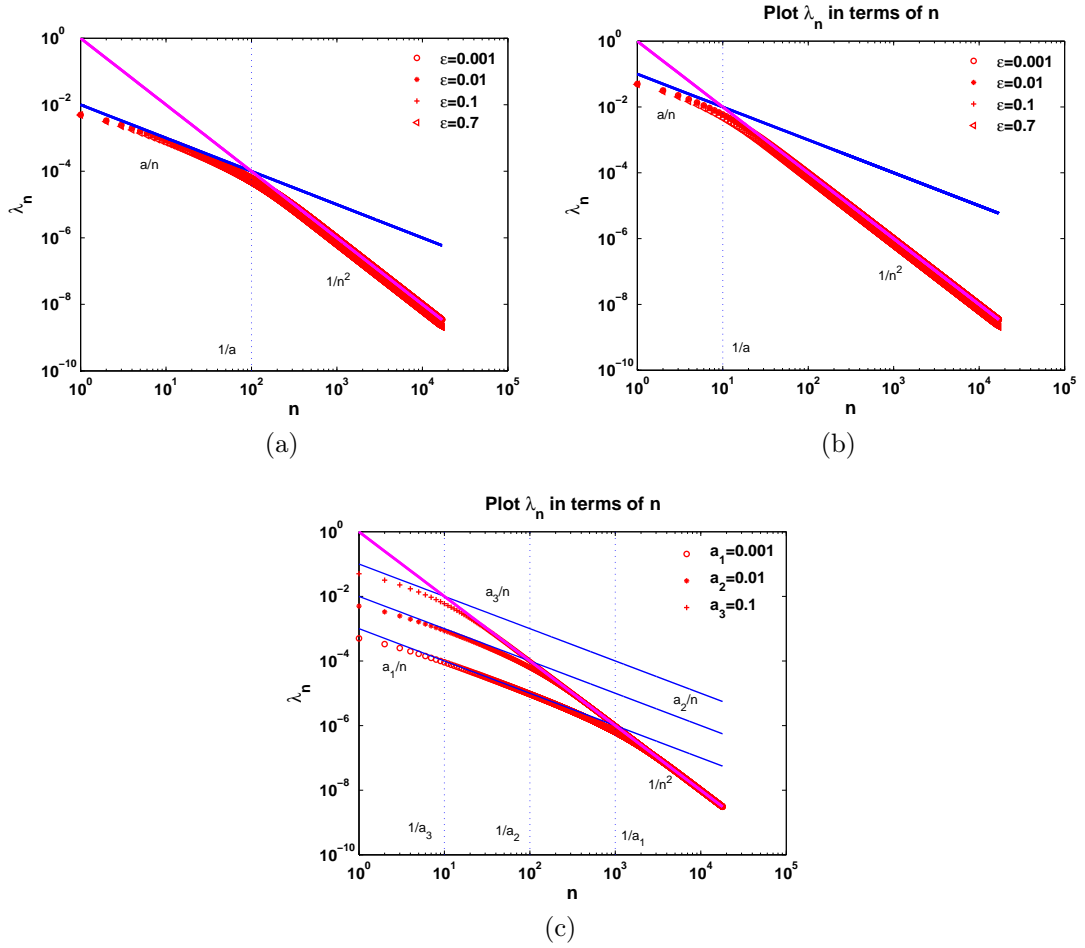


Figure 4.3: Eigenvalues λ_n of the operator $V\tilde{T}V$ for (a) $a = 0.01$ and four values ϵ : 0.001 (circles), 0.01 (stars), 0.1 (plus), and 0.7 (triangles); (b) $a = 0.1$ and four values ϵ : 0.001 (circles), 0.01 (stars), 0.1 (plus), and 0.7 (triangles); and (c) for $\epsilon = 0.01$ and three values of a : 0.001 (circles), 0.01 (stars), and 0.1 (plus). Solid lines show the asymptotic relations a/n and $1/n^2$, while vertical dotted lines indicate the separation $1/a$ between these asymptotic regimes. The coefficient A_ϵ in front of n^{-2} relation is close to 1 for all small targets, see (4.2.2).

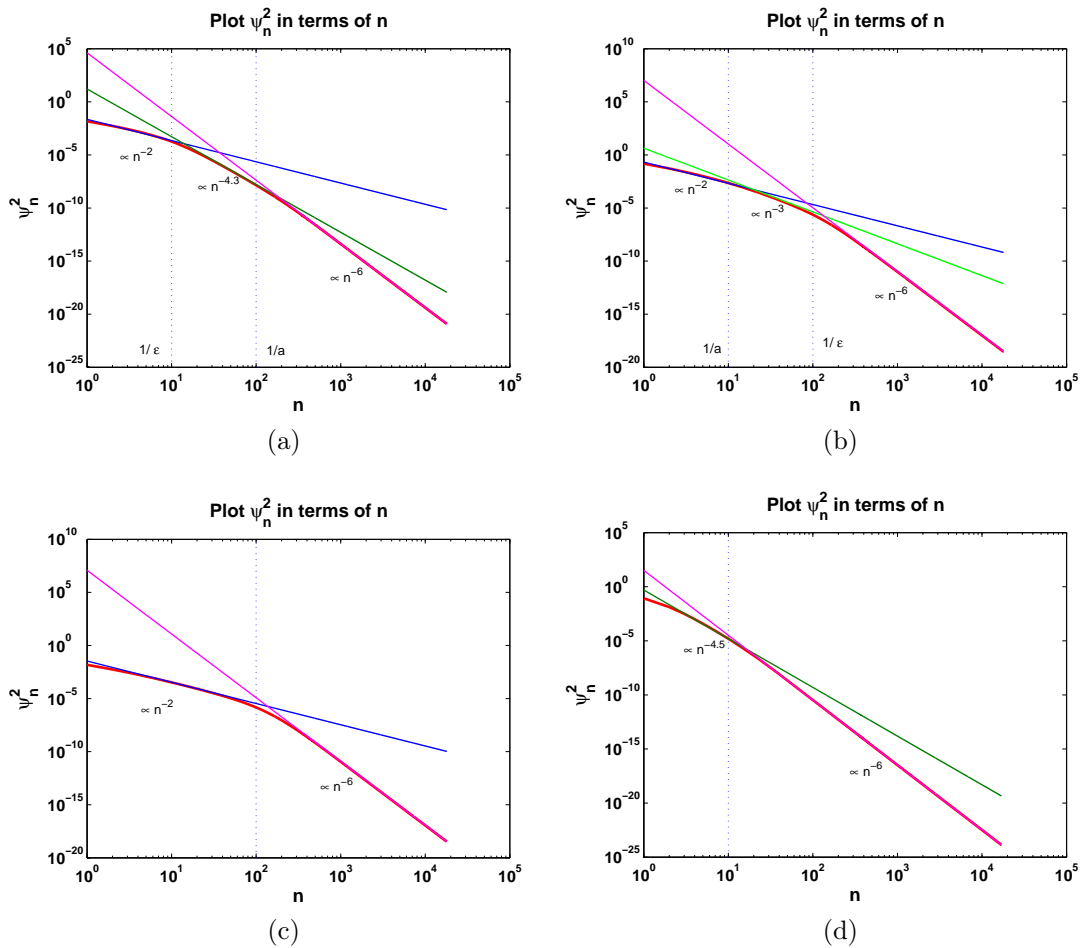


Figure 4.4: Spectral weights ψ_n^2 (shown by red solid line) for **(a)** $a = 0.01$ and $\epsilon = 0.1$; **(b)** $a = 0.1$ and $\epsilon = 0.01$; **(c)** $a = \epsilon = 0.01$; and **(d)** $a = 0.1$ and $\epsilon = 0.7$. In the first two plots, three asymptotic regimes can be distinguished according to Eqs. (4.2.3), (4.2.4), (4.2.5), while the intermediate regime disappears in the third plot and the first regime disappears in the last plot.

(i)

$$\psi_n^2 \sim \tilde{B}_{a,\epsilon} n^{-2} \quad (\max\{na, n\epsilon\} \ll 1), \quad (4.2.3)$$

i.e., there exists c'_1, n'_1, ϵ'_1 such that for all $n \geq n'_1$ and $\max\{na, n\epsilon\} < \epsilon'_1$, we have

$$\frac{1}{c'_1} < \left| \frac{\psi_n^2}{\tilde{B}_{a,\epsilon} n^{-2}} \right| < c'_1,$$

(ii)

$$\psi_n^2 \sim \tilde{B}'_{a,\epsilon} n^{-\alpha} \quad (\min\{na, n\epsilon\} \ll 1 \ll \max\{na, n\epsilon\}), \quad (4.2.4)$$

i.e., there exists c'_2, n'_2, ϵ'_2 such that for all n with $\max\{na, n\epsilon\} \geq n'_2$ and $\min\{na, n\epsilon\} < \epsilon'_2$, we have

$$\frac{1}{c'_2} < \left| \frac{\psi_n^2}{\tilde{B}'_{a,\epsilon} n^{-\alpha}} \right| < c'_2, \quad (3 \leq \alpha \leq 4.5),$$

(iii)

$$\psi_n^2 \sim B_{a,\epsilon} n^{-6} \quad (\min\{na, n\epsilon\} \gg 1), \quad (4.2.5)$$

i.e., there exists c'_3, n'_3, ϵ'_3 such that for all n with $\max\{na, n\epsilon\} \geq n'_3$, we have

$$\frac{1}{c'_3} < \left| \frac{\psi_n^2}{B_{a,\epsilon} n^{-6}} \right| < c'_3,$$

where $\tilde{B}_{a,\epsilon}, \tilde{B}'_{a,\epsilon}, B_{a,\epsilon}$ are constants.

The second regime is not easy to observe: when $\epsilon \ll a$, the power law α seems to be 3; otherwise, when $a \ll \epsilon$, $\alpha \sim 4.5$.

If $1 \ll \min\{1/a, 1/\epsilon\} \ll \max\{1/a, 1/\epsilon\}$, i.e., either $a \ll \epsilon \ll 1$, or $\epsilon \ll a \ll 1$ then we can observe all three regimes. If a or ϵ is not small enough, the first regime with n^{-2} may not be well established (Fig. 4.4d). If $a \sim \epsilon$, the second regime disappears, as illustrated on Fig. 4.4c. Fig. 4.4a,b show the difference in the second regime between the case of $a \ll \epsilon$ and $a \gg \epsilon$. When $\epsilon \rightarrow 0$, $\max\{1/a, 1/\epsilon\} \rightarrow \infty$, the third regime disappears, and one retrieves two regimes for point-like targets ($\epsilon = 0$).

When $\epsilon = 0$, we can obtain the asymptotic behavior of ψ_n^2 from their explicit computation (refer to Eqs. (B.2.7), (B.2.8) with $\epsilon = 0$):

(i)

$$\psi_n^2 \sim \tilde{B}_a n^{-2} \quad (na \ll 1), \quad (4.2.6)$$

4.2. NUMERICAL ASYMPTOTIC BEHAVIOR

i.e., there exists c'_1, n'_1, ϵ'_1 such that for all $n \geq n'_1$ and $na < \epsilon'_1$, we have

$$\frac{1}{c'_1} < \left| \frac{\psi_n^2}{\tilde{B}_a n^{-2}} \right| < c'_1,$$

(ii)

$$\psi_n^2 \sim \tilde{B}'_a n^{-3} \quad (na \gg 1), \quad (4.2.7)$$

i.e., there exists c'_2, n'_2, ϵ'_2 such that $na \geq n'_2$, we have

$$\frac{1}{c'_2} < \left| \frac{\psi_n^2}{\tilde{B}'_a n^{-3}} \right| < c'_2,$$

where $\tilde{B}_a, \tilde{B}'_a$ are constants.

In the same argument as on the disk, we get that

$$\sum_{n \geq 1} \frac{\psi_n^2}{\lambda_n^2} \simeq \frac{6D_2 \langle t_1 \rangle_b}{a}. \quad (4.2.8)$$

Since the eigenvalues $\lambda_n \simeq A_\epsilon n^{-2}$ is independent of a , it implies that $B_{a,\epsilon} \sim 1/a$ as $a \rightarrow 0$. Therefore, we plot $aB_{a,\epsilon}$ on Fig. 4.5b. The similar results as in 2-D are observed: for large ϵ , three curves for $a = 0.001$, $a = 0.01$ and $a = 0.1$ seem to be coincide, as expected, but strong deviations emerge at small ϵ . In conclusion, the reflection distance a plays an important role, especially for small targets.

Although above the asymptotic regimes for λ_n and ψ_n^2 remain conjectural, we investigate their consequences for the asymptotic behavior of the mean exit time. Using the asymptotic relations for large n , we get

$$\begin{aligned} \sum_{n \geq 1} \frac{\psi_n^2}{\lambda_n^2 (\lambda_n + \frac{D_1}{\lambda})} &\sim \int_1^\infty \frac{B_{a,\epsilon} x^{-6}}{A_\epsilon^2 x^{-4} (A_\epsilon x^{-2} + \frac{D_1}{\lambda})} dx \\ &= \frac{B_{a,\epsilon}}{A_\epsilon^3} \int_1^\infty \frac{dx}{1 + x^2 \frac{D_1}{\lambda A_\epsilon}} \sim \frac{B_{a,\epsilon}}{A_\epsilon^{5/2}} \frac{\pi}{2} \sqrt{\frac{\lambda}{D_1}}. \end{aligned}$$

From this asymptotic relation and Eq. (4.1.35), we obtain the asymptotic behavior for $\langle t_1 \rangle$,

$$\langle t_1 \rangle = \mathcal{T} - \frac{C_1}{\sqrt{\lambda}} + O\left(\frac{1}{\lambda}\right), \quad (4.2.9)$$

where

$$C_1 = C_{a,\epsilon} \frac{\sqrt{D_1}}{D_2}, \quad C_{a,\epsilon} = (1 - (1 - a)^2) \frac{B_{a,\epsilon}}{8A_\epsilon^{5/2}}. \quad (4.2.10)$$

Figure 4.6 shows the mean exit time $\langle t_1 \rangle$ as a function of λ , with $\epsilon = 0.01$, $D_1 = 1$, $D_2 = 5$ and three values of a : $a = 0.1$, 0.01 and 0.001 . In all cases of a , the mean exit time passes through a minimum at some positive desorption rate λ_c and then approaches the maximum as $\lambda \rightarrow \infty$. The optimal value λ_c as well as the height of the maximum at $\lambda \rightarrow \infty$ depend on a . The limiting mean exit time \mathcal{T} changes significantly with different small a . The asymptotic relation (4.2.9) accurately captures the limiting behavior.

Furthermore, understanding the asymptotic behavior of λ_n and ψ_n^2 also help us to investigate the relationship between $\langle t_1 \rangle$ and ϵ , a . Although we do not have enough investigations about λ_n and especially, ψ_n^2 , we can consider the case of non-intermittent bulk diffusion with reflex boundary ($a \rightarrow 0$), which formally correspond to the double limit $\lambda \rightarrow \infty$ and $a \rightarrow 0$, in the narrow escape limit ($\epsilon \rightarrow 0$).

For a fixed very small a , when $\epsilon \rightarrow 0$, Eqs. (4.2.1) and (4.2.3) give us

$$\begin{aligned}
 \lim_{\lambda \rightarrow \infty} \langle t_1 \rangle = \mathcal{T} &= \frac{1 - (1 - a)^2}{12D_2} \sum_{n \geq 1} \frac{\psi_n^2}{\lambda_n^2} \\
 &= \frac{1 - (1 - a)^2}{12D_2} \left(\sum_{n=1}^{1/\epsilon} \frac{\tilde{B}_{a,\epsilon} n^{-2}}{\tilde{A}_{a,\epsilon}^2 n^{-2}} + \sum_{n=1/\epsilon}^{1/a} \frac{\tilde{B}'_{a,\epsilon} n^{-\alpha}}{\tilde{A}_{a,\epsilon}^2 n^{-2}} + \sum_{n=1/a}^{\infty} \frac{B_{a,\epsilon} n^{-6}}{A_{a,\epsilon}^2 n^{-4}} \right) \\
 &= \frac{1 - (1 - a)^2}{12D_2} \left(\frac{\tilde{B}_{a,\epsilon}}{\tilde{A}_{a,\epsilon}^2} \frac{1}{\epsilon} + o\left(\frac{1}{\epsilon}\right) \right), \tag{4.2.11}
 \end{aligned}$$

where $\alpha \geq 3$.

Although we do not know more information about the $\tilde{A}_{a,\epsilon}$ and $\tilde{B}_{a,\epsilon}$, Eq. (4.2.11) gives us the divergence of \mathcal{T} with $1/\epsilon$, which is similar to the result from Ref. [22, 20, 21].

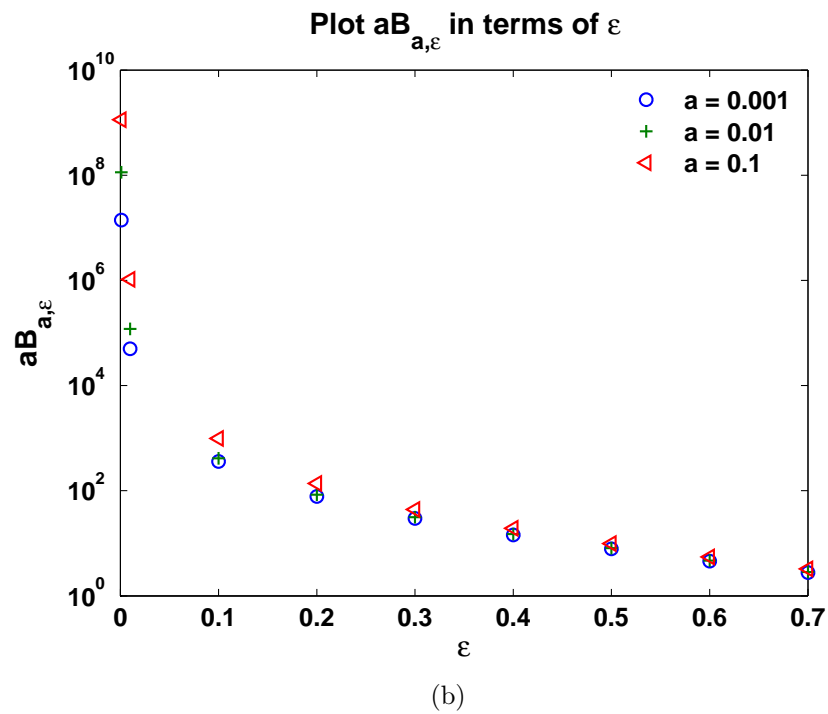
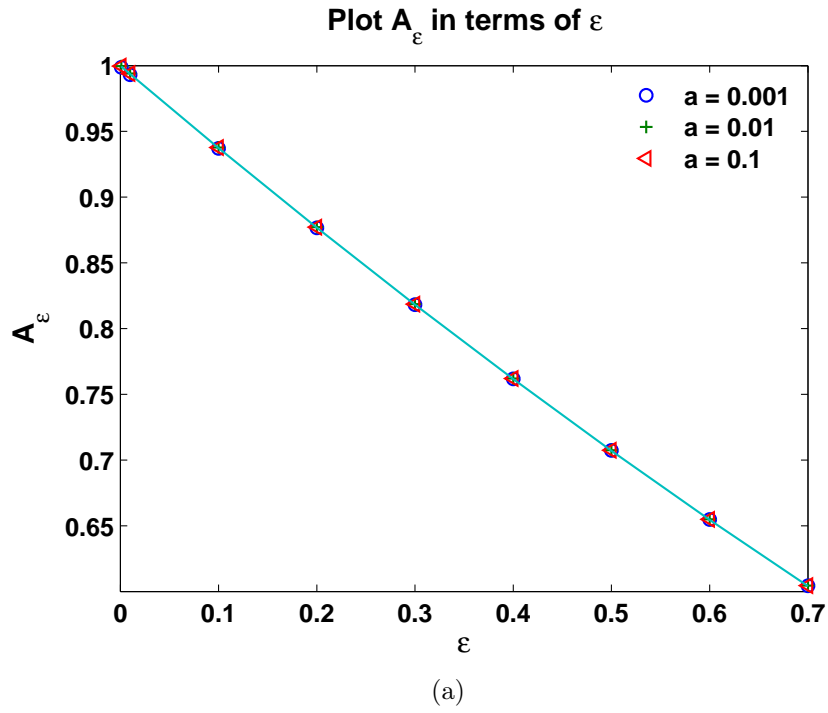


Figure 4.5: Coefficients A_ϵ , $aB_{a,\epsilon}$ from Eqs. (4.2.2), (4.2.5) versus ϵ . Three curves for $a = 0.001$, $a = 0.01$ and $a = 0.1$ coincide that illustrates the independence of A_ϵ of a .

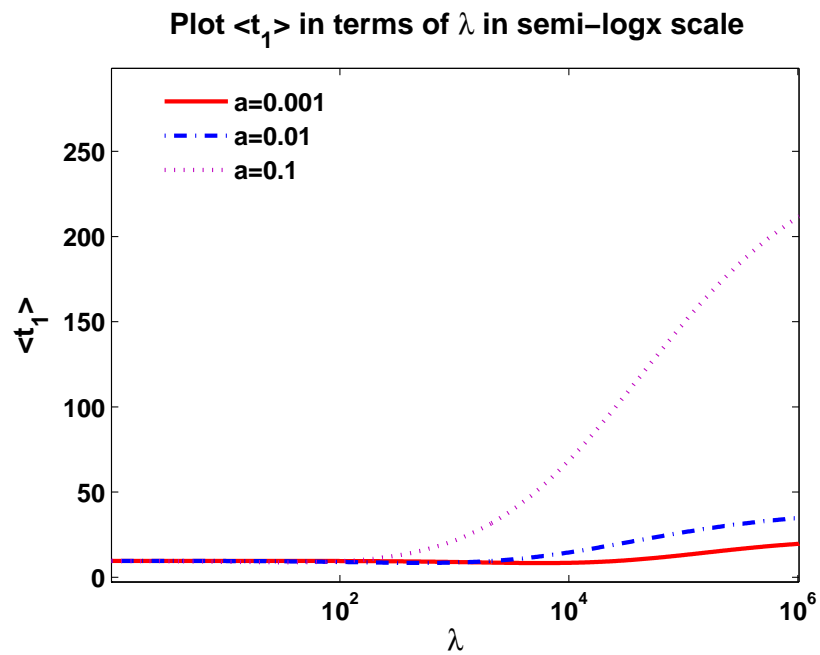


Figure 4.6: The mean time $\langle t_1 \rangle$ as a function of λ for $\epsilon = 0.01$, $D_1 = D_2 = 5$, and three values of a : 0.1 (green line), 0.01 (blue line) and 0.001 (red line).

Chapter 5

TORUS CASE

In this chapter, we describe an extension of the above problem to rectangles. We compute the mean exit time from a rectangle through a hole on its surface. As for the disk, we develop a spectral approach to this escape problem in which the mean exit time is explicitly expressed through the eigenvalues of a self-adjoint operator. This representation is well-suited to investigate the asymptotic behavior of the mean exit time in the limit of large desorption rate λ . Similar to the disk case, we show that the mean exit time diverges as $\sqrt{\lambda}$ for a point-like target and establish the asymptotic approach to a finite limit for extended targets. In all cases, the mean exit time is shown to asymptotically increase as λ goes to infinity. Most importantly, we investigate the role of the shape elongation on the optimality condition of surface-mediated diffusion. In particular, we prove that $D_{2,crit}$, the critical value for D_2 under which $\langle t_1 \rangle$ has a minimum at some positive λ , increases as the rectangle height R increases from $a/2$ to ∞ . This leads us to the conclusion that the function $f(R) = \frac{\langle t_1 \rangle_{\min}}{\langle t_1 \rangle_{\lambda=0}}$ has a minimum, i.e., there is an "optimal rectangle" for which the gain of surface-mediated diffusion over pure surface diffusion is maximal.

5.1 A self-adjoint operator formulation

We consider surface-mediated diffusion on a rectangle $[-\pi, \pi] \times [-R, R]$ when a target is located on horizontal edges. For convenience, the target is split into four pieces which are located near four corners: $[-\pi, -\pi + \epsilon] \times (-R)$, $[-\pi, -\pi + \epsilon] \times R$, $[\pi - \epsilon, \pi] \times (-R)$ and $[\pi - \epsilon, \pi] \times R$. This problem can be mapped onto the complex plane by periodically extending the rectangular pattern in both directions. The mapped target appears as an interval of length 2ϵ which is periodically repeated in two directions: $[(2k + 1)\pi - \epsilon + (2j + 1)Ri, (2k + 1)\pi + \epsilon + (2j + 1)Ri]$, $j, k \in \mathbb{Z}$. The "surface" is represented by horizontal lines at $y = (2j + 1)R$, $j \in \mathbb{Z}$. This problem is also equivalent to diffusion on a torus.

A particle starts at a point $x_0 + iy_0$. If this point lies on one of "surface" horizontal lines, i.e., $y_0 = (2j + 1)R$ for some $j \in \mathbb{Z}$, and it does not belong to the target, then a one-dimensional Brownian motion with the diffusion coefficient D_1 is started on

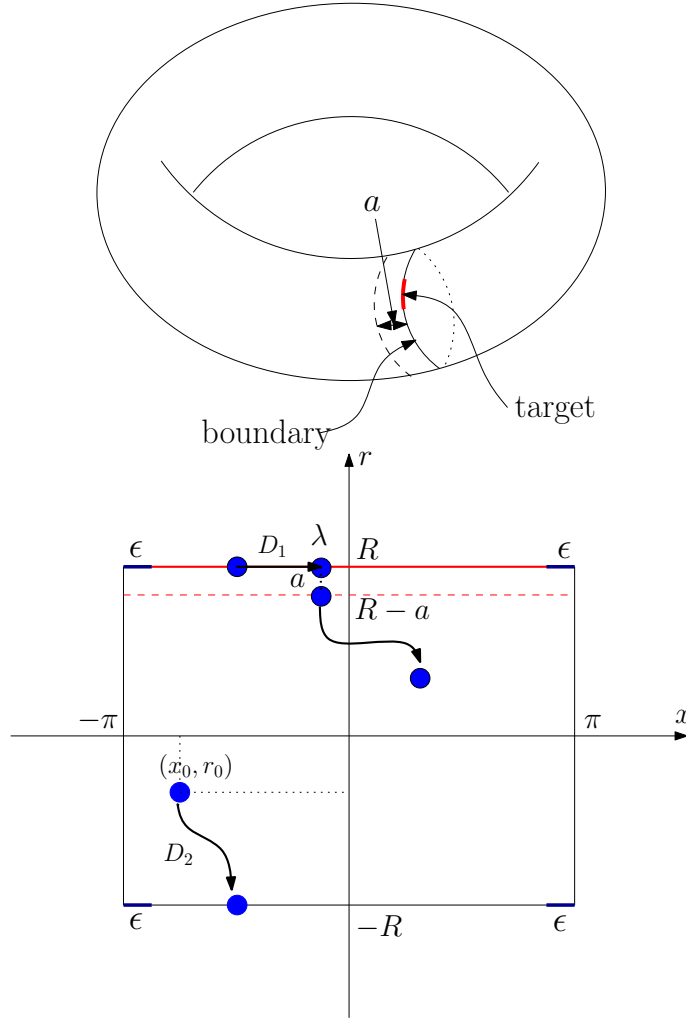


Figure 5.1: Surface-mediated diffusion in Torus (rectangle) case

this line. If the particle has not reached the target during a random time distributed by an exponential law with parameter $\lambda > 0$, then the particle is moved from its current position (x_1, y_0) to the point $(x_1, y_0 + a)$, from which a two-dimensional Brownian motion with the diffusion coefficient D_2 is started, until it reaches again a line $y = (2j + 1)R$ for some $j \in \mathbb{Z}$, for which the procedure starts over.

For a process started from a "surface" point $(x, (2j + 1)R)$, the mean exit time $t_1(x)$ is a 2π -periodic even function. When the process is started from a "bulk" point (x, y) , the mean exit time $t_2(x, y)$ is a 2π -periodic on the real line and $2R$ -periodic on the imaginary line.

Refer to the Mathematical Background 2.3, we establish the original equations

for these two functions t_1, t_2 :

$$\begin{cases} D_1 t_1''(x) + \lambda[t_2(x, R - a) - t_1(x)] = -1 \text{ for } x \in [-\pi + \epsilon, \pi - \epsilon], & (5.1.1) \\ D_2 \Delta t_2(x, r) = -1, & (5.1.2) \\ t_2(x, R) = t_1(x), \quad (x \in [-\pi, \pi]) & (5.1.3) \\ t_1(x) = 0 \text{ for } x \in [-\pi, -\pi + \epsilon] \cup [\pi - \epsilon, \pi], & (5.1.4) \end{cases}$$

and

$$\Delta = \frac{\partial^2}{\partial x^2} + \frac{\partial^2}{\partial r^2} \quad (5.1.5)$$

is the Laplace operator in Cartesian coordinates of the xr -plane.

By symmetry, $t_1(x)$ is an even function so it is sufficient to determine it on $[0, \pi]$ where it can be represented as a cosine series

$$t_1(x) = \sum_{n \geq 0} a_n \cos nx, \quad (5.1.6)$$

with unknown coefficients a_n .

As for the disk, the solution to Eq. (5.1.2) can be written as

$$t_2(x, r) = u(r) + v(x, r), \quad (5.1.7)$$

where $u(r)$ is the particular solution to the inhomogeneous (Poisson) equation $\Delta u = -\frac{1}{D_2}$, $u|_{\partial\mathbb{T}} = 0$ and $v(x, r)$ is the general solution to the Dirichlet problem $\Delta v = 0$, $v|_{\partial\mathbb{T}} = t_1$ ($\partial\mathbb{T}$ is the "surface" of the rectangle).

Solving the Poisson equation gives us

$$u(r) = \int_r^R \left(\int_0^{r_1} \frac{-1}{D_2} dr_2 \right) dr_1 = \frac{R^2 - r^2}{2D_2}. \quad (5.1.8)$$

In order to solve Dirichlet problem, we write v as

$$v(x, r) = \sum_{n \geq 0} b_n(r) a_n \cos nx. \quad (5.1.9)$$

We only consider the cases of n such that $b_n(r) a_n \neq 0$. In order to find $b_n(r)$ we first consider the boundary condition $v(x, \pm R) = t_1(x)$ which gives

$$b_n(R) = b_n(-R) = 1, \quad (5.1.10)$$

while $\Delta v = \frac{\partial^2 v}{\partial x^2} + \frac{\partial^2 v}{\partial r^2} = 0$ gives

$$\sum_{n \geq 0} [b_n''(r) - n^2 b_n(r)] a_n \cos nx = 0, \quad \forall x. \quad (5.1.11)$$

We identify the coefficients and use the condition $a_n \neq 0$ to obtain

$$b_n''(r) - n^2 b_n(r) = 0. \quad (5.1.12)$$

From Eq. (5.1.12), we write $b_n(r)$ which is the solution of Eq. (5.1.12) as

$$b_n(r) = \alpha \sinh nr + \beta \cosh nr. \quad (5.1.13)$$

From the boundary condition of v (see (5.1.10)), we get

$$\begin{cases} \alpha \sinh nR + \beta \cosh nR = 1, \\ -\alpha \sinh nR + \beta \cosh nR = 1 \end{cases} \quad \text{which implies} \quad \begin{cases} \alpha = 0, \\ \beta = \frac{1}{\cosh nR} \end{cases}$$

Hence, we obtain

$$b_n(r) = \frac{\cosh nr}{\cosh nR}$$

and

$$v(x, r) = \sum_{n \geq 0} a_n \frac{\cosh nr}{\cosh nR} \cos nx. \quad (5.1.14)$$

Combining (5.1.8) and (5.1.14), we immediately get that

$$t_2(x, r) = \frac{R^2 - r^2}{2D_2} + \sum_{n \geq 0} a_n \frac{\cosh nr}{\cosh nR} \cos nx. \quad (5.1.15)$$

Once more time, we define operators U, V on $L^2([0, \pi])$ satisfy $U = V^2$:

$$U \left(\sum_{n \geq 0} x_n \cos nx \right) = \sum_{n \geq 1} x_n \left(1 - \frac{\cosh n(R-a)}{\cosh nR} \right) \cos nx, \quad (5.1.16)$$

and

$$V \left(\sum_{n \geq 0} x_n \cos nx \right) = \sum_{n \geq 1} x_n \sqrt{1 - \frac{\cosh n(R-a)}{\cosh nR}} \cos nx. \quad (5.1.17)$$

Eq. (5.1.1) then is rewritten as

$$t_1''(x) = -\frac{1}{D_1} \left(1 + \lambda \frac{R^2 - (R-a)^2}{2D_2} \right) + \frac{\lambda}{D_1} U(t_1), \quad (5.1.18)$$

from which we obtain the solution t_1

$$t_1 = \frac{1}{D_1} \left(1 + \lambda \frac{R^2 - (R-a)^2}{2D_2} \right) \tilde{T}(1) - \frac{\lambda}{D_1} \tilde{T}U(t_1). \quad (5.1.19)$$

where the operator \tilde{T} is defined as in Chapter 3, i.e. $\tilde{T} = -\mathcal{E}T\mathcal{R}$ as an operator on $L^2([0, \pi])$, with T is defined as in Eqs. (3.2.9), \mathcal{R} is the natural restriction from $L^2([0, \pi])$ to $L^2([0, \pi - \epsilon])$ and \mathcal{E} is natural extension by 0 from $L^2([0, \pi - \epsilon])$ to $L^2([0, \pi])$.

Applying the operator V to both sides of Eq. (5.1.19), we get, writing $s_1 = V(t_1)$,

$$s_1 = \frac{1}{D_1} \left(1 + \lambda \frac{R^2 - (R - a)^2}{2D_2} \right) V\tilde{T}(1) - \frac{\lambda}{D_1} V\tilde{T}V(s_1),$$

which can be solved in s_1 as

$$s_1 = \frac{1}{D_1} \left(1 + \lambda \frac{R^2 - (R - a)^2}{2D_2} \right) \left(I + \frac{\lambda}{D_1} V\tilde{T}V \right)^{-1} (\psi), \quad (5.1.20)$$

where $\psi = V\tilde{T}(1)$.

The feature that $V\tilde{T}V$ is self-adjoint allows us to invert $(I + \frac{\lambda}{D_1} V\tilde{T}V)$ and to express the mean exit time in a spectral form.

We are interested in

$$\langle t_1 \rangle = \frac{1}{\pi} \int_0^\pi dx t_1(x) = \frac{1}{\pi} \langle t_1, 1 \rangle.$$

Hence, using Eqs. (5.1.19) and (5.1.20), we can write

$$\begin{aligned} \pi \langle t_1 \rangle &= \frac{1}{D_1} \left(1 + \lambda \frac{R^2 - (R - a)^2}{2D_2} \right) \langle \tilde{T}(1), 1 \rangle - \frac{\lambda}{D_1} \langle \tilde{T}V(s_1), 1 \rangle \\ &= \frac{1}{D_1} \left(1 + \lambda \frac{R^2 - (R - a)^2}{2D_2} \right) \langle \tilde{T}(1), 1 \rangle - \frac{\lambda}{D_1} \langle s_1, \psi \rangle, \end{aligned} \quad (5.1.21)$$

from which it follows that the knowledge of s_1 allows to compute $\langle t_1 \rangle$:

$$\langle t_1 \rangle = \frac{1}{\pi D_1} \left(1 + \lambda \frac{R^2 - (R - a)^2}{2D_2} \right) \left(\langle \tilde{T}(1), 1 \rangle - \frac{\lambda}{D_1} \left\langle \left(I + \frac{\lambda}{D_1} V\tilde{T}V \right)^{-1} \psi, \psi \right\rangle \right). \quad (5.1.22)$$

As for the disk, we can state that there is an orthonormal basis $(e_n)_{n \geq 0}$ of $\text{Im}(V\tilde{T}V)$ in $L^2([0, \pi])$ such that $V\tilde{T}V e_n = \lambda_n e_n$ and $\lambda_n \downarrow 0$ as $n \rightarrow \infty$.

When $\epsilon = 0$, the eigenbasis (e_n) is simply formed by cosine functions, and the analysis is straightforward (see below). When $\epsilon > 0$, we can write in spectral representation as

$$\psi = \sum_{n \geq 1} \psi_n e_n,$$

with coefficients $(\psi_n)_n$ forming a sequence in $\ell^2(\mathbb{N})$, $\psi_n = \langle \psi, e_n \rangle$. Using this representation, Eq. (5.1.20) is formally solved as

$$s_1 = \frac{1}{D_1} \left(1 + \lambda \frac{R^2 - (R-a)^2}{2D_2} \right) \sum_{n \geq 1} \frac{\psi_n}{1 + \frac{\lambda}{D_1} \lambda_n} e_n.$$

Plugging this expression into Eq. (5.1.22) we obtain

$$\langle t_1 \rangle = \frac{1}{\pi D_1} \left(1 + \lambda \frac{R^2 - (R-a)^2}{2D_2} \right) \left[\langle \tilde{T}(1), 1 \rangle - \frac{\lambda}{D_1} \sum_{n \geq 1} \frac{\psi_n^2}{1 + \frac{\lambda}{D_1} \lambda_n} \right]. \quad (5.1.23)$$

This spectral representation is almost identical to Eq. (3.2.21) for the disk, the only difference relies in the eigenvalues λ_n and spectral weights ψ_n (once D_2 is rescaled appropriately). Note that the surface extension 2π and the bulk "width" $2R$ between two horizontal edges for rectangles correspond to the disk perimeter 2π and disk diameter $2R$, respectively. While the disk is characterized by a single length scale (the radius of the disk=1), the advantage of rectangles is a possibility to separate these scales and thus to investigate the role of shape elongation.

5.1.1 Point-like target ($\epsilon = 0$)

For a point-like target ($\epsilon = 0$), the only difference with the disk lies in the eigenvalues λ_n for which Eq. (3.2.24) is replaced by

$$\lambda_n = \begin{cases} \left(1 - \frac{\cosh n(R-a)}{\cosh nR} \right) \frac{1}{n^2} & (n \geq 1), \\ 0 & (n = 0), \end{cases} \quad e_n = \begin{cases} \sqrt{2/\pi} \cos nx & (n \geq 1), \\ \sqrt{1/\pi} & (n = 0). \end{cases} \quad (5.1.24)$$

For $n \geq 1$, we have

$$\begin{aligned} \psi_n &= \langle \psi, e_n \rangle = \langle V\tilde{T}(1), e_n \rangle = \sqrt{2/\pi} \langle \tilde{T}(1), V(\cos nx) \rangle \\ &= \sqrt{2/\pi} \sqrt{1 - \frac{\cosh n(R-a)}{\cosh nR}} \left\langle \frac{\pi^2 - x^2}{2}, \cos nx \right\rangle = \sqrt{2\pi} \sqrt{1 - \frac{\cosh n(R-a)}{\cosh nR}} \frac{(-1)^{n+1}}{n^2}, \end{aligned} \quad (5.1.25)$$

while $\langle \psi, 1 \rangle = \langle V\tilde{T}(1), 1 \rangle = \langle \tilde{T}(1), V(1) \rangle = 0$. Substituting this expression into Eq. (5.1.23), we get

$$\begin{aligned}
 \langle t_1 \rangle_{\epsilon=0} &= \frac{1}{\pi D_1} \left(1 + \lambda \frac{R^2 - (R-a)^2}{2D_2} \right) \left(\langle \tilde{T}(1), 1 \rangle - \sum_{n \geq 1} \frac{2\pi \frac{\lambda}{D_1} \left(1 - \frac{\cosh n(R-a)}{\cosh nR} \right)}{n^2 \left(n^2 + \frac{\lambda}{D_1} \left(1 - \frac{\cosh n(R-a)}{\cosh nR} \right) \right)} \right) \\
 &= \frac{1}{\pi D_1} \left(1 + \lambda \frac{R^2 - (R-a)^2}{2D_2} \right) \left(\langle \tilde{T}(1), 1 \rangle - 2\pi \sum_{n \geq 1} \frac{1}{n^2} \right. \\
 &\quad \left. + 2\pi \sum_{n \geq 1} \frac{1}{n^2 + \frac{\lambda}{D_1} \left(1 - \frac{\cosh n(R-a)}{\cosh nR} \right)} \right) \\
 &= \frac{2}{D_1} \left(1 + \lambda \frac{R^2 - (R-a)^2}{2D_2} \right) \sum_{n \geq 1} \frac{1}{n^2 + \frac{\lambda}{D_1} \left(1 - \frac{\cosh n(R-a)}{\cosh nR} \right)}. \tag{5.1.26}
 \end{aligned}$$

Defining $\varepsilon_n \equiv \frac{\cosh n(R-a)}{\cosh nR}$, we have for $0 < a < 2R$:

$$\sum_{n \geq 0} n^4 \varepsilon_n \sim \sum_{n=0}^{n_0} n^4 \frac{e^{n(R-a)} + e^{-n(R-a)}}{e^{nR} + e^{-nR}} + \sum_{n=n_0}^{\infty} n^4 e^{-na} < \infty. \tag{5.1.27}$$

As for the disk, one can use Theorem 3.2.1 to obtain the asymptotic of the mean exit time $\langle t_1 \rangle_{\epsilon=0}$ as $\lambda \rightarrow \infty$

$$\begin{aligned}
 \langle t_1 \rangle_{\epsilon=0} &= \frac{2}{D_1} \left(1 + \lambda \frac{R^2 - (R-a)^2}{2D_2} \right) \left(\frac{\pi \sqrt{D_1}}{2\sqrt{\lambda}} - \frac{D_1}{2\lambda} + \frac{D_1}{\lambda} \sum_{n \geq 1} \frac{\varepsilon_n}{1 - \varepsilon_n} + O\left(\frac{1}{\lambda}\right) \right) \\
 &= \frac{R^2 - (R-a)^2}{2D_2 \sqrt{D_1}} \pi \sqrt{\lambda} + \frac{R^2 - (R-a)^2}{2D_2} \left(2 \sum_{n \geq 1} \frac{\varepsilon_n}{1 - \varepsilon_n} - 1 \right) + \frac{\pi}{\sqrt{D_1}} \frac{1}{\sqrt{\lambda}} \\
 &\quad + \left(2 \sum_{n \geq 1} \frac{\varepsilon_n}{1 - \varepsilon_n} - 1 \right) \frac{1}{\lambda} + O\left(\frac{1}{\lambda}\right) \\
 &= A_1 \sqrt{\lambda} + A_2 + \frac{A_3}{\sqrt{\lambda}} + O\left(\frac{1}{\lambda}\right), \tag{5.1.28}
 \end{aligned}$$

where

$$A_1 = \frac{R^2 - (R-a)^2}{2D_2} \frac{\pi}{\sqrt{D_1}}, \tag{5.1.29}$$

$$A_2 = \frac{R^2 - (R-a)^2}{2D_2} \left(2 \sum_{n \geq 1} \frac{\cosh n(R-a)}{\cosh nR - \cosh n(R-a)} - 1 \right), \tag{5.1.30}$$

$$A_3 = \frac{\pi}{\sqrt{D_1}}. \tag{5.1.31}$$

5.1. A SELF-ADJOINT OPERATOR FORMULATION

Similar to the 2-D case, we can compute $\frac{d\langle t_1 \rangle_{\epsilon=0}}{d\lambda}$ and show that $\frac{d\langle t_1 \rangle_{\epsilon=0}}{d\lambda} > 0$ at large λ , from which combine with Eq. (5.1.28) allows us to conclude that $\langle t_1 \rangle_{\epsilon=0}$ asymptotically increases to infinity as $\lambda \rightarrow \infty$, as illustrated on Fig. 5.2a.

As a result, if $\left. \frac{\partial \langle t_1 \rangle_{\epsilon=0}}{\partial \lambda} \right|_{\lambda=0} < 0$, then $\langle t_1 \rangle_{\epsilon=0}$ has a minimum in terms of λ . We compute

$$\begin{aligned}
 \left. \frac{\partial \langle t_1 \rangle_{\epsilon=0}}{\partial \lambda} \right|_{\lambda=0} &= \frac{2}{D_1} \left(\frac{R^2 - (R-a)^2}{2D_2} \sum_{n \geq 1} \frac{1}{n^2} - \frac{1}{D_1} \sum_{n \geq 1} \frac{1 - \frac{\cosh n(R-a)}{\cosh nR}}{n^4} \right) < 0 \\
 \Leftrightarrow \frac{R^2 - (R-a)^2}{2D_2} \frac{\pi^2}{6} &< \frac{1}{D_1} \sum_{n \geq 1} \frac{1 - \frac{\cosh n(R-a)}{\cosh nR}}{n^4} \\
 \Leftrightarrow D_2 > D_{2,\text{crit}} &= D_1 \frac{\pi^2 (R^2 - (R-a)^2)}{12 \sum_{n \geq 1} \frac{1 - \frac{\cosh n(R-a)}{\cosh nR}}{n^4}}. \tag{5.1.32}
 \end{aligned}$$

If $D_2 > D_{2,\text{crit}}$, then $\langle t_1 \rangle_{\epsilon=0}$ has a minimum.

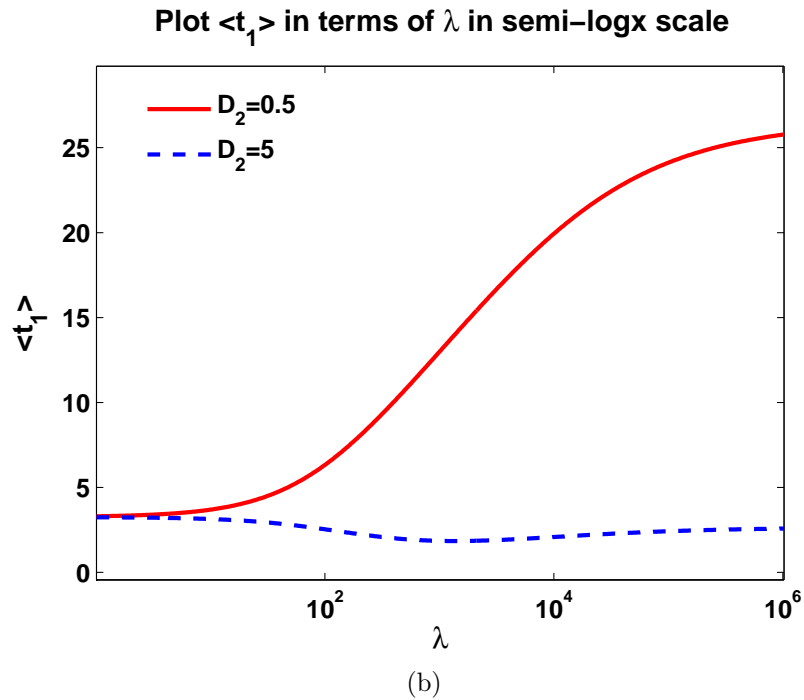
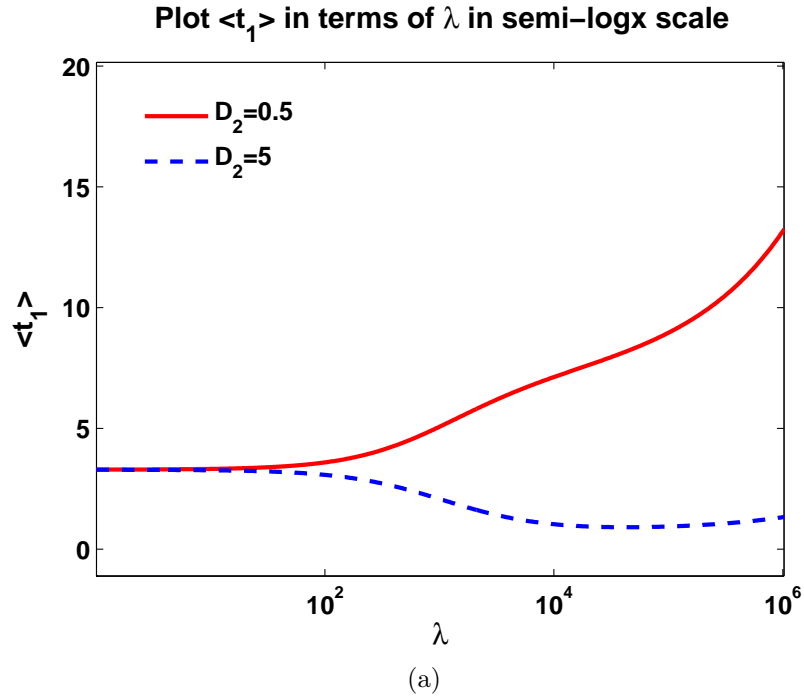


Figure 5.2: Mean exit time $\langle t_1 \rangle$ as a function of λ for $\epsilon = 0$ (a) and $\epsilon = 0.01$ (b), with $a = 0.01$ and $D_1 = 1$. When $D_2 = 0.5 < D_{2,\text{crit}}$ (blue solid line), $\langle t_1 \rangle$ monotonously increases with λ so that the smallest mean exit time corresponds to $\lambda = 0$ (surface diffusion without intermittence). When $D_2 = 2 > D_{2,\text{crit}}$ (red dashed line), $\langle t_1 \rangle$ starts first to decrease with λ , passes through a minimum and monotonously increases to infinity.

5.1.2 Extended target ($\epsilon > 0$)

As for the disk, the mean exit time $\langle t_1 \rangle$ to an extended target ($\epsilon > 0$) converges to a finite limit as $\lambda \rightarrow \infty$. Theorem (3.2.2) can be proved for rectangles case in the same way as in Sec. 3.2.2, we have

$$\sum_{n \geq 1} \frac{\psi_n^2}{\lambda_n} = \langle \tilde{T}(1), 1 \rangle, \quad \sum_{n \geq 1} \frac{\psi_n^2}{\lambda_n^2} < \infty, \quad \sum_{n \geq 1} \frac{\psi_n^2}{\lambda_n^3} = \infty. \quad (5.1.33)$$

Consequently, Eqs. (5.1.23), (5.1.33) yield the mean exit time for surface diffusion phase:

$$\langle t_1 \rangle_{\lambda=0} = \frac{1}{\pi D_1} \sum_{n \geq 1} \frac{\psi_n^2}{\lambda_n} = \frac{1}{\pi D_1} \langle \tilde{T}(1), 1 \rangle = \frac{(\pi - \epsilon)^3}{3\pi D_1}. \quad (5.1.34)$$

Plugging Eq. (5.1.33) into Eq. (5.1.23), we obtain

$$\langle t_1 \rangle = \frac{1}{\pi} \left(\frac{1}{\lambda} + \frac{R^2 - (R - a)^2}{2D_2} \right) \sum_{n \geq 1} \frac{\psi_n^2}{\lambda_n \left(\frac{D_1}{\lambda} + \lambda_n \right)}. \quad (5.1.35)$$

In the limit $\lambda \rightarrow \infty$, Eq. (5.1.35) yields the mean exit time for the bulk diffusion phase:

$$\mathcal{T} = \lim_{\lambda \rightarrow \infty} \langle t_1 \rangle = \frac{R^2 - (R - a)^2}{2\pi D_2} \sum_{n \geq 1} \frac{\psi_n^2}{\lambda_n^2}. \quad (5.1.36)$$

Remark 5.1.1. From (5.1.36) and (5.1.33), we obtain the asymptotic behavior for $\langle t_1 \rangle$:

$$\langle t_1 \rangle = \mathcal{T} - \frac{D_1}{\lambda} \frac{R^2 - (R - a)^2}{2\pi D_2} \sum_{n=1}^{\infty} \frac{\psi_n^2}{\lambda_n^2 \left(\lambda_n + \frac{D_1}{\lambda} \right)} + \frac{S}{\pi \lambda} + o\left(\frac{1}{\lambda}\right). \quad (5.1.37)$$

We also have the following theorem whose proof is similar to the Theorem 3.2.4.

Theorem 5.1.1. The function $\lambda \mapsto \langle t_1 \rangle$, where $\langle t_1 \rangle$ defined in (5.1.23) is asymptotically increasing as $\lambda \rightarrow +\infty$. Moreover, if

$$\left. \frac{d\langle t_1 \rangle}{d\lambda} \right|_{\lambda=0} < 0,$$

then the function $\langle t_1 \rangle$ passes through a minimum which is located at $\lambda_{\min} > 0$.

Remark 5.1.2. The theorem (5.1.1) allows us to determine the critical value for the bulk diffusion coefficient $D_{2,\text{crit}}$ above which bulk excursions are beneficial. The

existence of the optimal value λ (that minimizes the function $\langle t_1 \rangle$) depends on this ratio. If $D_2 > D_{2,\text{crit}}$, with

$$\begin{aligned} D_{2,\text{crit}} &= D_1 \frac{(R^2 - (R - a)^2) \langle \tilde{T}(1), 1 \rangle}{2 \|V\tilde{T}(1)\|^2} \\ &= D_1 \frac{\pi(\pi - \epsilon)^3 (R^2 - (R - a)^2)}{12} \left(\sum_{n \geq 1} \frac{1 - \frac{\cosh n(R-a)}{\cosh nR}}{n^4} \left[(\pi - \epsilon) \cos n\epsilon + \frac{\sin n\epsilon}{n} \right]^2 \right)^{-1}, \end{aligned} \quad (5.1.38)$$

then $\langle t_1 \rangle$ starts first to decrease with λ , passes through a minimum then monotonously increases.

5.2 Dependence on the value R

The rectangle case allows one to investigate the role of the domain elongation on the optimality condition for surface-mediated diffusion. In fact, the shape of a disk is fully characterized by a single length scale, its radius K (where in this thesis we fix as 1 and stretch the other parameters into scale $1/L$). In turn, the rectangle has two sides $2\pi L$ (again, in this thesis, we fix $L = 1$) and $2R$ representing two length scales. Changing the aspect ratio π/R , one can study how the mean exit time and the search efficiency depend on the domain elongation.

First, we will show that $D_{2,\text{crit}}$ increases to infinity as $R \rightarrow \infty$. On other words, surface-mediated diffusion becomes less and less efficient for rectangles elongated in the vertical direction. In the opposite limit $R = a/2$, every reflection by distance a moves the particles back to the (opposite) surface, fully excluding the bulk diffusion phase. As a consequence, there should exist an optimal value of R for which the intermittent search strategy is most efficient.

Theorem 5.2.1. $D_{2,\text{crit}}$ defined in Eq. (5.1.38) monotonously increases to infinity as $R \rightarrow \infty$.

Proof. It is convenient to write Eq. (5.1.38) as

$$D_{2,\text{crit}} = D_1 \frac{\pi(\pi - \epsilon)^3 (R^2 - (R - a)^2)}{12} \left(\sum_{n \geq 1} f_n g_n \right)^{-1}, \quad (5.2.1)$$

where

$$f_n = \frac{1}{n^4} \left[(\pi - \epsilon) \cos n\epsilon + \frac{\sin n\epsilon}{n} \right]^2, \quad (5.2.2)$$

$$g_n = 1 - \frac{\cosh n(R - a)}{\cosh nR}, \quad (5.2.3)$$

i.e., f_n are independent of R .

Setting $R = a + \delta$, one can rewrite

$$g_n = 1 - \frac{\cosh n\delta}{\cosh n(a + \delta)}, \quad (5.2.4)$$

and

$$D_{2,crit} = D_1 \frac{\pi(\pi - \epsilon)^3 (2a\delta + a^2)}{12} \left(\sum_{n \geq 1} f_n g_n \right)^{-1}. \quad (5.2.5)$$

Taking the derivative of $D_{2,crit}$ with respect to δ yields

$$\frac{dD_{2,crit}}{d\delta} = \frac{D_1 \pi(\pi - \epsilon)^3 2a \sum_{n \geq 1} f_n g_n - (a^2 + 2a\delta) \sum_{n \geq 1} f_n \frac{dg_n}{d\delta}}{12 [\sum_{n \geq 1} f_n g_n]^2} \quad (5.2.6)$$

$$= D_1 \frac{\pi(\pi - \epsilon)^3 2a \sum_{n \geq 1} f_n h_n}{12 [\sum_{n \geq 1} f_n g_n]^2}, \quad (5.2.7)$$

where

$$h_n = g_n - (a/2 + \delta) \frac{d}{d\delta} g_n \quad (5.2.8)$$

$$= 1 - \frac{\cosh n\delta}{\cosh n(a + \delta)} - (a/2 + \delta) \frac{n \sinh na}{\cosh^2 n(a + \delta)}. \quad (5.2.9)$$

Writing $h_n = \frac{\tilde{h}_n}{\cosh^2 n(a + \delta)}$, where

$$\tilde{h}_n := \cosh^2 n(a + \delta) - \cosh n(a + \delta) \cosh n\delta - (a/2 + \delta)n \sinh na, \quad (5.2.10)$$

we will show that $\tilde{h}_n > 0$ for $\delta > -a/2$.

Taking the derivative with respect to δ , one finds

$$\begin{aligned} \frac{d\tilde{h}_n}{d\delta} &= 2n \cosh n(a + \delta) \sinh n(a + \delta) - n \sinh n\delta \cosh n(a + \delta) \\ &\quad - n \cosh n\delta \sinh n(a + \delta) - n \sinh na \\ &= n [\sinh n(a + 2\delta + a) - \sinh n(a + 2\delta) - \sinh na] \\ &= n \{ \sinh n(a + 2\delta) (\cosh na - 1) + \sinh na (\cosh n(a + 2\delta) - 1) \} > 0 \end{aligned} \quad (5.2.11)$$

when $(a + 2\delta) > 0$.

Finally, \tilde{h}_n vanishes at $\delta = -a/2$. We conclude that $\tilde{h}_n > 0$ for $\delta > -a/2$ and any $n \geq 1$.

As a consequence, $h_n > 0$ for all $\delta > -a/2$ and all $n \geq 1$ so that $D_{2,crit}$ monotonously

increases as R increases from $a/2$ to infinity.

Moreover, since

$$|f_n| \leq \frac{(\pi - \epsilon)^2}{n^4} + \frac{2(\pi - \epsilon)}{n^5} + \frac{1}{n^6}, \quad (5.2.12)$$

$$|g_n| \leq 1, \quad (5.2.13)$$

one has

$$\left| \sum_{n \geq 1} f_n g_n \right| \leq (\pi - \epsilon)^2 \zeta(4) + 2(\pi - \epsilon) \zeta(5) + \zeta(6) < \infty. \quad (5.2.14)$$

As a consequence, the sum in Eq. (5.2.1) remains bounded, while $R^2 - (R - a)^2 \rightarrow \infty$ as $R \rightarrow \infty$ so that $D_{2,crit} \rightarrow \infty$ as $R \rightarrow \infty$ that completes the proof. \square

Theorem 5.2.2. *For $D_{2,crit}$ defined in Eq. (5.1.38), we have*

$$D_{2,crit} \rightarrow D_1 \Delta_{a,\epsilon} \text{ as } R \rightarrow \frac{a}{2}, \quad (5.2.15)$$

where

$$\Delta_{a,\epsilon} = D_1 \frac{\pi(\pi - \epsilon)}{12} a \left(\sum_{n \geq 1} f_n n \tanh \frac{na}{2} \right)^{-1}, \quad (5.2.16)$$

and f_n are defined in Eq. (5.2.2).

Proof. Setting $R = \xi + \frac{a}{2}$, $D_{2,crit}$ can be rewritten as

$$D_{2,crit} = D_1 \frac{\pi(\pi - \epsilon)^3}{12} 2a\xi \left[\sum_{n \geq 1} f_n g_n \right]^{-1}, \quad (5.2.17)$$

with g_n is defined in (5.2.3) and is rewritten as

$$g_n = 1 - \frac{\cosh n \left(\frac{a}{2} - \xi \right)}{\cosh n \left(\frac{a}{2} + \xi \right)}. \quad (5.2.18)$$

We would like to prove that $\sum_{n \geq 1} f_n \frac{g_n}{\xi}$ converges to $\sum_{n \geq 1} f_n n \tanh \frac{na}{2}$ as $\xi \rightarrow 0$. Indeed, we have that

$$\begin{aligned} g_n(\xi) &= 1 - \frac{e^{n(\xi - \frac{a}{2})} + e^{n(-\xi + \frac{a}{2})}}{e^{n(\xi + \frac{a}{2})} + e^{-n(\xi + \frac{a}{2})}} \\ &= \frac{\left[e^{n(\xi + \frac{a}{2})} - e^{n(-\xi + \frac{a}{2})} \right] + \left[e^{-n(\xi + \frac{a}{2})} - e^{n(\xi - \frac{a}{2})} \right]}{e^{n(\xi + \frac{a}{2})} + e^{-n(\xi + \frac{a}{2})}} \\ &= \frac{e^{n\frac{a}{2}} \left[e^{n\xi} - e^{-n\xi} \right] + e^{-n\frac{a}{2}} \left[e^{-n\xi} - e^{n\xi} \right]}{e^{n(\xi + \frac{a}{2})} + e^{-n(\xi + \frac{a}{2})}} \\ &= \left[e^{n\xi} - e^{-n\xi} \right] \frac{\left(e^{n\frac{a}{2}} - e^{-n\frac{a}{2}} \right)}{e^{n(\xi + \frac{a}{2})} + e^{-n(\xi + \frac{a}{2})}} \\ &= \left[e^{n\xi} - e^{-n\xi} \right] \mathbf{E}(n, \xi), \end{aligned} \quad (5.2.19)$$

where $\mathbf{E}(n, \xi) = \frac{(e^{n\frac{a}{2}} - e^{-n\frac{a}{2}})}{e^{n(\xi+\frac{a}{2})} + e^{-n(\xi+\frac{a}{2})}}$.

We have

$$|\mathbf{E}(n, \xi)| \leq e^{-n\xi}. \quad (5.2.20)$$

Since

$$\begin{aligned} e^{n\xi} - e^{-n\xi} &= 2n\xi + (n\xi)^2 (e^{n\xi t_0} - e^{-n\xi t_0}) \\ &= 2n\xi + \theta_1(n, \xi) \end{aligned} \quad (5.2.21)$$

for some $t_0 \in [0, 1]$, where

$$\theta_1(n, \xi) = (n\xi)^2 (e^{n\xi t_0} - e^{-n\xi t_0}), \quad (5.2.22)$$

satisfies

$$|\theta_1(n, \xi)| \leq 2(n\xi)^2 e^{n\xi}, \quad (5.2.23)$$

and

$$\begin{aligned} e^{n(\xi+\frac{a}{2})} + e^{-n(\xi+\frac{a}{2})} &= e^{n\frac{a}{2}} + e^{-n\frac{a}{2}} \\ &+ e^{n\frac{a}{2}} (e^{n\xi} - 1) + e^{-n\frac{a}{2}} (e^{-n\xi} - 1) \end{aligned} \quad (5.2.24)$$

$$\begin{aligned} &= e^{n\frac{a}{2}} + e^{-n\frac{a}{2}} + n\xi e^{n\frac{a}{2}} e^{n\xi t_1} - n\xi e^{-n\frac{a}{2}} e^{-n\xi t_2} \\ &= e^{n\frac{a}{2}} + e^{-n\frac{a}{2}} + \theta_2(n, \xi) \end{aligned} \quad (5.2.25)$$

for some $t_1, t_2 \in [0, 1]$, where

$$\theta_2(n, \xi) = n\xi e^{n\frac{a}{2}} e^{n\xi t_1} - n\xi e^{-n\frac{a}{2}} e^{-n\xi t_2}, \quad (5.2.26)$$

bounded by

$$|\theta_2(n, \xi)| \leq 2n\xi e^{n\frac{a}{2}} e^{n\xi}, \quad (5.2.27)$$

we get that

$$\begin{aligned} g_n(\xi) &= 2n\xi \frac{e^{n\frac{a}{2}} - e^{-n\frac{a}{2}}}{e^{n\frac{a}{2}} + e^{-n\frac{a}{2}} + \theta_2(n, \xi)} + \theta_1(n, \xi) \mathbf{E}(n, \xi) \\ &= 2n\xi \frac{e^{n\frac{a}{2}} - e^{-n\frac{a}{2}}}{e^{n\frac{a}{2}} + e^{-n\frac{a}{2}}} \\ &+ 2n\xi \frac{\theta_2(n, \xi)}{e^{n\frac{a}{2}} + e^{-n\frac{a}{2}}} \mathbf{E}(n, \xi) + \theta_1(n, \xi) \mathbf{E}(n, \xi) \\ &= 2n\xi \frac{e^{n\frac{a}{2}} - e^{-n\frac{a}{2}}}{e^{n\frac{a}{2}} + e^{-n\frac{a}{2}}} + \mathbf{F}(n, \xi) \end{aligned} \quad (5.2.28)$$

where

$$\mathbf{F}(n, \xi) = 2n\xi \frac{\theta_2(n, \xi)}{e^{n\frac{a}{2}} + e^{-n\frac{a}{2}}} \mathbf{E}(n, \xi) + \theta_1(n, \xi) \mathbf{E}(n, \xi) \quad (5.2.29)$$

satisfies

$$\begin{aligned} |\mathbf{F}(n, \xi)| &\leq 2n\xi \frac{|\theta_2(n, \xi)|}{e^{n\frac{a}{2}}} \mathbf{E}(n, \xi) + \theta_1(n, \xi) \mathbf{E}(n, \xi) \\ &\leq 4(n\xi)^2 e^{n\xi} \mathbf{E}(n, \xi) + 2(n\xi)^2 e^{n\xi} \mathbf{E}(n, \xi) \\ &\leq 6(n\xi)^2. \end{aligned} \quad (5.2.30)$$

We get

$$\begin{aligned} \left| \sum_{n=1}^{\infty} f_n \frac{g_n(\xi)}{\xi} - \sum_{n=1}^{\infty} \left(f_n 2n \frac{(e^{n\frac{a}{2}} - e^{-n\frac{a}{2}})}{e^{n\frac{a}{2}} + e^{-n\frac{a}{2}}} \right) \right| &\leq \sum_{n=1}^{\infty} |f_n| \left| \frac{g_n(\xi)}{\xi} - 2n \frac{(e^{n\frac{a}{2}} - e^{-n\frac{a}{2}})}{e^{n\frac{a}{2}} + e^{-n\frac{a}{2}}} \right| \\ &\leq \sum_{n=1}^{\infty} |f_n| \frac{|\mathbf{F}(n, \xi)|}{\xi} \\ &\leq 6\xi \sum_{n=1}^{\infty} (|f_n| n^2) \\ &\leq \xi M \rightarrow 0 \text{ as } \xi \rightarrow 0, \quad (M < \infty) \end{aligned} \quad (5.2.31)$$

since

$$|f_n| \leq \frac{(\pi - \epsilon)^2}{n^4} + \frac{2(\pi - \epsilon)}{n^5} + \frac{1}{n^6}.$$

Therefore,

$$\lim_{\xi \rightarrow 0} \sum_{n=1}^{\infty} f_n \frac{g_n(\xi)}{\xi} = \sum_{n=1}^{\infty} \left(f_n 2n \frac{e^{n\frac{a}{2}} - e^{-n\frac{a}{2}}}{e^{n\frac{a}{2}} + e^{-n\frac{a}{2}}} \right) = \sum_{n=1}^{\infty} f_n 2n \tanh \frac{na}{2}. \quad (5.2.32)$$

that implies Eq. (5.2.16) and completes the proof.

In particular, as $a \rightarrow 0$, one gets

$$\lim_{a \rightarrow 0} \Delta_{a, \epsilon} = \frac{\pi(\pi - \epsilon)^3}{6} \left(\sum_{n \geq 1} f_n n^2 \right)^{-1}. \quad (5.2.33)$$

Finally, if $\epsilon \rightarrow 0$, f_n goes to π^2/n^4 so that $\Delta_{0,0} = 1$. This is not surprising that the limiting case $R \rightarrow a/2$ corresponds to pure surface diffusion phase. \square

According to Theorems 5.2.1 and 5.2.2, $D_1 \Delta_{a, \epsilon}$ is the minimal value of the critical diffusion coefficient $D_2, crit$ under fixed a , ϵ , D_1 and variable R . One can thus distinguish two cases for fixed a , ϵ , D_1 and R varying from $a/2$ to infinity:

- (1) If $D_2 < D_1\Delta_{a,\epsilon}$ then for any $R \geq a/2$, $D_2 < D_{2,crit}(R)$ (since $D_{2,crit}(R)$ is a increasing function of R) implying that the minimal value of $\langle t_1 \rangle$ is reached at $\lambda_{\min} = 0$: $\langle t_1 \rangle_{\min} = \langle t_1 \rangle_{\lambda=0}$. On other words, surface diffusion is optimal for any $R \geq a/2$ in that case.
- (2) If $D_2 > D_1\Delta_{a,\epsilon}$ then there exists a value R_0 such that $D_{2,crit}(R_0) = D_2$. Hence,
 - (2a) when $a/2 < R \leq R_0$, one has $\Delta < D_{2,crit}(R) \leq D_2 = D_{2,crit}(R_0)$, so that there is an optimal value of $\lambda_{\min} > 0$ that minimizes $\langle t_1 \rangle$;
 - (2b) when $R_0 < R$, $D_{2,crit}(R) > D_2$, and the optimal value of $\lambda_{\min} = 0$: $\langle t_1 \rangle_{\min} = \langle t_1 \rangle_{\lambda=0}$, i.e., surface diffusion is optimal.

Note that that limiting case $R = a/2$ means the particle always stays on the boundary, so that $\langle t_1 \rangle_{\min} = \langle t_1 \rangle_{\lambda=0}$.

The above arguments can be reformulated in terms of the ratio $f(R) = \frac{\langle t_1 \rangle_{\min}}{\langle t_1 \rangle_{\lambda=0}}$, i.e., the "gain" in the search time that intermittent surface-mediated diffusion may bring as compared to pure surface diffusion. By construction, $f(R) \leq 1$. From the above results, we have $f(a/2) = 1$. If D_2/D_1 exceeds $\Delta_{a,\epsilon}$, then there exists R_0 such that $D_{2,crit}(R_0) = D_2$. In this case, $\forall R > R_0$, $f(R) = 1$. Hence, we conclude that there exists an optimal value $R_{\min} \in [a/2, R_0]$ which gives $f(R_{\min}) = \min_R \{f(R)\}$. In other words, one can determine the rectangular shape (i.e., R_{\min}) which provides the highest "gain" in the search time.

5.3 Numerical asymptotic behavior

As in previous chapters, the purpose of this section is giving the numerical asymptotic behavior of \mathcal{T} , the mean exit time for non-intermittent pure bulk diffusion. Although we have another parameter R in this rectangle case, we obtain the same results as in 2-D case:

- We can state Theorem 5.3.1 which is an analogue of Theorem 3.3.1. The proof for those theorems are given generally in Appendix A.
- We believe that $\psi_n^2 \sim n^{-6}$ as $n \rightarrow \infty$, from which combines to Theorem 5.3.1, we obtain the asymptotic behavior $\mathcal{T} - \langle t_1 \rangle \sim \frac{1}{\sqrt{\lambda}}$ (see Eqs. (5.3.9), (5.3.10)).
- The asymptotic behavior of \mathcal{T} , the mean exit time for non-intermittent pure bulk diffusion is $\mathcal{T} \sim \ln(1/\epsilon)$ (see Eq. (5.3.12)).

The following theorem, stated similarly to Theorem 3.3.1 in 2-D case, shows the asymptotic behavior of λ_n as $n \rightarrow \infty$.

Theorem 5.3.1. *Let $(\lambda_n)_{n \geq 1}$ be the decreasing sequence of eigenvalues of the operator $V\tilde{T}V$, where the operators \tilde{T} and V are defined in Eqs. (3.2.9) and (5.1.17). We have*

$$\lambda_n \sim A_\epsilon n^{-2}, \quad (5.3.1)$$

where A_ϵ depends only on ϵ .

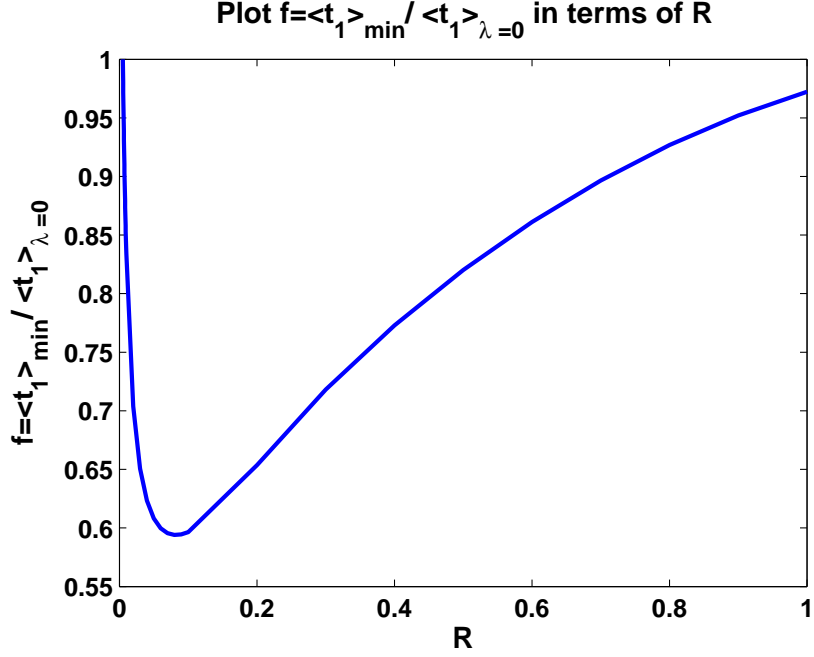


Figure 5.3: Function $f(R) = \frac{\langle t_1 \rangle_{\min}}{\langle t_1 \rangle_{\lambda=0}}$ versus R with fixed $D_1 = 1$, $D_2 = 2$, $a = 0.01$, $\epsilon = 0.01$, $R \in [a/2, 1]$. The minimum is obtained at $R \sim 0.08$ where $f(R = 0.08) = 0.594$.

Proof. The proof of this theorem is analogous to Theorem 3.3.1. \square

For the spectral weights, we believe that $\psi_n^2 \sim \frac{1}{n^6}$ as $n \rightarrow \infty$ (shown in Fig. 5.5). Consequently, Theorem 5.3.1 and this conjecture lead to the asymptotic behavior of $\langle t_1 \rangle_{\epsilon > 0}$ in the formulas (5.3.9) and (5.3.10). The rest of this section is devoted for being evidence to these conjectures. Since it is limited by the perturbations of λ_n and ψ_n^2 when ϵ is big, in this chapter we limit ourselves at $\epsilon \leq 1.2$.

The next part gives the numerical computations of the eigenvalues λ_n and the spectral weights ψ_n^2 (see Appendix B.3 for computational details). Figure 5.4 allows one to distinguish in three kinds of regimes for λ_n , for small, intermediate, and large n as in the following conjecture:

Conjecture 5.3.2. Let $(\lambda_n)_{n \geq 1}$ be defined in Theorem 5.3.1, we have
(i)

$$\lambda_n \simeq A_{a,R,\epsilon}^{(1)} n^0 \quad (\max\{na, n(2R - a)\} \ll 1), \quad (5.3.2)$$

i.e., there exists c_1, n_1, ϵ_1 such that for all $n \geq n_1$ and $\max\{na, n(2R - a)\} < \epsilon_1$, we

have

$$\frac{1}{c_1} < \left| \frac{\lambda_n}{A_{a,R,\epsilon}^{(1)} n^0} \right| < c_1,$$

(ii)

$$\lambda_n \simeq A_{a,R,\epsilon}^{(2)} n^{-1} \quad (\max\{na, n(2R-a)\} \gg 1 \gg \min\{na, n(2R-a)\}), \quad (5.3.3)$$

i.e., there exists c_2, n_2, ϵ_2 such that for all n , $\max\{na, n(2R-a)\} \geq n_2$ and $\min\{na, n(2R-a)\} < \epsilon_2$, we have

$$\frac{1}{c_2} < \left| \frac{\lambda_n}{A_{a,R,\epsilon}^{(2)} n^{-1}} \right| < c_2,$$

(iii)

$$\lambda_n \simeq A_\epsilon n^{-2} \quad (\min\{na, n(2R-a)\} \gg 1), \quad (5.3.4)$$

i.e., there exists c_3, n_3 such that for all n , $\min\{na, n(2R-a)\} \geq n_3$, we have

$$\frac{1}{c_3} < \left| \frac{\lambda_n}{A_\epsilon n^{-2}} \right| < c_3,$$

where $A_{a,R,\epsilon}^{(1)}$, $A_{a,R,\epsilon}^{(2)}$ and A_ϵ are three constants.

Theorem 5.3.1 proves the third (large n) asymptotic relation for λ_n and shows that the constant A_ϵ weakly depends on a and R .

In Fig. 5.4, the transition between three asymptotic regimes is determined by $1/(2R-a)$ and $1/a$ (and is independent of ϵ). One can see that these asymptotic relations accurately approximate the eigenvalues λ_n .

The behavior of A_ϵ is shown on Fig. 5.6b and Fig. 5.7b. As expected, it weakly depends on a and R . Although it is limited by $\epsilon \leq 1.2$, these numerical results show

$$A_\epsilon = (1 - \epsilon/\pi)^2. \quad (5.3.5)$$

According to the first case in Theorem C.0.1, the coefficient $A_{a,\epsilon}^{(1)}$ is equal to $a(2R-a)/2$ when $\epsilon = 0$. In Figs. 5.6a and 5.7a, we plot $\frac{2A_{a,R,\epsilon}^{(1)}}{a(2R-a)}$, this ratio approaches 1 as $\epsilon \rightarrow 0$.

Figure 5.5 shows that the asymptotic behavior of the spectral weights ψ_n^2 is more complicated. For each triple value of (a, R, ϵ) , one can distinguish three asymptotic regimes:

5.3. NUMERICAL ASYMPTOTIC BEHAVIOR

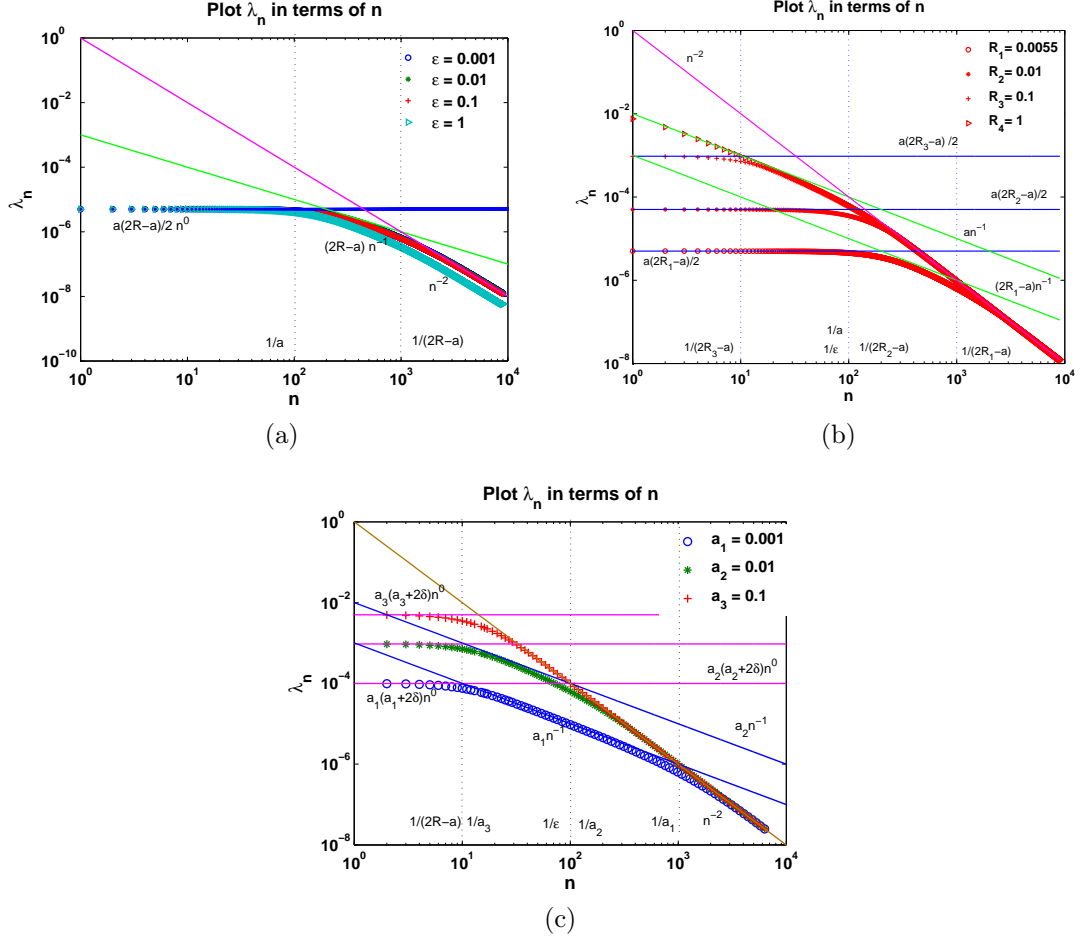


Figure 5.4: Eigenvalues λ_n of the operator $V\tilde{T}V$ (from left to right, up to down) for (a) $a = 0.01$, $R = 0.0055$ and four values ϵ : 0.001 (circles), 0.01 (stars), 0.1 (plus) and 1 (triangle); (b) for $\epsilon = 0.01$, $a = 0.01$ and four values of R : 0.0055 (circles), 0.01 (stars), 0.1 (plus), and 1 (triangle); and (c) for $\epsilon = 0.01$, $R = 0.1$ and three values of a : 0.001 (circles), 0.01 (stars) and 0.1 (plus). Solid lines show the asymptotic relations $a(2R - a)/2n^0$, a/n , $(2R - a)/n$ and $1/n^2$. The coefficient A_ϵ in front of n^{-2} relation is close to 1 for all small targets, except for $\epsilon = 1$, see Eq. (5.3.5). The first plot shows that λ_n weakly depends on ϵ . The second plot shows that for $R = R_1$ ($1 < R_1 < a$), there are three separated kinds of regimes of λ_n , the coefficient in front of n^{-1} relation is close to $2R_1 - a$; for $R = R_2$ ($1 < R = a$), the second regime disappears; for $R = R_3$ ($1 < a < R$), there are three separated kinds of regimes of λ_n , the coefficient in front of n^{-1} relation is close to a ; for $R = R_4$ ($R \geq 1$), the first regime disappears. In the last plot, it shows the dependence of λ_n in terms of a . Similar to the second plot, the second regime disappears when $a_2 = R$.

5.3. NUMERICAL ASYMPTOTIC BEHAVIOR

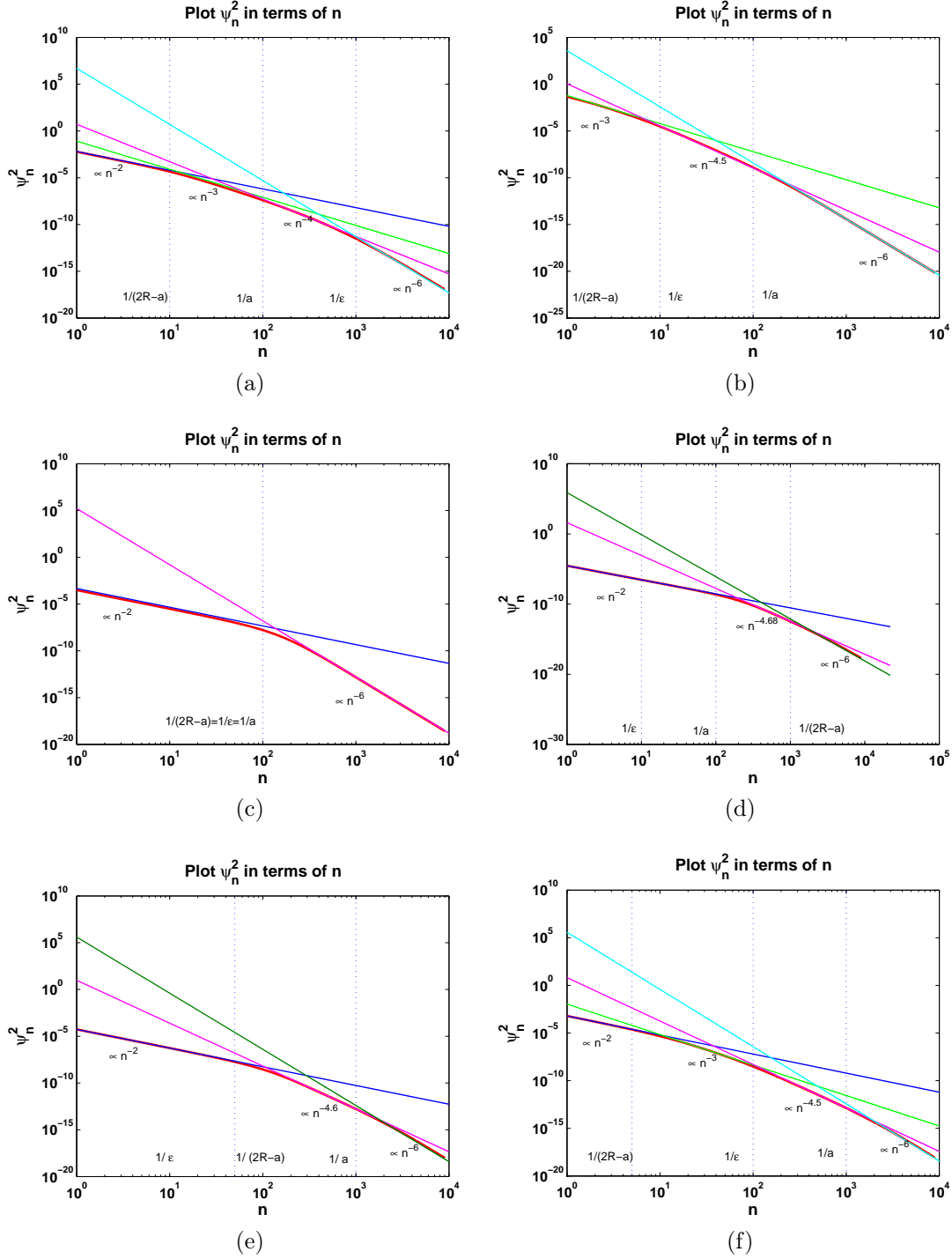


Figure 5.5: Spectral weights ψ_n^2 (shown by red solid line) for (a) $a = 0.01, R = 0.1$ and $\epsilon = 0.001$; (b) $a = 0.01, R = 1$ and $\epsilon = 0.1$; (c) $a = R = \epsilon = 0.01$; (d) $a = 0.01, R = 0.0055$ and $\epsilon = 0.1$; (e) $a = 0.001, R = 0.01$ and $\epsilon = 0.1$; and (f) $a = 0.001, R = 0.1$ and $\epsilon = 0.01$. In (a) and (f), there are four distinguished asymptotic regimes (the second regime in Conjecture 5.3.3 is separated into two different regimes), while the first regime disappears in (b) and the intermediate regimes disappears in (c).

Conjecture 5.3.3. Let ψ_n are the spectral weights of the function $V\tilde{T}(1)$ in the eigenbasis of the operator $V\tilde{T}V$

(i)

$$\psi_n^2 \simeq B_{a,R,\epsilon}^{(1)} n^{-2} \quad (\max\{na, n(2R-a)\} \ll 1), \quad (5.3.6)$$

i.e., there exists c'_1, n'_1, ϵ'_1 such that for all $n \geq n'_1$ and $\max\{na, n(2R-a)\} < \epsilon_1$, we have

$$\frac{1}{c'_1} < \left| \frac{\psi_n^2}{B_{a,R,\epsilon}^{(1)} n^{-2}} \right| < c'_1,$$

(ii)

$$\psi_n^2 \simeq B_{a,R,\epsilon}^{(2)} n^{-\alpha}, \quad (3 \leq \alpha < 6) \quad (\max\{na, n(2R-a)\} \gg 1 \gg \min\{na, n(2R-a), n\epsilon\}), \quad (5.3.7)$$

i.e., there exists c'_2, n'_2, ϵ'_2 such that for all n , $\max\{na, n(2R-a)\} \geq n'_2$ and $\min\{na, n(2R-a), n\epsilon\} < \epsilon_2$, we have

$$\frac{1}{c'_2} < \left| \frac{\psi_n^2}{B_{a,R,\epsilon}^{(2)} n^{-\alpha}} \right| < c'_2,$$

(iii)

$$\psi_n^2 \simeq B_{a,R,\epsilon}^{(4)} n^{-6} \quad (\min\{na, n(2R-a), n\epsilon\} \gg 1), \quad (5.3.8)$$

i.e., there exists c'_4, n'_4 such that for all n , $\min\{na, n(2R-a), n\epsilon\} \geq n'_4$, we have

$$\frac{1}{c'_4} < \left| \frac{\psi_n^2}{B_{a,R,\epsilon}^{(4)} n^{-6}} \right| < c'_4.$$

The second regime is more complicated. It can be two separated regimes (Fig. 5.5 a,f) (if $\min\{1/a, 1/(2R-a)\} < 1/\epsilon$), it can be only one regime (Fig. 5.5d,e) or it does not happen (Fig. 5.5 c). In order to observe all the regimes, one needs $2R-a \neq a \neq \epsilon$, $2R-a \neq 0$ and $a, \epsilon \ll 1$. If $2R-a$, a or ϵ is not small enough, the first regime (see (5.3.6)) may not be well established (Fig. 5.5 b). If $a \sim \epsilon$, $a \sim 2R-a$, $2R-a \sim \epsilon$ the second regime disappears, as illustrated on Fig. 5.5c. Finally, when $\epsilon \rightarrow 0$, $\max\{1/a, 1/\epsilon, 1/(2R-a)\} \rightarrow \infty$, the last regime disappears, and one retrieves three regimes for point-like targets (see Theorem C.0.1).

The behavior of the coefficients $B_{a,R,\epsilon}^{(1)}$ is shown on Fig. 5.6c and Fig. 5.7c. As expected, from the first case of Theorem C.0.1, $B_{a,R,\epsilon}^{(1)}/(\pi a(a+2\delta))$ approaches 1 as $\epsilon \rightarrow 0$ (point-like target). Moreover, such normalized coefficient weakly depends on a and R (either curves for $a = 0.01$, $a = 0.1$ in Fig. 5.7c or curves for $R = 0.0055$, $R = 0.01$, $R = 0.1$ in Fig. 5.6c almost coincide).

Fig 5.6d and Fig. 5.7d show the behavior of $B_{a,R,\epsilon}^{(4)}/(2\pi)$ as ϵ . As observation, although A_ϵ weakly depends on a and R , these parameters play significant roles on $B_{a,R,\epsilon}^{(4)}$.

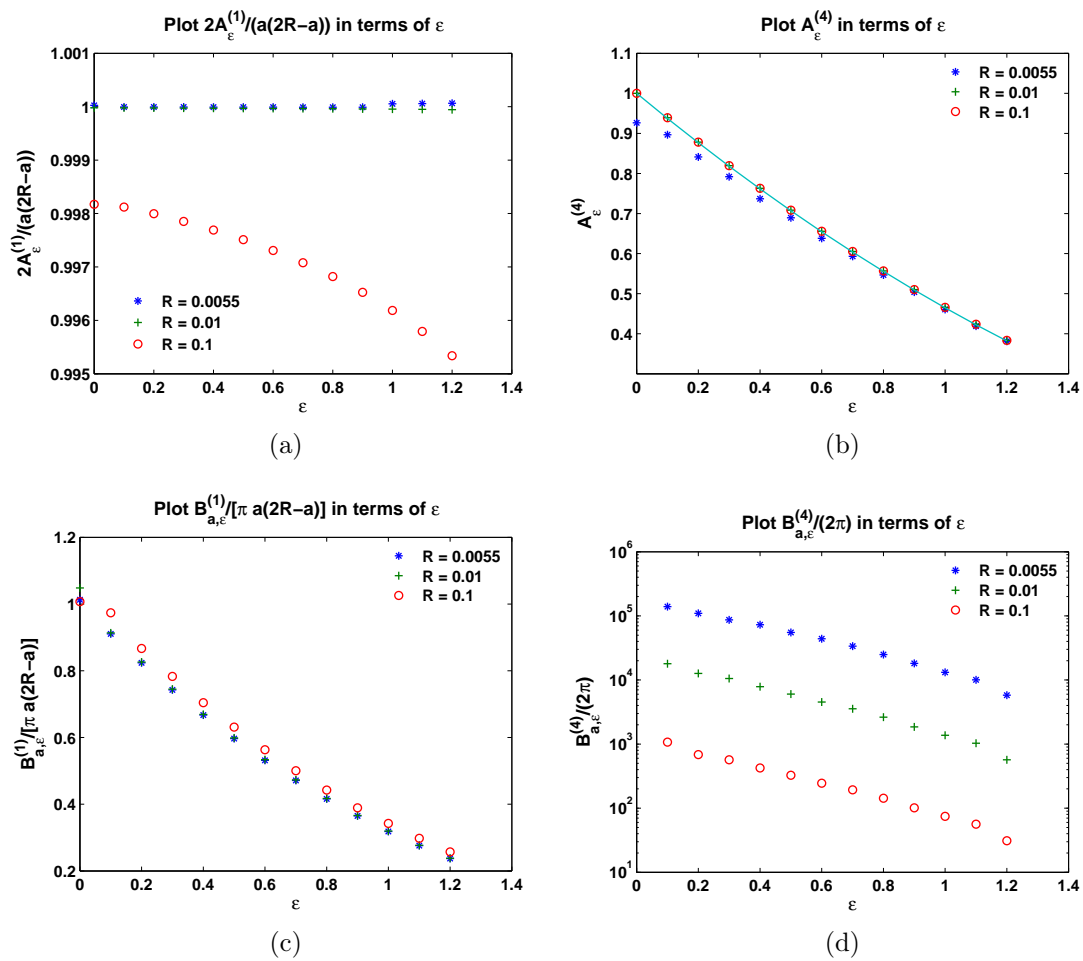


Figure 5.6: Coefficients $A_{\epsilon}^{(4)}$, $2A_{a,R,\epsilon}^{(1)}/(a(2R-a))$, $B_{a,\epsilon}^{(1)}/(\pi a(2R-a))$, and $B_{a,R,\epsilon}^{(4)}/(2\pi)$ from Conjectures (5.3.2), (5.3.3) versus ϵ . Four curves for fixed $a = 0.01$ and three values of R : $R = 0.1$, $R = 0.01$, and $R = 0.0055$ coincide that illustrates the independence of $A_{\epsilon}^{(4)}$ of R .

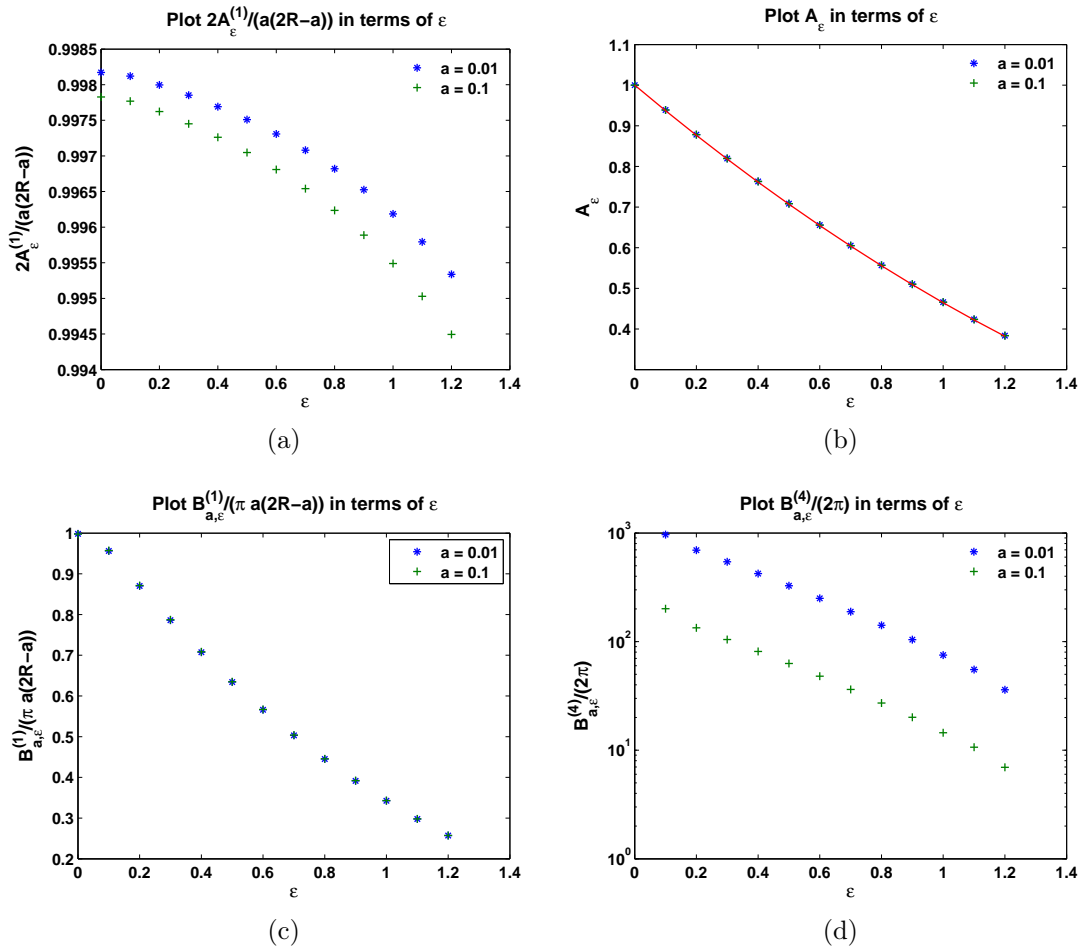


Figure 5.7: Coefficients $A_{\epsilon}^{(4)}$, $2A_{a,\epsilon}^{(1)}/(a(a+2\delta))$, $B_{a,\epsilon}^{(1)}/(\pi a(a+2\delta))$, and $\tilde{B}_{a,\epsilon}/(2\pi)$ from Conjectures (5.3.2), (5.3.3) versus ϵ . Four curves for fixed $R = 0.1$ and two values of a : $a = 0.1$ and $a = 0.01$ coincide that illustrates the independence of $A_{\epsilon}^{(4)}$ of a .

5.3. NUMERICAL ASYMPTOTIC BEHAVIOR

Although the above asymptotic regimes for λ_n and ψ_n^2 remain conjectural, we use the asymptotic relations of λ_n and ψ_n (for large n), to get the asymptotic behavior of $\langle t_1 \rangle_{\epsilon > 0}$.

$$\begin{aligned} \sum_{n \geq 1} \frac{\psi_n^2}{\lambda_n^2 (\lambda_n + \frac{D_1}{\lambda})} &\sim \int_1^\infty \frac{B_{a,R,\epsilon}^{(4)} x^{-6}}{A_\epsilon^2 x^{-4} (A_\epsilon x^{-2} + \frac{D_1}{\lambda})} dx \\ &= \frac{B_{a,R,\epsilon}^{(4)}}{A_\epsilon^3} \int_1^\infty \frac{dx}{1 + x^2 \frac{D_1}{\lambda A_\epsilon}} \sim \frac{B_{a,R,\epsilon}^{(4)}}{A_\epsilon^{5/2}} \frac{\pi}{2} \sqrt{\frac{\lambda}{D_1}}. \end{aligned}$$

Consequently, we get

$$\langle t_1 \rangle = \mathcal{T} - \frac{C_1}{\sqrt{\lambda}} + O\left(\frac{1}{\lambda}\right), \quad (5.3.9)$$

where

$$C_1 = C_{a,R,\epsilon} \frac{\sqrt{D_1}}{D_2}, \quad C_{a,R,\epsilon} = (R^2 - (R - a)^2) \frac{B_{a,R,\epsilon}^{(4)}}{8A_\epsilon^{5/2}}. \quad (5.3.10)$$

Figures 5.8 and 5.9 show the mean exit time $\langle t_1 \rangle$ as a function of λ for $\epsilon = 0.01$, $R = 2$ and three values of a : 0.001, 0.01 and 0.1 (Fig. 5.8) and for $\epsilon = 0.01$, $a = 0.01$ and four values of R : 0.0055, 0.01, 0.1 and 2 (Fig. 5.9). In the cases of R big ($R = 2$), the mean exit time passes through a minimum at some intermediate desorption rate λ_c and then approaches the maximum as $\lambda \rightarrow \infty$. One can clearly see that the optimal value λ_c as well as the height of the maximum at $\lambda \rightarrow \infty$ depend on a and R .

In the cases of R small ($R = 0.0055$, $R = 0.01$, $R = 0.1$), the mean exit time seems to be decreasing at the end which is contrary to Theorem (5.1.1). However, this is not a contradiction. In those cases, the facts are that $R^2 - (R - a)^2$ is very small while λ is not big enough and it is limited in computing λ_n and ψ_n^2 for n is not big enough. Hence, the second term in the formula of the function $\frac{d\langle t_1 \rangle}{d\lambda}$ (which can be computed from Eq. (5.1.23) with $S = \sum_{n \geq 1} \frac{\psi_n^2}{\lambda_n^2}$):

$$\pi \frac{d\langle t_1 \rangle}{d\lambda} = -\frac{S}{\lambda^2} + \frac{1}{\lambda^2} \frac{D_1 (R^2 - (R - a)^2)}{2D_2} \sum_{n \geq 1} \frac{\psi_n^2}{\lambda_n (\lambda_n + \frac{D_1}{\lambda})^2} + \frac{D_1}{\lambda^3} \sum_{n \geq 0} \frac{\psi_n^2 (2\lambda_n + D_1/\lambda)}{\lambda_n^2 (\lambda_n + D_1/\lambda)^2}, \quad (5.3.11)$$

is not big enough to make $\frac{d\langle t_1 \rangle}{d\lambda} > 0$. In order to observe the eventual increase of $\langle t_1 \rangle$ in those cases, one needs λ large enough ($\lambda > 10^6$), hence, it is necessary to solve more λ_n and ψ_n^2 ($n \gg 10^4$).

In the final part, we focus on the behavior of the mean exit time $\langle t_1 \rangle_{\epsilon > 0}$ in the case of $\lambda \rightarrow \infty$, a is very small, and R big enough. In this situation, when $\epsilon \rightarrow 0$,

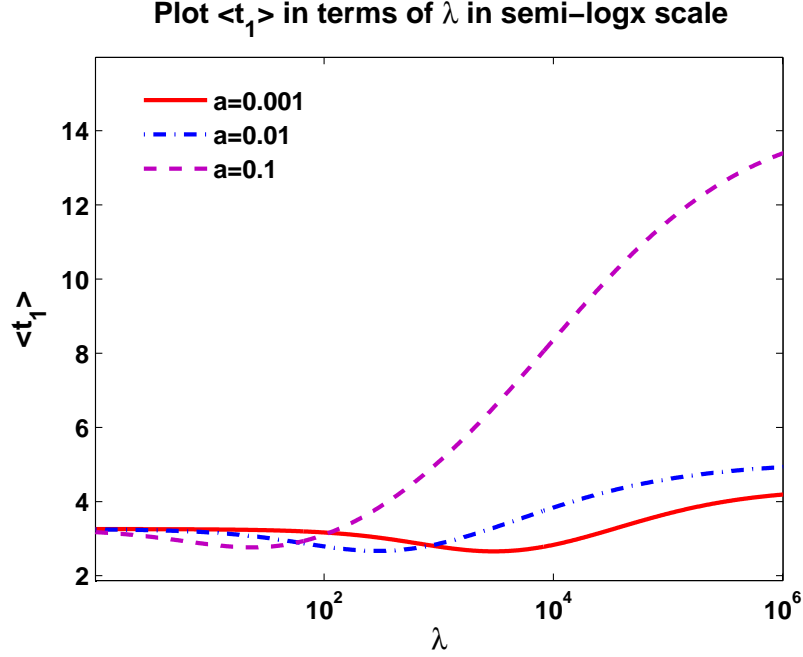


Figure 5.8: The mean time $\langle t_1 \rangle$ as a function of λ for $\epsilon = 0.01$, $R = 2$, $D_1 = 1$, $D_2 = 5$, and three values of a : 0.1 (dash pink line), 0.01 (dash-dot blue line), 0.001 (red solid line).

we use Conjectures (5.3.2) and (5.3.3) to get

$$\begin{aligned}
 \lim_{\lambda \rightarrow \infty} \langle t_1 \rangle &= \mathcal{T} = \frac{R^2 - (R - a)^2}{2\pi D_2} \sum_{n \geq 1} \frac{\psi_n^2}{\lambda_n^2} & (5.3.12) \\
 &= \frac{R^2 - (R - a)^2}{2\pi D_2} \left(\sum_{n=1}^{1/\epsilon} \frac{B_{a,R,\epsilon}^{(2)} n^{-3}}{A_{a,R,\epsilon}^{(2)2} n^{-2}} + \sum_{n=1/\epsilon}^{1/a} \frac{B_{a,R,\epsilon}^{(3)} n^{-\alpha}}{A_{a,R,\epsilon}^{(2)2} n^{-2}} + \sum_{n=1/a}^{\infty} \frac{B_{a,R,\epsilon}^{(4)} n^{-6}}{A_{a,R,\epsilon}^{(3)2} n^{-4}} \right) \\
 &= \frac{R^2 - (R - a)^2}{2\pi D_2} \left(\frac{B_{a,R,\epsilon}^{(2)}}{A_{a,R,\epsilon}^{(2)2}} \ln \left(\frac{1}{\epsilon} \right) + o(\ln(1/\epsilon)) \right), & (5.3.13)
 \end{aligned}$$

with $\alpha > 3$.

This logarithmic divergence is similar to the result from Ref. [21] which describes the mean exit time for non-intermittent bulk diffusion (2D Brownian motion) in the narrow escape limit ($\epsilon \rightarrow 0$).

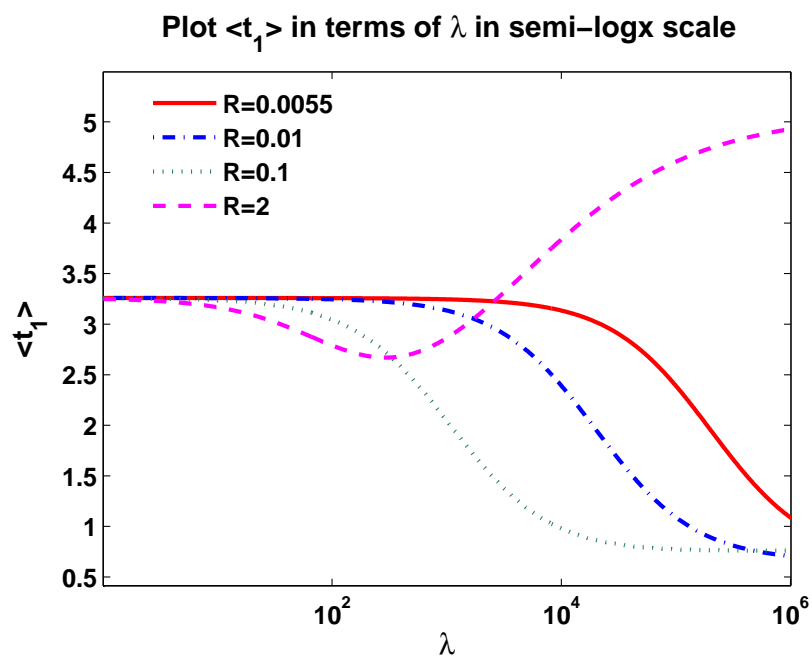


Figure 5.9: The mean time $\langle t_1 \rangle$ as a function of λ for $\epsilon = 0.01$, $a = 0.01$, $D_1 = 1$, $D_2 = 5$, and four values of R : 0.0055 (solid red line), 0.01 (dash-dot blue line), 0.1 (dot green line) and 2 (dash pink line).

Appendix A

Asymptotic behavior of the eigenvalues of the operator $V\tilde{T}V$

Proof of Theorems 3.3.1 and 5.3.1.

We state the following theorem which generalizes Theorem 3.3.1 and 5.3.1:

Theorem A.0.4. *Let $(\lambda_n)_{n \geq 1}$ be the decreasing sequence of eigenvalues of the operator $V\tilde{T}V$, where the operators \tilde{T} is defined in Eq. (3.2.9) and the operator V is defined by*

$$V(E_n) = \sqrt{1 - \varepsilon_n} E_n, \quad (\text{A.0.1})$$

with E_n are the orthonormal eigenvectors of V and $0 \leq \varepsilon_n \leq 1$.

We have

$$\lambda_n \sim A_\epsilon n^{-2}, \quad (\text{A.0.2})$$

where A_ϵ depends only on ϵ .

Proof. In order to prove this statement, we first investigate the following problem:

Let A and B are two compact, positive, self-adjoint operators. We assume that the eigenvalues of the operator A are ordered in a decreasing sequence: $\lambda_1(A) \geq \lambda_2(A) \geq \dots \geq \lambda_n(A) \geq \dots \geq 0$. We recall the variational principle as following

Proposition A.0.5 (Variational Principle). *Let \mathcal{F}_n be the set of n -dimensional subspaces F on $L^2[a, b]$, then*

$$\lambda_n(A) = \max_{F \in \mathcal{F}_n} \min_{0 \neq x \in A; x \in F} \frac{\langle Ax, x \rangle}{\langle x, x \rangle}. \quad (\text{A.0.3})$$

The max is taken over F , the subspace associated with the first n eigenvectors of A .

We state the following lemmas which will be needed to prove the Theorem A.0.4.

Lemma A.0.6. *We make the assumption that $\lambda_n(A)$, $\lambda_n(A + B)$ are the n^{th} eigenvalues of the operators A and $A + B$. Then, we have*

$$\lambda_n(A) - \|B\| \leq \lambda_n(A + B) \leq \lambda_n(A) + \|B\|, \quad (\text{A.0.4})$$

where $\|\cdot\|$ define the norm of an operator in $L^2[a, b]$ space.

Proof. Let $F(A)$ be the subspace of $L^2[a, b]$ associated with the first n eigenvectors of A . For all $x \in F(A)$, we have

$$\langle (A + B)x, x \rangle = \langle Ax, x \rangle + \langle Bx, x \rangle.$$

According to the variational principle, we have

$$\langle Ax, x \rangle \geq \min_{x \in A} \frac{\langle Ax, x \rangle}{\langle x, x \rangle} \|x\|^2 = \lambda_n(A) \|x\|^2. \quad (\text{A.0.5})$$

Besides, we have

$$|\langle Bx, x \rangle| \leq \|B\| \|x\|^2. \quad (\text{A.0.6})$$

It follows from Eqs. (A.0.5) and (A.0.6) that

$$\langle (A + B)x, x \rangle \geq \lambda_n(A) \|x\|^2 - \|B\| \|x\|^2.$$

This gives

$$\min_{0 \neq x \in F(A)} \frac{\langle (A + B)x, x \rangle}{\|x\|^2} \geq \lambda_n(A) - \|B\|.$$

Again, according to the variational principle, we thus get

$$\lambda_n(A + B) \geq \lambda_n(A) - \|B\|.$$

In the same manner, if we take $F(A + B)$ be associated to the first n eigenvectors of $A + B$, we can get

$$\lambda_n(A + B) \leq \lambda_n(A) + \|B\|,$$

and the lemma A.0.6 follows. \square

Lemma A.0.7. *With the notations used in Lemma A.0.6, if $\text{rank}(B) < n < \infty$, then*

$$\lambda_{n+\text{rank}(B)}(A) \leq \lambda_n(A + B) \leq \lambda_{n-\text{rank}(B)}(A). \quad (\text{A.0.7})$$

Proof. We call $F'(A)$ the subspace of $L^2[a, b]$ associated with the first $n + \text{rank}(B)$ eigenvectors of A .

By the variational principle, we have

$$\forall x \in F'(A) \cap \ker(B), \|x\| = 1 : \langle (A + B)x, x \rangle = \langle Ax, x \rangle \geq \lambda_{n+\text{rank}(B)}(A).$$

Consequently,

$$\min_{x \in F'(A) \cap \ker(B); \|x\|=1} \langle (A + B)x, x \rangle \geq \lambda_{n+\text{rank}(B)}(A).$$

Since

$$\dim(F'(A) \cap \ker(B)) = \dim F'(A) - \dim B(F'(A)) \geq n,$$

we have

$$\lambda_n(A + B) \geq \min_{0 \neq x \in \ker(B) \cap F'(A); \|x\|=1} \langle (A + B)x, x \rangle.$$

So, we conclude that

$$\lambda_n(A + B) \geq \lambda_{n+\text{rank}(B)}(A). \quad (\text{A.0.8})$$

The second inequality in (A.0.7) of this Lemma is obtained when we put $A' = A + B$, $B' = -B$, $n' = n - \text{rank}(B)$ and apply the conclusion (A.0.8) for A' , B' and n' instead of A , B and n . \square

We now call π_N be the orthogonal projection on the first N eigenvectors of B .

By the property of an orthogonal projection, we can rewrite

$$B = \pi_N B \pi_N + (I - \pi_N) B (I - \pi_N),$$

then

$$A + B = A + \pi_N B \pi_N + (I - \pi_N) B (I - \pi_N).$$

We note that

$$\text{rank}(\pi_N B \pi_N) = N,$$

and

$$\|(I - \pi_N) B (I - \pi_N)\| \leq \lambda_N(B). \quad (\text{A.0.9})$$

By applying lemma A.0.6, we get $\forall n \geq N$,

$$\begin{aligned} \lambda_n(A + \pi_N B \pi_N) - \|(I - \pi_N) B (I - \pi_N)\| &\leq \lambda_n(A + B), \\ \lambda_n(A + B) &\leq \lambda_n(A + \pi_N B \pi_N) + \|(I - \pi_N) B (I - \pi_N)\|. \end{aligned}$$

From (A.0.9), we obtain

$$\lambda_n(A + \pi_N B \pi_N) - \lambda_N(B) \leq \lambda_n(A + B) \leq \lambda_n(A + \pi_N B \pi_N) + \lambda_N(B).$$

According to lemma A.0.7,

$$\lambda_{n+N}(A) - \lambda_N(B) \leq \lambda_n(A + B) \leq \lambda_{n-N}(A) + \lambda_N(B).$$

We can thus conclude that

$$\forall N, \forall n \geq N : \lambda_{n+N}(A) - \lambda_N(B) \leq \lambda_n(A + B) \leq \lambda_{n-N}(A) + \lambda_N(B). \quad (\text{A.0.10})$$

Lemma A.0.8. *Let $\{\lambda_n(A)\}$ and $\{\lambda_n(B)\}$ be the eigenvalues of two self-adjoint operators A and B . If $\lambda_n(A) \sim cn^{-s}$ and $\lambda_N(B) = \rho^N$ where c and ρ are some constants, $0 \leq \rho < 1$, then*

$$\lambda_n(A + B) \sim cn^{-s}.$$

Proof. Indeed, by applying (A.0.10), if we choose $N(n) = n^\delta$, with $\delta < 1$, then we obtain from (A.0.10) that

$$c(n + n^\delta)^{-s}(1 + o(1)) - \rho^{n^\delta} \leq \lambda_n(A + B) \leq c(n - n^\delta)^{-s}(1 + o(1)) + \rho^{n^\delta},$$

Let $n \rightarrow \infty$, we have

$$cn^{-s}(1 + o(1)) \leq \lambda_n(A + B) \leq cn^{-s}(1 + o(1)).$$

Hence, we conclude that $\lambda_n(A + B) \sim cn^{-s}$. \square

We turn back to prove the Theorem A.0.4.

We consider the eigenpairs of the operator $V\tilde{T}V$, where \tilde{T} is defined in Eq. (3.2.9), and V is defined by

$$V(E_n) = \sqrt{1 - \varepsilon_n} E_n = \left(1 - \sum_{m \geq 1} \binom{\alpha}{m} \varepsilon_n^m\right) E_n \simeq \left(1 - \frac{1}{2} \varepsilon_n\right) E_n$$

where $\{E_n\}$ are the eigenvectors of the operator V , $0 \leq \varepsilon_n \leq 1$ and $\binom{\alpha}{m} = \prod_{k=1}^m \frac{\alpha - k + 1}{k}$ are binomial coefficients. In this thesis, ε_n can either be $(1 - a)^n$ ($0 \leq a \leq 1$) (2-D case) or be $\frac{\cosh n(R-a)}{\cosh nR}$ ($0 \leq a \leq 2R$, $R > 0$) (rectangle case). The last approximate equality is valid for $\varepsilon_n \rightarrow 0$ as $n \rightarrow \infty$.

Putting

$$R(E_n) = \left(\sum_{m \geq 1} \binom{\alpha}{m} \varepsilon_n^m\right) E_n,$$

then,

$$V\tilde{T}V = (I - R)\tilde{T}(I - R) = \tilde{T} - R\tilde{T} - \tilde{T}R - R\tilde{T}R.$$

Let us denote by K_N the image of the orthonormal projection on the first N^{th} eigenvectors of R and R_N the image of the orthonormal projection on the rest eigenvectors of R . By definition, $R = K_N + R_N$. Then,

$$\begin{aligned} V\tilde{T}V &= \tilde{T} - (K_N + R_N)\tilde{T} - \tilde{T}(K_N + R_N) + (K_N + R_N)\tilde{T}(K_N + R_N) \\ &= \tilde{T} - \underbrace{K_N\tilde{T} - \tilde{T}K_N + K_N\tilde{T}K_N + K_N\tilde{T}R_N + R_N\tilde{T}K_N}_{\text{these operators have the finite rank, which equal to } N} - R_N\tilde{T} - \tilde{T}R_N + R_N\tilde{T}R_N. \end{aligned} \tag{A.0.11}$$

We note that $\text{rank}(K_N) = N$ and in formula (A.0.11), whenever there is a K_N , we have an operator of rank N .

Moreover, $-R_N\tilde{T} - \tilde{T}R_N + R_N\tilde{T}R_N$ has the norm dominated by the N^{th} eigenvalue of R :

$$\begin{aligned} \|-R_N\tilde{T} - \tilde{T}R_N + R_N\tilde{T}R_N\| &\leq \|R_N\tilde{T}\| + \|\tilde{T}R_N\| + \|R_N\tilde{T}R_N\| \\ &\leq c\|R_N\| \leq c\lambda_N(R) \leq c\varepsilon_N, \end{aligned}$$

since $\lambda_N(R) = \sum_{m \geq 1} \binom{\alpha}{m} \varepsilon_n^m \leq \varepsilon_N$.

Hence, refer to Lemma A.0.8, we get that

$$\lambda_n(V\tilde{T}V) \sim \lambda_n(\tilde{T}).$$

Particularly, in Chapters 3 and 5, as the operator \tilde{T} is defined in Eq. (3.2.9), we have $\lambda_n(\tilde{T}) = \nu_n \sim A_\epsilon n^{-2}$ where $\nu_n = \frac{(1-\epsilon/\pi)^2}{(n+1/2)^2}$ is defined in Eq.(3.2.11). Consequently, we get that $\lambda_n(V\tilde{T}V) \sim A_\epsilon n^{-2}$ and $A_\epsilon \simeq \left(1 - \frac{\epsilon}{\pi}\right)^2$. \square

Appendix B

Numerical computation of spectral characteristics

B.1 2-D case

We briefly present a numerical algorithm to compute the spectral characteristics λ_n and ψ_n . In order to compute the eigenvalues λ_n and the eigenvectors e_n of the operator $V\tilde{T}V$, we get an explicit representation of this operator in the basis $\cos n\theta$. First, we find

$$\tilde{T}(\cos n\theta) = \begin{cases} \frac{\cos n\theta - \cos n(\pi - \epsilon)}{n^2}, & 0 \leq \theta < \pi - \epsilon, \\ 0, & \pi - \epsilon \leq \theta \leq \pi, \end{cases} \quad (\text{B.1.1})$$

and

$$\tilde{T}(1)(\theta) = \begin{cases} \frac{(\pi - \epsilon)^2 - \theta^2}{2}, & 0 \leq \theta < \pi - \epsilon, \\ 0, & \pi - \epsilon \leq \theta \leq \pi, \end{cases} \quad (\text{B.1.2})$$

from which the expansion of $\tilde{T}(\cos n\theta)$ ($n \geq 0$) in the basis $\{\cos n\theta\}$ of $L^2_{\text{even}}[0, \pi]$ is

$$\tilde{T}(\cos n\theta) = \sum_{m \geq 0} \mathbf{T}_{mn} \cos m\theta \quad n \geq 0, \quad (\text{B.1.3})$$

where the coefficients \mathbf{T}_{mn} are defined by

$$\begin{aligned} \frac{\pi}{2} \mathbf{T}_{mn} &= \begin{cases} \langle \tilde{T}(\cos n\theta), \cos m\theta \rangle, & \text{if } m \geq 1 \\ \frac{1}{2} \langle \tilde{T}(\cos n\theta), 1 \rangle, & \text{if } m = 0 \end{cases} \\ &= \begin{cases} \frac{1}{2} (1 - \delta_{mn}) \frac{(-1)^{m+n+1}}{mn} \left[\frac{\sin(m-n)\epsilon}{m-n} - \frac{\sin(m+n)\epsilon}{m+n} \right] + \frac{1}{2} \delta_{mn} \frac{1}{n^2} \left(\pi - \epsilon + \frac{\sin 2n\epsilon}{2n} \right) & (m \geq 1; n \geq 1), \\ \frac{1}{2} \frac{(-1)^{n+1}}{n^2} \left[(\pi - \epsilon) \cos n\epsilon + \frac{\sin n\epsilon}{n} \right], & (m = 0; n \geq 1), \\ \frac{(-1)^{m+1}}{m^2} \left[(\pi - \epsilon) \cos m\epsilon + \frac{\sin m\epsilon}{m} \right], & (m \geq 1; n = 0), \\ \frac{(\pi - \epsilon)^3}{6}, & (m = 0; n = 0). \end{cases} \end{aligned} \quad (\text{B.1.4})$$

In turn, the operator V has a diagonal representation:

$$\mathbf{V}_{mn} = \begin{cases} \sqrt{1 - (1 - a)^m} & (m = n; m, n \geq 0), \\ 0 & (m \neq n; m, n \geq 0). \end{cases} \quad (\text{B.1.5})$$

Combining these results, the operator $V\tilde{T}V$ is represented by the infinite-dimensional matrix \mathbf{VTV} whose elements are

$$[\mathbf{VTV}]_{m,n} = \frac{1}{\pi} \sqrt{1 - (1 - a)^n} \sqrt{1 - (1 - a)^m} \left\{ \delta_{mn} \frac{1}{n^2} \left(\pi - \epsilon + \frac{\sin 2n\epsilon}{2n} \right) - (1 - \delta_{mn}) \frac{(-1)^{m+n}}{mn} \left[\frac{\sin(m-n)\epsilon}{m-n} - \frac{\sin(m+n)\epsilon}{m+n} \right] \right\} \quad (m \geq 1; n \geq 1), \quad (\text{B.1.6})$$

and $[\mathbf{VTV}]_{m,n} = 0$ if $m = 0$ or $n = 0$. Solving the eigenvalues $\{\lambda_n\}$ and the eigenvectors $\{e_n\}$ of the operator $V\tilde{T}V$ is equivalent to finding the eigenpairs of the associated matrix \mathbf{VTV} . Note that this matrix is symmetric.

The matrix \mathbf{VTV} is diagonalized in Matlab that finds the eigenvalues λ_n and the coefficients v_{mn} determining the orthonormal basis $\{e_n\}_{n \geq 0}$ as

$$e_n(\theta) = \sqrt{\frac{1}{\pi}} v_{0n} + \sqrt{\frac{2}{\pi}} \sum_{m \geq 1} v_{mn} \cos m\theta. \quad (\text{B.1.7})$$

The spectral weights ψ_n are then given as

$$\psi_n = \langle \psi, e_n \rangle = \sqrt{\frac{2}{\pi}} \sum_{m \geq 1} v_{mn} \langle \psi, \cos m\theta \rangle, \quad (\text{B.1.8})$$

where

$$\langle \psi, \cos m\theta \rangle = \sqrt{1 - (1 - a)^m} \frac{(-1)^{m+1}}{m^2} \left[(\pi - \epsilon) \cos m\epsilon + \frac{\sin m\epsilon}{m} \right],$$

and $\langle \psi, 1 \rangle = \langle V\tilde{T}(1), 1 \rangle = \langle \tilde{T}(1), V(1) \rangle = 0$.

In our computation, the size of matrix VTV in this 2-D case is 22000×22000 .

B.2 3-D case

We briefly present a numerical algorithm to compute the spectral characteristics λ_n and ψ_n . In order to compute the eigenvalues λ_n and the eigenvectors e_n of the operator $V\tilde{T}V$, we get an explicit representation of this operator in the basis $\{P_n(x)\}$. First, we find

$$\tilde{T}(P_n)(x) = \begin{cases} \frac{P_n(x) - P_n(\alpha_\epsilon)}{n(n+1)}, & -1 \leq x < \alpha_\epsilon, \\ 0, & \alpha_\epsilon \leq \theta \leq 1, \end{cases} \quad (n \geq 1) \quad (\text{B.2.1})$$

and

$$\tilde{T}(1)(x) = \begin{cases} \log \frac{1-x}{1-\alpha_\epsilon}, & -1 \leq x < \alpha_\epsilon, \\ 0, & \alpha_\epsilon \leq x \leq 1, \end{cases} \quad (n=0) \quad (\text{B.2.2})$$

from which the expansion of $\tilde{T}(P_n)(x)$ ($n \geq 0$) in the basis $\{P_n(x)\}$ of $L^2[-1, 1]$ is

$$\tilde{T}(P_n)(x) = \sum_{m \geq 0} \mathbf{T}_{mn} P_m(x) \quad n \geq 0, \quad (\text{B.2.3})$$

where the coefficients \mathbf{T}_{mn} are defined by

$$\begin{aligned} \mathbf{T}_{mn} &= \sqrt{\frac{2n+1}{2}} \sqrt{\frac{2m+1}{2}} \langle \tilde{T}(P_n)(x), P_m(x) \rangle \\ &= \begin{cases} (1 - \delta_{mn}) \frac{\sqrt{2n+1}\sqrt{2m+1}}{2} \frac{1}{(n+1)(m+1)} \\ \quad \times \frac{(n-m)uP_m(\alpha_\epsilon)P_n(\alpha_\epsilon) + (m+1)P_{n-1}(\alpha_\epsilon)P_m(\alpha_\epsilon) - (n+1)P_{m-1}(\alpha_\epsilon)P_n(\alpha_\epsilon)}{m(m+1) - n(n+1)} \\ \quad + \delta_{mn} \frac{2n+1}{2} \frac{1}{n(n+1)} \left[-P_n(\alpha_\epsilon) \frac{\alpha_\epsilon P_n(\alpha_\epsilon) - P_{n-1}(\alpha_\epsilon)}{n+1} + \frac{F_n(\alpha_\epsilon) + 1}{2n+1} \right], & (m \geq 0; n \geq 1), \\ \frac{\sqrt{2m+1}}{2} \frac{1}{m(m+1)} \left[\left(1 + \frac{m\alpha_\epsilon}{m+1}\right) P_m(\alpha_\epsilon) + \frac{P_{m-1}(\alpha_\epsilon)}{(m+1)(2m+1)} \right], & (n=0; m \geq 1). \end{cases} \end{aligned}$$

In turn, the operator V has a diagonal representation:

$$\mathbf{V}_{mn} = \begin{cases} \sqrt{1 - (1-a)^m} & (m = n; m, n \geq 0), \\ 0 & (m \neq n; m, n \geq 0). \end{cases} \quad (\text{B.2.4})$$

Combining these results, the operator $V\tilde{T}V$ is represented by the infinite-dimensional matrix \mathbf{VTV} whose elements are

$$\begin{aligned} [\mathbf{VTV}]_{m,n} &= \frac{\sqrt{2n+1}\sqrt{2m+1}}{2} \sqrt{1 - (1-a)^n} \sqrt{1 - (1-a)^m} \\ &\quad \times \left\{ \delta_{mn} \frac{1}{n(n+1)} \left[-P_n(\alpha_\epsilon) \frac{\alpha_\epsilon P_n(\alpha_\epsilon) - P_{n-1}(\alpha_\epsilon)}{n+1} + \frac{F_n(\alpha_\epsilon) + 1}{2n+1} \right] \right. \\ &\quad + (1 - \delta_{mn}) \frac{1}{(m+1)(n+1)} \\ &\quad \left. \times \frac{(n-m)\alpha_\epsilon P_m(\alpha_\epsilon)P_n(\alpha_\epsilon) + (m+1)P_{n-1}(\alpha_\epsilon)P_m(\alpha_\epsilon) - (n+1)P_{m-1}(\alpha_\epsilon)P_n(\alpha_\epsilon)}{m(m+1) - n(n+1)} \right\}, \end{aligned} \quad (\text{B.2.5})$$

if $m \geq 1; n \geq 1$ and $[\mathbf{VTV}]_{m,n} = 0$ if $m = 0$ or $n = 0$. Solving the eigenvalues $\{\lambda_n\}$ and the eigenvectors $\{e_n\}$ of the operator $V\tilde{T}V$ is equivalent to finding the eigenpairs of the associated matrix \mathbf{VTV} . Note that this matrix is symmetric.

The matrix \mathbf{VTV} is diagonalized in Matlab that finds the eigenvalues λ_n and the coefficients v_{mn} determining the orthonormal basis $\{e_n\}_{n \geq 0}$ as

$$e_n = \sum_{m \geq 0} v_{mn} \sqrt{\frac{2m+1}{2}} P_m(x). \quad (\text{B.2.6})$$

The spectral weights ψ_n are then given as

$$\psi_n = \langle \psi, e_n \rangle = \sum_{m \geq 1} v_{mn} \sqrt{\frac{2m+1}{2}} \langle \psi, P_m \rangle, \quad (\text{B.2.7})$$

where

$$\langle \psi, P_m \rangle = \frac{\sqrt{2m+1}}{2} \frac{\sqrt{1-(1-a)^m}}{m(m+1)} \left[\left(1 + \frac{m\alpha_\epsilon}{m+1} \right) P_m(\alpha_\epsilon) + \frac{P_{m-1}(\alpha_\epsilon)}{(m+1)(2m+1)} \right], \quad (\text{B.2.8})$$

and $\langle \psi, 1 \rangle = \langle V\tilde{T}(1), 1 \rangle = \langle \tilde{T}(1), V(1) \rangle = 0$.

In 3-D case, we compute matrix $[VTV]_{N \times N}$ with the size $N = 22000$.

B.3 Rectangle case

We briefly present a numerical algorithm to compute the spectral characteristics λ_n and ψ_n . In order to compute the eigenvalues λ_n and the eigenvectors e_n of the operator $V\tilde{T}V$, we get an explicit representation of this operator in the basis $\cos n\theta$. First, we find

$$\tilde{T}(\cos n\theta) = \begin{cases} \frac{\cos n\theta - \cos n(\pi-\epsilon)}{n^2}, & 0 \leq \theta < \pi - \epsilon, \\ 0, & \pi - \epsilon \leq \theta \leq \pi, \end{cases} \quad (\text{B.3.1})$$

and

$$\tilde{T}(1)(\theta) = \begin{cases} \frac{(\pi-\epsilon)^2 - \theta^2}{2}, & 0 \leq \theta < \pi - \epsilon, \\ 0, & \pi - \epsilon \leq \theta \leq \pi, \end{cases} \quad (\text{B.3.2})$$

from which the expansion of $\tilde{T}(\cos n\theta)$ ($n \geq 0$) in the basis $\{\cos n\theta\}$ of $L^2_{\text{even}}[0, \pi]$ is

$$\tilde{T}(\cos n\theta) = \sum_{m \geq 0} \mathbf{T}_{mn} \cos m\theta \quad n \geq 0, \quad (\text{B.3.3})$$

where the coefficients \mathbf{T}_{mn} are defined by

$$\begin{aligned} \frac{\pi}{2} \mathbf{T}_{mn} &= \begin{cases} \langle \tilde{T}(\cos n\theta), \cos m\theta \rangle, & \text{if } m \geq 1 \\ \frac{1}{2} \langle \tilde{T}(\cos n\theta), 1 \rangle, & \text{if } m = 0 \end{cases} \\ &= \begin{cases} \frac{1}{2} (1 - \delta_{mn}) \frac{(-1)^{m+n+1}}{mn} \left[\frac{\sin(m-n)\epsilon}{m-n} - \frac{\sin(m+n)\epsilon}{m+n} \right] + \frac{1}{2} \delta_{mn} \frac{1}{n^2} \left(\pi - \epsilon - \frac{\sin 2m\epsilon}{2m} \right) & (m \geq 1; n \geq 1), \\ \frac{1}{2} \frac{(-1)^{n+1}}{n^2} \left[(\pi - \epsilon) \cos n\epsilon + \frac{\sin n\epsilon}{n} \right], & (m = 0; n \geq 1), \\ \frac{(-1)^{m+1}}{m^2} \left[(\pi - \epsilon) \cos m\epsilon + \frac{\sin m\epsilon}{m} \right], & (m \geq 1; n = 0), \\ \frac{(\pi-\epsilon)^3}{6}, & (m = 0; n = 0). \end{cases} \end{aligned} \quad (\text{B.3.4})$$

In turn, the operator V has a diagonal representation:

$$\mathbf{V}_{mn} = \begin{cases} \sqrt{1 - \frac{\cosh m(R-a)}{\cosh mR}} & (m = n; m, n \geq 0), \\ 0 & (m \neq n; m, n \geq 0). \end{cases} \quad (\text{B.3.5})$$

Combining these results, the operator $V\tilde{T}V$ is represented by the infinite-dimensional matrix \mathbf{VTV} whose elements are

$$\begin{aligned} [\mathbf{VTV}]_{m,n} = & \frac{1}{\pi} \sqrt{1 - \frac{\cosh n(R-a)}{\cosh nR}} \sqrt{1 - \frac{\cosh m(R-a)}{\cosh mR}} \left\{ \delta_{mn} \frac{1}{n^2} \left(\pi - \epsilon - \frac{\sin 2n\epsilon}{2n} \right) \right. \\ & \left. - (1 - \delta_{mn}) \frac{(-1)^{m+n}}{mn} \left[\frac{\sin(m-n)\epsilon}{m-n} - \frac{\sin(m+n)\epsilon}{m+n} \right] \right\} \quad (m \geq 1; n \geq 1), \end{aligned} \quad (\text{B.3.6})$$

and $[\mathbf{VTV}]_{m,n} = 0$ if $m = 0$ or $n = 0$. Solving the eigenvalues $\{\lambda_n\}$ and the eigenvectors $\{e_n\}$ of the operator $V\tilde{T}V$ is equivalent to finding the eigenpairs of the associated matrix \mathbf{VTV} . Note that this matrix is symmetric.

The matrix \mathbf{VTV} is diagonalized in Matlab that finds the eigenvalues λ_n and the coefficients v_{mn} determining the orthonormal basis $\{e_n\}_{n \geq 0}$ as

$$e_n(\theta) = \sqrt{\frac{1}{\pi}} v_{0n} + \sqrt{\frac{2}{\pi}} \sum_{m \geq 1} v_{mn} \cos m\theta. \quad (\text{B.3.7})$$

The spectral weights ψ_n are then given as

$$\psi_n = \langle \psi, e_n \rangle = \sqrt{\frac{2}{\pi}} \sum_{m \geq 1} v_{mn} \langle \psi, \cos m\theta \rangle, \quad (\text{B.3.8})$$

where

$$\langle \psi, \cos m\theta \rangle = \sqrt{1 - \frac{\cosh m(R-a)}{\cosh mR}} \frac{(-1)^{m+1}}{m^2} \left[(\pi - \epsilon) \cos m\epsilon + \frac{\sin m\epsilon}{m} \right],$$

and $\langle \psi, 1 \rangle = \langle V\tilde{T}(1), 1 \rangle = \langle \tilde{T}(1), V(1) \rangle = 0$.

In the rectangle case, since we have one more parameter R and it requires to run much more the computation of the eigenvalues λ_n and spectral weights ψ_n^2 (for different values of a, R, ϵ). In the restriction of the time, in our computations, we compute matrix VTV in the size of $10^4 \times 10^4$.

Appendix C

Proof of Theorem 5.1.1

Theorem C.0.1. For point-like target ($\epsilon = 0$), Eqs. (5.1.24) and (5.1.25) imply for fixed R and small a the existence of the following distinct asymptotic behaviors:

- (1) If $na \ll 1$ and $n(2R - a) \ll 1$ then $\lambda_n \simeq \frac{a(2R-a)}{2}n^0$ and $\psi_n^2 \simeq \pi a(2R - a)n^{-2}$,
i.e.
 $\exists c_1, c'_1, n_1, \epsilon_1, \epsilon'_1$, such that $\forall n \geq n_1$ but $na < \epsilon_1$, $n(2R - a) < \epsilon'_1$, we have
 $\frac{1}{c_1} < \left| \frac{\lambda_n}{a(2R-a)n^0/2} \right| < c_1$ and $\frac{1}{c'_1} < \left| \frac{\psi_n^2}{\pi a(2R-a)n^{-2}} \right| < c'_1$.
- (2) If $na \gg 1$ and $n(2R - a) \ll 1$ then $\lambda_n \simeq (2R - a)n^{-1}$ and $\psi_n^2 \simeq 2\pi(2R - a)n^{-3}$,
i.e.
 $\exists c_2, c'_2, n_2, \epsilon_2$ such that $\forall n$, with $na \geq n_2$, but $n(2R - a) < \epsilon_2$ we have
 $\frac{1}{c_2} < \left| \frac{\lambda_n}{(2R-a)n^{-1}} \right| < c_2$ and $\frac{1}{c'_2} < \left| \frac{\psi_n^2}{2\pi(2R-a)n^{-3}} \right| < c'_2$.
- (3) If $na \ll 1$ and $n(2R - a) \gg 1$ then $\lambda_n \simeq an^{-1}$ and $\psi_n^2 \simeq 2\pi an^{-3}$, i.e.
 $\exists c_3, c'_3, n_3, \epsilon_3$, such that $\forall n$, with $n(2R - a) \geq n_3$ but $na < \epsilon_3$, we have
 $\frac{1}{c_3} < \left| \frac{\lambda_n}{an^{-1}} \right| < c_3$ and $\frac{1}{c'_3} < \left| \frac{\psi_n^2}{2\pi an^{-3}} \right| < c'_3$.
- (4) If $na \gg 1$ and $n(2R - a) \gg 1$ then $\lambda_n \simeq n^{-2}$ and $\psi_n^2 \simeq 2\pi n^{-4}$, i.e.
 $\exists c_4, c'_4, n_4$ such that $\forall n$, with $\min\{na, n(2R - a)\} \geq n_4$, we have $\frac{1}{c_4} < \left| \frac{\lambda_n}{n^{-2}} \right| < c_4$ and $\frac{1}{c'_4} < \left| \frac{\psi_n^2}{2\pi n^{-4}} \right| < c'_4$.

Proof. Indeed, Eqs. (5.1.24) , (5.1.25) gives us:

$$\lambda_n = \begin{cases} \left(1 - \frac{\cosh n(R-a)}{\cosh nR}\right) \frac{1}{n^2}, & (n \geq 1), \\ 0, & (n = 0). \end{cases} \quad \psi_n^2 = \begin{cases} 2\pi \left(1 - \frac{\cosh n(R-a)}{\cosh nR}\right) \frac{1}{n^4}, & (n \geq 1), \\ 0, & (n = 0). \end{cases}$$

- (1) If $\max\{na, n(2R - a)\} \ll 1$ which means $\exists \epsilon_1, n_1$ such that $\forall n \geq n_1$, we have

$na < \epsilon_1$ and $n(2R - a) < \epsilon_1$, then we have

$$\begin{aligned}
 1 - \frac{\cosh n(R-a)}{\cosh nR} &= 1 - \cosh na + \sinh na \tanh nR \\
 &= 1 - \left(1 + \frac{n^2 a^2}{2!} + \sum_{i=2}^{\infty} \frac{(na)^{2i}}{(2i)!} \right) \\
 &\quad + \left(na + \sum_{i=1}^{\infty} \frac{(na)^{2i+1}}{(2i+1)!} \right) \left(nR + \sum_{j=2}^{\infty} (nR)^{2j-1} \frac{B_{2j} 4^j (4^j - 1)}{(2j)!} \right) \\
 &= \frac{n^2 a(2R-a)}{2} + \sum_{i=2}^{\infty} \frac{(na)^{2i}}{(2i)!} + \sum_{i=0}^{\infty} \frac{(na)^{2i+1}}{(2i+1)!} \sum_{j+i \geq 2}^{\infty} (nR)^{2j-1} \frac{B_{2j} 4^j (4^j - 1)}{(2j)!}.
 \end{aligned} \tag{C.0.1}$$

where the numbers B_k appearing are Bernoulli numbers. Divide $1 - \frac{\cosh n(R-a)}{\cosh nR}$ by $n^2 a(2R-a)/2$ we get

$$\begin{aligned}
 \frac{1 - \frac{\cosh n(R-a)}{\cosh nR}}{n^2 a(2R-a)/2} &= 1 + \frac{2a}{2R-a} \sum_{i=2}^{\infty} \frac{(na)^{2i-2}}{(2i)!} \\
 &\quad + 2 \sum_{i=0}^{\infty} \frac{(na)^{2i}}{(2i+1)!} \sum_{j+i \geq 2}^{\infty} (nR)^{2j-2} \frac{B_{2j} 4^j (4^j - 1)}{(2j)!}.
 \end{aligned} \tag{C.0.2}$$

Since $na < \epsilon_1$, $n(2R-a) < \epsilon_1 \forall n \geq n_1$, we have $nR < \epsilon_1$ and

$$\begin{aligned}
 1 \leq \frac{1 - \frac{\cosh n(R-a)}{\cosh nR}}{n^2 a(2R-a)/2} &\leq 1 + \frac{2a}{2R-a} \sum_{i=2}^{\infty} \frac{\epsilon_1^{2i-2}}{(2i)!} + 2 \sum_{i=0}^{\infty} \frac{\epsilon_1^{2i}}{(2i+1)!} \sum_{j+i \geq 2}^{\infty} \epsilon_1^{2j-2} \frac{B_{2j} 4^j (4^j - 1)}{(2j)!} \\
 &\leq 1 + \frac{2a}{2R-a} \epsilon_1^2 \sum_{i=2}^{\infty} \frac{1}{(2i)!} + 2\epsilon_1^2 \sum_{i=0}^{\infty} \frac{1}{(2i+1)!} \sum_{j+i \geq 2}^{\infty} \frac{B_{2j} 4^j (4^j - 1)}{(2j)!}.
 \end{aligned} \tag{C.0.3}$$

Therefore, we obtain

$$1 \leq \frac{\lambda_n}{\frac{n^2 a(2R-a)}{2}} \leq 1 + c_1, \quad 1 \leq \frac{\psi_n^2}{\pi a(2R-a)n^{-2}} \leq 1 + c_1. \tag{C.0.4}$$

where $c_1 = \frac{2a}{2R-a} \epsilon_1^2 \sum_{i=2}^{\infty} \frac{1}{(2i)!} + 2\epsilon_1^2 \sum_{i=0}^{\infty} \frac{1}{(2i+1)!} \sum_{j+i \geq 2}^{\infty} \frac{B_{2j} 4^j (4^j - 1)}{(2j)!}$.

(2) If $n(2R-a) \ll 1 \ll na$ which means $\exists \epsilon_2, n_2$ such that $\forall n: na \geq n_2$, but

$n(2R - a) < \epsilon_2$, then we have

$$\begin{aligned}
 1 - \frac{\cosh n(R-a)}{\cosh nR} &= 1 - \cosh na + \sinh na \tanh nR \\
 &= 1 - \frac{e^{na} + e^{-na}}{2} + \frac{e^{na} - e^{-na}}{2} \frac{e^{2nR} - 1}{e^{2nR} + 1} \\
 &= 1 - \frac{e^{na}}{e^{2nR} + 1} - \frac{e^{-na}}{2} \left(1 + \frac{e^{2nR} - 1}{e^{2nR} + 1} \right) \\
 &= 1 - \frac{1}{e^{n(2R-a)} + e^{-na}} - \frac{e^{n(2R-a)}}{e^{2nR} + 1} \\
 &= \frac{e^{n(2R-a)} - 1}{e^{n(2R-a)} + e^{-na}} + \frac{e^{-na}}{e^{n(2R-a)} + e^{-na}} - \frac{e^{n(2R-a)}}{e^{2nR} + 1} \\
 &= \frac{e^{n(2R-a)} - 1}{e^{n(2R-a)} + e^{-na}} + \frac{1 - e^{n(2R-a)}}{e^{2nR} + 1} \\
 &= \frac{\sum_{i=1}^{\infty} \frac{n^i(2R-a)^i}{i!}}{\sum_{i=0}^{\infty} \frac{n^i(2R-a)^i}{i!} + e^{-na}} - \frac{1 - \sum_{i=1}^{\infty} \frac{n^i(2R-a)^i}{i!}}{e^{2nR} + 1}. \quad (\text{C.0.5})
 \end{aligned}$$

Divide $1 - \frac{\cosh n(R-a)}{\cosh nR}$ by $n(2R - a)$ we get

$$\begin{aligned}
 \frac{1 - \frac{\cosh n(R-a)}{\cosh nR}}{n(2R - a)} &= \frac{\sum_{i=0}^{\infty} \frac{n^i(2R-a)^i}{(i+1)!}}{\sum_{i=0}^{\infty} \frac{n^i(2R-a)^i}{(i)!} + e^{-na}} - \frac{\sum_{i=1}^{\infty} \frac{n^i(2R-a)^i}{i!}}{n(2R - a)(e^{2nR} + 1)} \\
 &= 1 - \frac{\sum_{i=1}^{\infty} n^i(2R - a)^i \left(\frac{1}{i!} - \frac{1}{(i+1)!} \right) + e^{-na}}{\sum_{i=0}^{\infty} \frac{n^i(2R-a)^i}{i!} + e^{-na}} - \frac{\sum_{i=0}^{\infty} \frac{n^i(2R-a)^i}{(i+1)!}}{e^{2nR} + 1}. \quad (\text{C.0.6})
 \end{aligned}$$

Since $n(2R - a) < \epsilon_2$, $na > n_2$, we get

$$\begin{aligned}
 1 - \sum_{i=1}^{\infty} (\epsilon_2)^i \left(\frac{1}{i!} - \frac{1}{(i+1)!} \right) + e^{-n_2} - \frac{1 + \sum_{i=1}^{\infty} \frac{(\epsilon_2)^i}{(i+1)!}}{2} &\leq \frac{1 - \frac{\cosh n(R-a)}{\cosh nR}}{n(2R - a)} \leq 1, \\
 1/2 - \epsilon_2 - e^{-n_2} - \epsilon_2 \sum_{i=1}^{\infty} \frac{1}{(i+1)!} &\leq \frac{1 - \frac{\cosh n(R-a)}{\cosh nR}}{n(2R - a)} \leq 1. \quad (\text{C.0.7})
 \end{aligned}$$

Therefore, we obtain

$$1 - c_2 \leq \frac{\lambda_n}{n(2R - a)} \leq 1, \quad \text{and } c_2 \leq \frac{\psi_n^2}{2\pi n(2R - a)} \leq 1 \quad (\text{C.0.8})$$

where $c_2 = 1/2 + \epsilon_2 + e^{-n_2} + \epsilon_2 \sum_{i=1}^{\infty} \frac{1}{(i+1)!}$.

(3) If $na \ll 1 \ll n(2R - a)$ which means $\exists \epsilon_3, n_3$ such that $\forall n: n(2R - a) \geq n_3$, but $na < \epsilon_3$, then we have

$$\begin{aligned}
 1 - \frac{\cosh n(R - a)}{\cosh nR} &= 1 - \cosh na + \sinh na \tanh nR \\
 &= 1 - \cosh na + \sinh na \left(1 - \frac{2e^{-2nR}}{1 + e^{-2nR}} \right) \\
 &= 1 - \left(1 + \sum_{i=1}^{\infty} \frac{(na)^i (-1)^i}{i!} \right) - \sum_{i=0}^{\infty} \frac{(na)^{2i+1}}{(2i+1)!} \frac{2e^{-2nR}}{1 + e^{-2nR}} \\
 &= \sum_{i=1}^{\infty} \frac{(na)^i (-1)^{i-1}}{i!} - \sum_{i=0}^{\infty} \frac{(na)^{2i+1}}{(2i+1)!} \frac{2e^{-2nR}}{1 + e^{-2nR}} \quad (\text{C.0.9})
 \end{aligned}$$

Divide $1 - \frac{\cosh n(R-a)}{\cosh nR}$ by na we get

$$\frac{1 - \frac{\cosh n(R-a)}{\cosh nR}}{na} = 1 + \sum_{i=2}^{\infty} \frac{(na)^{i-1} (-1)^{i-1}}{i!} - \sum_{i=0}^{\infty} \frac{(na)^{2i}}{(2i+1)!} \frac{2e^{-2nR}}{1 + e^{-2nR}}. \quad (\text{C.0.10})$$

Since $na < \epsilon_3$, $n(2R - a) \geq n_3$, we get $nR \geq n_3/2$ and

$$\begin{aligned}
 1 - \sum_{i=1}^{\infty} \frac{(na)^{2i-1}}{(2i)!} - \sum_{i=0}^{\infty} \frac{(na)^{2i}}{(2i+1)!} \frac{2e^{-2nR}}{1 + e^{-2nR}} &\leq \frac{1 - \frac{\cosh n(R-a)}{\cosh nR}}{na} \leq 1 + \sum_{i=1}^{\infty} \frac{(na)^{2i}}{(2i+1)!}, \\
 1 - \sum_{i=1}^{\infty} \frac{\epsilon_3^{2i-1}}{(2i)!} - \sum_{i=0}^{\infty} \frac{\epsilon_3^{2i}}{(2i+1)!} 2e^{-n_3} &\leq \frac{1 - \frac{\cosh n(R-a)}{\cosh nR}}{na} \leq 1 + \sum_{i=1}^{\infty} \frac{\epsilon_3^{2i}}{(2i+1)!}, \\
 1 - \epsilon_3 \sum_{i=1}^{\infty} \frac{1}{(2i)!} - 2e^{-n_3} \sum_{i=0}^{\infty} \frac{1}{(2i+1)!} &\leq \frac{1 - \frac{\cosh n(R-a)}{\cosh nR}}{na} \leq 1 + \epsilon_3^2 \sum_{i=1}^{\infty} \frac{1}{(2i+1)!}. \quad (\text{C.0.11})
 \end{aligned}$$

Therefore, we obtain

$$1 - c_3 \leq \frac{\lambda_n}{na} \leq 1 + c'_3, \quad \text{and} \quad 1 - c_3 \leq \frac{\psi_n^2}{2\pi na} \leq 1 + c'_3 \quad (\text{C.0.12})$$

where $c_3 = 1 - \sum_{i=1}^{\infty} \frac{\epsilon_3^{2i-1}}{(2i)!} - \sum_{i=0}^{\infty} \frac{\epsilon_3^{2i}}{(2i+1)!} 2e^{-n_3}$ and $c'_3 = 1 + \epsilon_3^2 \sum_{i=1}^{\infty} \frac{1}{(2i+1)!}$.

(4) If $\min\{na, n(2R - a)\} \gg 1$ which means $\exists n_4$ such that $\forall n: na \geq n_4$ and $n(2R - a) \geq n_4$, then we have

$$\begin{aligned}
 1 - \frac{\cosh n(R - a)}{\cosh nR} &= 1 - \frac{e^{n(R-a)} + e^{-n(R-a)}}{e^{nR} + e^{-nR}} \\
 &= 1 - \frac{e^{-na} + e^{-n(2R-a)}}{1 + e^{-2nR}}. \quad (\text{C.0.13})
 \end{aligned}$$

Since $na \geq n_4$, $n(2R - a) \geq n_4$, we get $nR \geq n_4$ and

$$1 - 2e^{-n_4} \leq 1 - \frac{\cosh n(R - a)}{\cosh nR} \leq 1. \quad (\text{C.0.14})$$

Therefore, we obtain

$$1 - c_4 \leq \frac{\lambda_n}{n^{-2}} \leq 1, \quad \text{and } c_4 < \frac{\psi_n^2}{2\pi n^{-4}} < 1, \quad (\text{C.0.15})$$

where $c_4 = 2e^{-n_4}$.

□

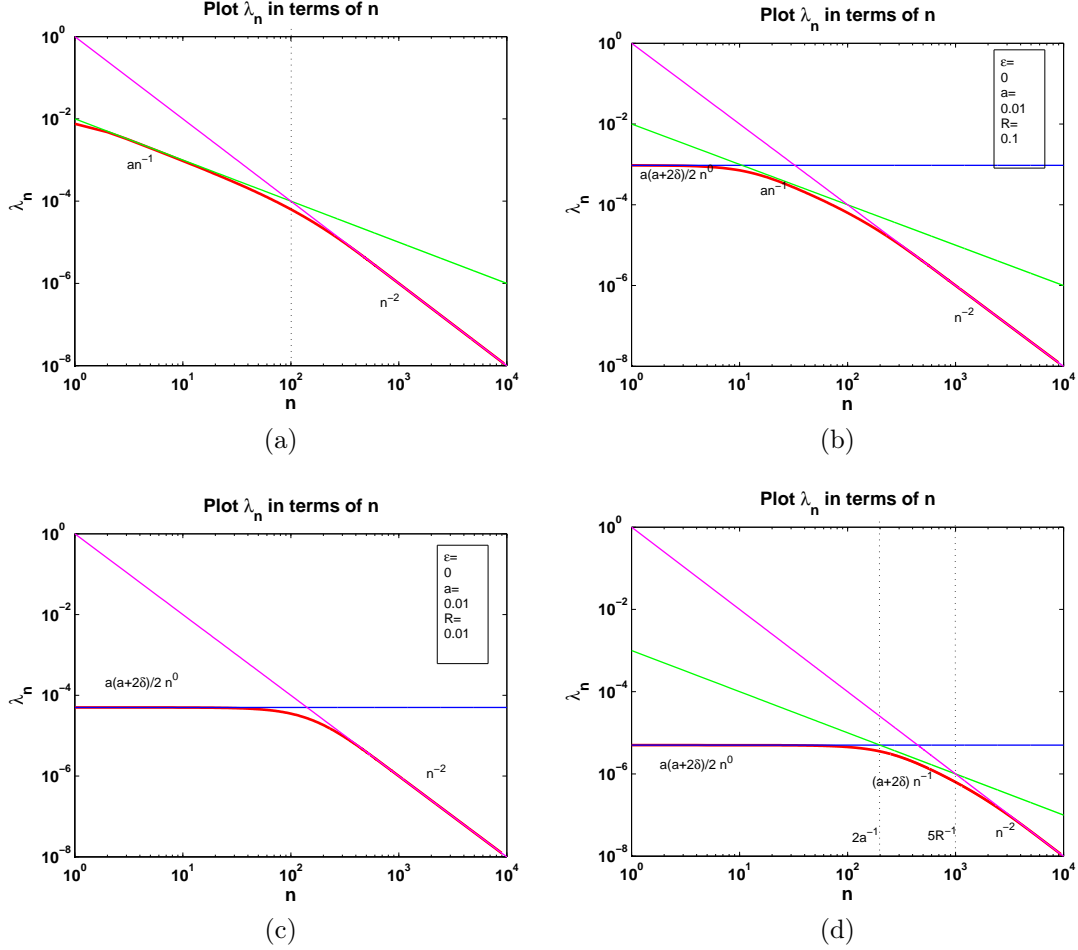


Figure C.1: Eigenvalues λ_n of the operator $V\tilde{T}V$ for $\epsilon = 0$, $a = 0.01$ and four values R (from left to right, up to down): **(a)** $R = 1$; **(b)** $R = 0.1$; **(c)** $R = 0.01$ and **(d)** $R = 0.0055$. Solid lines show the asymptotic relations $a(2R - a)/2n^0$, $A_{a,R}^{(2)}n^{-1}$ and n^{-2} , where $A_{a,R}^{(2)}$ can be a or $a + 2\delta$ ($\delta = 2R - a$). We observe that in the case **a** ($R \geq 1$), the first regime disappears and $A_{a,R}^{(2)} = a$; in the case **b** ($1 < a < R$), there are three separated regimes $a(2R - a)/2n^0$, an^{-1} and n^{-2} ; in the case **c** ($1 < R = a$), the second regime disappears; in the case **d** ($1 < R < a$), there are three separated regimes $a(2R - a)/2n^0$, $(2R - a)n^{-1}$ and n^{-2} .

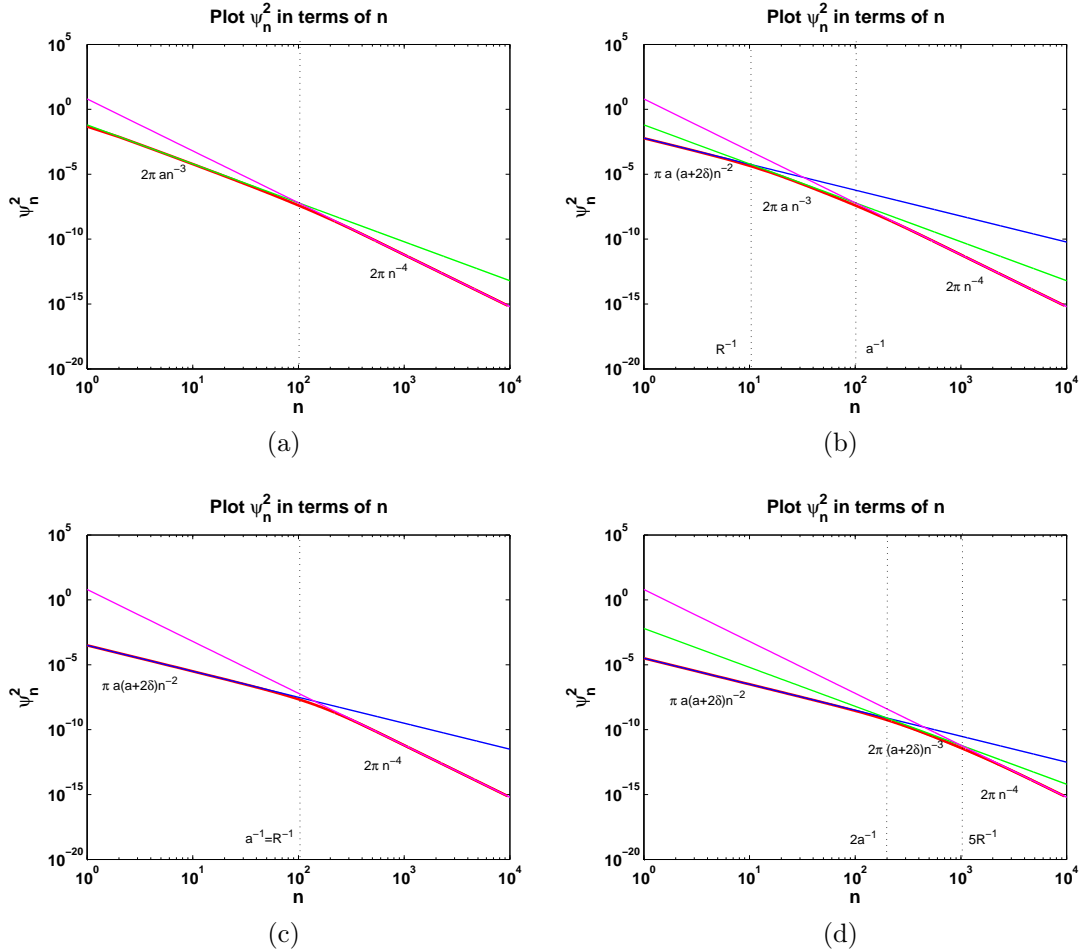


Figure C.2: Coefficients ψ_n^2 for $\epsilon = 0$, $a = 0.01$ and four values R : **(a)** $R = 1$; **(b)** $R = 0.1$; **(c)** $R = 0.01$ and **(d)** $R = 0.0055$. Straight lines show the asymptotic relations $\pi a(2R - a)n^{-2}$, $B_{a,R}^{(2)}n^{-3}$ and $2\pi n^{-4}$, where $B_{a,R}^{(2)}$ can be $2\pi a$ or $2\pi(2R - a)$. In the case **a** ($R \geq 1$), the first regime disappears and $B_{a,R}^{(2)} = 2\pi a$; in the case **b** ($1 < a < R$), there are three separated regimes $\pi a(2R - a)n^{-2}$, $2\pi a n^{-3}$ and $2\pi n^{-4}$; in the case **c** ($1 < R = a$), the second regime disappears; in the case **d** ($1 < R < a$), there are three separated regimes $\pi a(2R - a)n^{-2}$, $2\pi(2R - a)n^{-3}$ and $2\pi n^{-4}$.

Bibliography

- [1] O. Bénichou, D. S. Grebenkov, P. E. Levitz, C. Loverdo, and R. Voituriez. Optimal reaction time for surface-mediated diffusion. *Phys. Rev. Lett.*, 105, 2010.
- [2] O. Bénichou, D. S. Grebenkov, P. E. Levitz, C. Loverdo, and R. Voituriez. Mean first-passage time of surface-mediated diffusion in spherical domains. *J. Stat. Phys.*, 142(4):657–685, 2011.
- [3] O. Bénichou, D.S. Grebnkov, L. Hillairet, X.L. Phun, and M. Zinsmeister. Mean exit time for surface-mediated diffusion: spectral analysis and asymptotic behavior. *In preparation*.
- [4] O. Bénichou, C. Loverdo, M. Moreau, and R. Voituriez. Intermittent search strategies. *Rev. Mod. Phys.*, 83, 2011.
- [5] P. C. Bressloff and J. M. Newby. Stochastic models of intracellular transport. *Rev. Mod. Phys.*, 85, 2013.
- [6] Haim Brezis. *Functional analysis, Sobolev spaces and partial differential equations*. Universitext. Springer, New York, 2011.
- [7] T. Calandre, O. Bénichou, D. S. Grebenkov, and R. Voituriez. The interfacial territory covered by surface-mediated diffusion. *Phys. Rev. E*, 85, 2012.
- [8] T. Calandre, O. Bénichou, D. S. Grebenkov, and R. Voituriez. Splitting probabilities and interfacial territory covered by 2d and 3d surface-mediated diffusion. *Phys. Rev. E*, 89, 2014.
- [9] S. A. Isaacson and J. M. Newby. Uniform asymptotic approximation of diffusion to a small target. *Phys. Rev. E*, 88, 2013.
- [10] R. Metzler, G. Oshanin, and S. Redner, editors. *First-Passage Phenomena and Their Applications*. World Scientific Publisher, 2014.
- [11] S. Redner. *A Guide to First-Passage Processes*. Cambridge University Press, Cambridge, 2001.

- [12] J. Reingruber and D. Holcman. Diffusion in narrow domains and application to phototransduction. *Phys. Rev. E*, 79, 2009.
- [13] J.A. Revelli, C.E. Budde, O. Prato, D. Deza, and H.S. Wio. Bulk mediated surface diffusion: non markovian desorption with finite first moment. *Eur. Phys. J. B*, 43:65, 2005.
- [14] F. Rojo and C.E Budde. Enhanced diffusion through surface excursion: A master-equation approach to the narrow-escape-time problem. *Phys. Rev. E*, 84:021117, 2011.
- [15] F. Rojo, C.E Jr. Budde, H.S. Wio, and C.E Budde. Enhanced transport through desorption-mediated diffusion. *Phys. Rev. E*, 87:012115, 2013.
- [16] F. Rojo, P.A. Pury, and C.E Budde. Intermittent pathways towards a dynamical target.
- [17] J.-F. Rupprecht, O. Bénichou, D. S. Grebenkov, and R. Voituriez. Exact mean exit time for surface-mediated diffusion. *Phys. Rev. E*, 86, 2012.
- [18] J.-F. Rupprecht, O. Bénichou, D. S. Grebenkov, and R. Voituriez. Kinetics of active surface-mediated diffusion in spherically symmetric domains. *J. Stat. Phys.*, 147, 2012.
- [19] Z. Schuss, A. Singer, and D. Holcman. The narrow escape problem for diffusion in cellular microdomains. *Proc. Nat. Ac. Sci.*, 104:16098, 2007.
- [20] A. Singer, Z. Schuss, and D. Holcman. Narrow escape. II. The circular disk. *J. Stat. Phys.*, 122(3):465–489, 2006.
- [21] A. Singer, Z. Schuss, and D. Holcman. Narrow escape. III. Non-smooth domains and Riemann surfaces. *J. Stat. Phys.*, 122(3):491–509, 2006.
- [22] A. Singer, Z. Schuss, D. Holcman, and R. S. Eisenberg. Narrow escape. I. *J. Stat. Phys.*, 122(3):437–463, 2006.

Xuan Lan PHUN

PROCESSUS DE TRANSPORT INTERMITTENT SUR SURFACES

Résumé :

Comment les protéines trouvent-elles leur chemin vers les rares endroits des molécules d'ADN où elles peuvent perpétuer le processus de vie?

De nombreuses études récentes tendent à prouver que seule une dynamique intermittente, c'est à dire à (au moins) deux régimes permet ce processus.

L'objet principal de cette thèse est une étude rigoureuse d'un modèle simplifié de dynamique intermittente. Dans ce modèle la molécule alterne des dynamiques browniennes dans le "bulk" et sur la "surface" (i.e. la molécule d'ADN dans l'exemple plus haut) jusqu'à ce qu'elle atteigne sa cible, une petite fenêtre sur la surface: le temps passé par la molécule à la surface est naturellement modélisé comme une variable exponentielle de paramètre λ . Le principal résultat de la thèse est que quels que soient les paramètres, la recherche purement "par le bulk" n'est jamais optimale, ce qui légitime la thèse de la dynamique intermittente. On y caractérise aussi le cas où le temps optimal est atteint pour $\lambda > 0$.

L'outil mathématique nouveau est l'introduction d'un opérateur autoadjoint et de sa base orthonormée de vecteurs propres. Cette étude permet d'obtenir un développement asymptotique à λ grand du temps moyen d'atteinte de la cible. Par ailleurs, un modèle nouveau est introduit: c'est celui du tore qui porte un paramètre supplémentaire, à savoir son module. Il est montré dans cette thèse que certaines valeurs du module conduisent à prouver que la stratégie intermittente est considérablement meilleure que celle de la pure diffusion dans le bulk.

Mots clés : le temps moyen de sortie, la diffusion de surface médiée, le transport intermittent, les processus de recherche, d'analyse spectrale.

INTERMITTENT TRANSPORT PROCESSES ON SURFACES

Abstract :

How do proteins find their way towards the rare places on DNA molecules where they need to go in order to perpetuate the life process?

Many recent works tend to show that only an intermittent dynamics, that is a dynamics with two or more regimes, allows this process.

The main goal of this PhD is a rigorous study of a simplified model of intermittent dynamics.

In this model the molecule alternates diffusion in the bulk with a different kind of diffusion on the surface until it reaches its target consisting in a small window on the surface. The time spent by the molecule on the surface is naturally modeled as following an exponential law with parameter λ . The main result of this thesis is to show that, whatever the parameters are, a pure bulk strategy is never optimal, thus reinforcing the hypothesis of intermittent dynamics. One also characterizes the case where the optimal time is attained for $\lambda > 0$.

The new mathematical tool is the introduction of a self-adjoint operator and the use of its orthonormal basis of eigenvectors. This tool allows to obtain a precise asymptotic behavior of the mean exit time for λ large. Besides that a new geometrical model is developed, called the torus model. This new model carries a new parameter, namely its modulus. It is shown in this thesis that for some values of the modulus the optimized exit time is significantly (allowing experimental checking for instance) shorter than the pure bulk search.

Keywords : mean exit time, surface-mediated diffusion, intermittent transport, search processes, spectral analysis.



MAPMO UMR 6628 - CNRS
Rue de Chartres - BP6759
45067 ORLÉANS CEDEX

